

On the Manifestation of Chiral Symmetry in Nuclei and Dense Nuclear Matter

G.E. Brown^(a) and Mannque Rho^(b,c)

(a) *Department of Physics and Astronomy, State University of New York
Stony Brook, NY 11794, USA*

(b) *Service de Physique Théorique, CE Saclay, 91191 Gif-sur-Yvette, France*

(c) *Department of Physics, Seoul National University, Seoul, Korea and Department of
Physics, Yonsei University, Seoul, Korea*

(May 20, 2019)

Abstract

This article reviews our view on how chiral symmetry, its pattern of breaking and restoration under extreme conditions manifest themselves in the nucleon, nuclei, nuclear matter and dense hadronic matter. We discuss how first-principle (QCD) calculations of the properties of finite nuclei can be effectuated by embedding the “standard nuclear physics approach” into the framework of effective field theories of nuclei that incorporate chiral dynamics and then exploit the predictive power of the theory to accurately compute such solar neutrino processes as the proton-proton fusion and the “hep” process and such cosmological nucleosynthesis process as thermal neutron-proton capture etc. The Brown-Rho (BR) scaling that implements chiral symmetry property of baryon-rich medium is re-interpreted in terms of “vector manifestation” of hidden local symmetry à la Harada-Yamawaki. We present a clear *direct* evidence and a variety of *indirect* evidences for BR scaling in nuclear processes at normal nuclear matter density probed by weak and electromagnetic fields and at higher density probed by heavy-ion collisions and compact-star observables. We develop the notion of “broadband equilibration” in heavy-ion processes and sharpen the role of strangeness in the formation of compact stars and their collapse into black-holes. We revisit the Cheshire-Cat phenomenon first discovered in the skyrmion structure of baryons and more recently revived in the form of “quark-hadron continuity” in mapping low-density structure of hadrons to high-density structure of quarks and gluons and argue once more for the usefulness and power of effective field theories based on chiral symmetry under extreme conditions. It is shown how color-flavor locking in terms of QCD variables and hidden local symmetry in terms of hadronic variables are connected and how BR scaling fits into this “continuity” scheme exhibiting a novel aspect of the Cheshire Cat phenomenon.

Contents

1	INTRODUCTION	3
2	FROM QUARK TO NUCLEON	5
2.1	Modeling the Nucleon in QCD	5
2.2	The Chiral Bag Lagrangian	7
3	EFFECTIVE FIELD THEORIES IN NUCLEAR PHYSICS	11
3.1	Chiral Symmetry in Nuclear Processes	11
3.2	Objectives of EFTs in Nuclear Physics	12
3.3	Effective Chiral Lagrangians	14
3.4	Nucleon-Nucleon Scattering	15
3.5	The PKMR Approach: <i>More Effective EFT</i>	19
3.5.1	<i>NN scattering</i>	19
3.5.2	<i>Electroweak response functions: Accurate postdictions and predictions</i>	22
3.5.3	<i>The chiral filter: Two sides of the same coin</i>	28
3.5.4	<i>An interpretation of hard-core correlation in an effective field theory</i>	29
4	“VECTOR MANIFESTATION” OF CHIRAL SYMMETRY	33
5	LANDAU FERMI LIQUID FROM CHIRAL LAGRANGIANS	37
5.1	Fluctuating Around Zero-Density Vacuum	37
5.2	Skyrmion vs. Q-Ball	38
5.3	Effective Chiral Lagrangian for Many-Nucleon Systems	39
5.4	Brown-Rho Scaling	41
5.5	Landau Mass and BR Scaling	43
6	INDIRECT EVIDENCES FOR BR SCALING	44
6.1	Indications in Finite Nuclei	44
6.2	The Anomalous Gyromagnetic Ratio in Nuclei	45
6.3	Axial Charge Transitions in Heavy Nuclei	46
6.4	Axial-Vector Coupling Constant g_A^* in Dense Matter	47
6.5	Evidences from “On-Shell” Vector Mesons	49
7	DIRECT EVIDENCE FROM THE $(e, e'p)$ RESPONSE FUNCTIONS IN NUCLEI	50
8	BR SCALING IN CHIRAL RESTORATION	54
8.1	Bag Constant and Scalar Field Energy	54
8.2	“Nambu Scaling” in Temperature	55
8.3	“Nambu Scaling” in Density	57

9 SIGNALS FROM HEAVY-ION COLLISIONS	58
9.1 Top-Down and Bottom-Up and How They Connect	59
9.2 Distinguishing Rapp/Wambach and Brown/Rho	61
10 “BROAD-BAND EQUILIBRATION” OF STRANGENESS IN HEAVY-ION COLLISIONS	63
10.1 Kaons and Chiral Symmetry	63
10.2 Equilibration vs. Dropping Kaon Mass	63
10.3 The Equilibrium K^+/π^+ Ratio	67
10.4 The Top-Down Scenario of K^\pm Production	68
10.5 Partial Decoupling of the Vector Interaction	70
10.5.1 <i>Theoretical and experimental evidences</i>	70
10.5.2 <i>Kaons at GSI</i>	73
10.6 Schematic Model	74
10.6.1 <i>First try with the simplest form</i>	74
10.6.2 <i>Implications on kaon condensation and maximum neutron-star mass</i>	74
10.7 Discussions	76
11 EFFECTIVE FIELD THEORIES FOR DENSE QCD	78
11.1 Color-Flavor Locking for $N_F = 3$	78
11.1.1 <i>Instability at high density</i>	78
11.1.2 <i>Symmetry breaking and excitations</i>	79
11.1.3 <i>Chiral Lagrangians and qualitons</i>	80
11.2 Complementarity of Hidden Gauge Symmetry and Color Gauge Symmetry and BR Scaling	83
11.2.1 <i>Quark number susceptibility</i>	83
11.2.2 <i>Color-isospin locking</i>	84
11.2.3 <i>Implications of the lattice measurements of quark number susceptibility</i>	84
11.2.4 <i>Link to BR scaling and Landau parameter F_1</i>	86
11.3 Kaon Condensation: <i>Encore Cheshire Cat</i>	87

1 INTRODUCTION

In a recent unpublished paper, Morgenstern and Meziani [1] reported a remarkable result of their extensive analysis of the longitudinal and transverse response functions in medium-weight and heavy nuclei and concluded that the available world data showed unequivocally the quenching of $\sim 20\%$ in the longitudinal response function and the only viable way to explain this quenching is to invoke the Brown-Rho (BR) scaling [2] formulated to account for the change of the strong-interaction vacuum induced by matter density. Partly motivated by this development and other indirectly related developments including the most recent one on color-flavor-locking and color superconductivity, we shall make in this review *our* overview of evidences that indicate both directly and indirectly that the BR scaling is indeed operative in finite nuclei and dense (and superdense) nuclear matter. We shall develop our arguments starting with the basic structure of the nucleon, then go to that of nuclei and of nuclear matter and finally to that of dense matter that one expects to create in relativistic heavy-ion collisions and find in the interior of highly compact stars. The principal theme will be that the chiral symmetry of quantum chromodynamics – its spontaneous breaking in free space and partial or full restoration in medium – underlies the common feature from elementary hadrons to complex dense systems. We admit that our views are not necessarily shared by others in all details and that some points may not be fully correct. We are however confident that the general theme that we have developed and we shall review here will survive the experimental test that is to come.

It was recognized a long time ago that chiral symmetry, now identified as an essential ingredient of QCD associated with the light-mass up (u), down (d) and strange (s) quarks, with its “hidden” realization in Nambu-Goldstone mode plays an important role in nuclear physics. In fact, the emphasis on its role in a variety of nuclear processes predates even the advent of QCD proper and subsequent acceptance as *the correct* theory of strong interactions [3]. Among the time-tested and established is the role of chiral symmetry in exchange currents in electro-weak processes in nuclei [4, 5] and its subsequent importance in probing nuclear structure at various electron machines, now out of operation, throughout the world [6]. Since our early review on the subject [3], there has been continuous and significant evolution in the field specifically associated with the role of QCD in nuclear physics, more or less unnoticed by workers in other areas of physics. The evolution touched on the structure of the nucleon, the proton and the neutron, starting with the notion of a “little bag” [7], the recognition of the preeminent importance of Goldstone pion clouds in both the nucleon structure and nuclear forces [7, 8], followed by the resurrection of the Skyrme soliton model that contains baryons – which are fermions – in a bosonic field theory [9, 10] and then the emergence of the notion of “Cheshire Cat phenomenon.” At present, the issue of both “spontaneous” breaking and restoration of chiral symmetry occupies one of the central positions in current activities in both nuclear and hadron physics communities. The development up to 1995 has been summarized in a recent monograph by Nowak, Rho and Zahed [11].

It is now becoming clearer in which direction the chiral symmetry of QCD will steer

the *next* generation of nuclear and hadronic physicists, with the advent of new accelerators such as the Jefferson Laboratory (JL) and the RHIC at Brookhaven – both of which are already operating – and ALICE/LHC at CERN – which is to come in a few years. On one hand, the electron machine at the JL will probe deeper into shorter distance properties of the nucleon-nucleon interactions, exploring how the chiral structure of the nucleon in medium changes from hadronic over to quark/gluon picture as shorter distances are probed. As will be repeatedly stressed, one does not expect any abrupt phase transitions along the way; as the change will most likely be continuous (for a multitude of reasons we will discuss), it will then be a matter of economy which language will be more efficient for given processes with given conditions, implying that there will be a continuous map between the various descriptions. This continuity will play a central role in our discussion and will later be referred, quite broadly, to as “Cheshire Cat Phenomenon.”

On the other hand, the heavy-ion machines at RHIC and ALICE/LHC will create systems at high temperature and density, mimicking the early Universe. At high temperatures, QCD predicts a phase transition from chiral symmetry in the Goldstone mode to that in the Wigner mode with a consequent change in confinement/deconfinement. This is more or less confirmed on lattice in QCD. Indications are coming out already from available experimental data that such a transition has been seen. Matter at high density is a completely different matter. Up to date, it has not been feasible to put density on lattice, so there is no model-independent theoretical indication for a similar phase change as density is increased. Theoretical models however do predict that there can be a series of phase changes including the chiral symmetry restoration. As will be discussed in this article, there are a variety of processes involving nuclei and nuclear matter that provide, albeit indirect, evidence for such phase changes, most intriguingly of which are possible signals from compact (neutron) stars.

Going to the physics of matter under extreme conditions — high temperature, high density or both – encompasses a multitude of scales. At low density $\rho < \rho_0$ (where ρ_0 is nuclear matter density), one can rely on the rich phenomenology available in the guise of standard nuclear physics to work with an effective Lagrangian field theory that is anchored on the premise of quantum chromodynamics (QCD), e.g., chiral perturbation theory. We may call this “phenomenological perturbation approach (PPA).” However as one approaches the density ρ_0 , an effective field theory constructed in the matter-free vacuum encounters difficulty and becomes more or less unpredictable: Presently there is no way to derive a nucleus starting from a first-principle Lagrangian, not to mention denser hadronic matter. The reason why this is so will be explained in the course of this review. The attitude we will adopt here is then to develop a generic description of dense matter based on global characteristics of hadrons in the environment of surrounding dense medium. For this, we exploit the chiral structure of the QCD vacuum and the excitations thereon (i.e., hadrons) following the notion of “vector manifestation” recently proposed and developed by Harada and Yamawaki [12]. In the Harada-Yamawaki scenario, chiral restoration from the spontaneously broken mode to an unbroken mode takes place with the massless pions (in the chiral limit) coming together with the would-be scalar Goldstone bosons that are the longitudinal components of massive vector mesons, with the massless

vector mesons consequently decoupling. This scheme requires that near the chiral phase transition — independently of whatever form it may take, the vector (ρ and ω) meson masses drop as the chiral transition point is approached bottom-up. This, we will see, provides a compelling theoretical support to BR scaling. We will also see that most remarkably, this scenario will be further supported by QCD structure of quark condensates in medium associated with color-flavor locking.

BR scaling as originally formulated in [2] corresponded to a mean-field approximation in a large N_c effective chiral Lagrangian theory (where N_c is the number of colors in QCD) with the strong interaction vacuum ¹ “sliding” with density (or temperature) of the system. For a given density, say, quantum fluctuations or loop corrections are to be calculated for correlation functions etc with a chiral Lagrangian whose parameters are suitably defined at the sliding vacuum appropriate to physical processes of given kinematical conditions. How this works out has been explained in the literature but will be summarized in the review at pertinent places. We propose that the way the BR-scaling mean-field quantities vary as a function of the medium condition (density or temperature) should roughly match with the change of the vacuum suggested by Harada-Yamawaki’s vector manifestation. As mentioned above, at small external conditions (e.g., at low density), the PPA using phenomenological Lagrangians fixed in free space will be in no disagreement with the notion of BR scaling. However as density increases, fluctuations are to be built on a vacuum modified from the free-space one. At some point, this effect can no longer be accessed adequately by the PPA. This can be seen in what we call “sobar” description as explained in a later section. Eventually a correct theory will have to approach Landau Fermi-liquid fixed point at normal nuclear matter density. We will show how this comes about with BR scaling chiral Lagrangians: BR scaling and a Landau parameter can be identified.

One of the major themes of this review is that this picture combining the vector manifestation of chiral symmetry, color-flavor locking and BR scaling passes several tests in nuclear and dense hadronic systems. This, we believe, points to the validity of the notion that understanding what goes on in many-body systems of nucleons at high density and understanding the chiral structure of the nucleon at the QCD level relies on the same principle, a long standing issue in nuclear and hadronic physics. We shall summarize the evidences accumulated since our earlier publication [3, 13].

2 FROM QUARK TO NUCLEON

2.1 Modeling the Nucleon in QCD

For concrete applications of QCD to physical hadronic processes, the only model that purports to encode QCD and at the same time is versatile enough for a wide range of strong interaction physics has been, and still is, the bag model. All other models

¹Throughout this article, the terminology vacuum will be used in the generalized sense of a ground state in the presence of matter.

of equal versatility can be considered as belonging to the same class. There is a long history in the development of this model which, as we shall mention later, continues even today in the guise of string theory and large N Yang-Mills gauge theory. The first such model that incorporates confinement and asymptotic freedom of QCD is the MIT bag model [14]. However it was realized early on that since this model by construction lacks chiral symmetry, it could not be directly applied to the description of nuclear interactions, the domain of strong interaction physics most thoroughly and accurately studied. A simple stability argument showed that the bag for the nucleon must have a bag size typically of ~ 1 fm, essentially the confinement scale implicit in the model. And this is simply too big if one naively applies the picture to nuclear systems. As a possible way to reconcile this simple bag modeling of QCD with the “size crisis”, it was proposed in 1979 [7] to implement the spontaneously broken chiral symmetry and bring in pion cloud to the model. How to introduce pion cloud to the MIT bag producing a “chiral bag” was already known and discussed in the literature [15]. It consisted of adding into the model Goldstone pion fields outside of the bag and imposing chiral-invariant boundary conditions that assure both chiral invariance and confinement. The initial idea in [7] was to use the pressure generated by the external pion cloud to squeeze the bag to a smaller size so as to accommodate the standard nuclear physics picture of meson exchange interactions. At the time the idea was proposed, we had no idea how to squash the bag into a “little bag” in a way consistent with the premise of QCD. We simply dialed the parameters of the model such that the size diminished from ~ 1 fm to ~ 0.3 fm, a size known to be a spatial cutoff between two nucleons. We now know that this prescription was not natural and in fact totally unnecessary. How to reconcile the bag size and nuclei can now be put in the form of what is known as “Cheshire Cat Principle” [16]².

Apart from the concern with the nucleon size in nuclei and *apparent* incompatibility with the successful standard meson-exchange potential picture, the “little bag” was not indispensable for understanding the wide variety of nucleon dynamics as has been argued by Thomas and his co-workers [8, 18]. In fact, this latter approach where the pion field enters only as a fluctuating field at the bag boundary with its size comparable to that of the original MIT one has been reasonably successful in a wide range of applications to those nucleon and nuclear processes that are dominated by pionic perturbative effects and in which nonperturbative chiral effects play a subdominant role [18].

It is now well understood how both the “big cloudy bag” of [8] and the “little bag” of [7] can be accommodated in a unified framework of the chiral bag model. In fact, we now know how to shrink the bag even further from the “little bag” and eventually obtain a “point bag,” the skyrmion [9, 10] which can be considered as the limit that the bag size is shrunk to zero. What has transpired from the development since late 1970’s/early 1980’s up until now is that the bag size that appears in the simple confinement model is more like a gauge degree of freedom [20, 21] and depending upon the gauge choice, it can be of any size without changing basic physics. That physics should not depend upon the confinement (bag) size is known as “Cheshire cat phenomenon” and

²A historical note: Simultaneously and independently of [16], a similar idea was proposed based on phenomenology by Brown et al [17].

has been amply reviewed in the literature (for an exhaustive list of references, see [11, 22, 23]). Unfortunately there is no known exact formulation of this “Cheshire-Cat gauge theory.” This is mainly because there is no exact bosonization of QCD known in four dimensions, the skyrmion limit corresponding to the totally bosonized theory, and the chiral bag partially bosonized. Asking what size of the chiral bag is needed for a particular phenomenology is like asking what gauge choice is optimal in gauge theories that are solved only partially as is the case with QCD. In practice, what bag size is optimal depends upon what physical processes are concerned.

Thus far our argument has been phrased in the framework of a bag picture. The notion of Cheshire Cat is however much more general than in this restricted context. It is a reflection of a variety of “duality” in the problem which is a statement that there are a variety of different ways of describing the same physical process. In other areas of physics (such as string theories, condensed matter physics etc), such a notion can even be formulated in an exact way. In the strong interaction dynamics, however, the notion is at best approximate and hence its predictive power semi-quantitative. Even so, it is sufficiently versatile as to be applied to a variety of problems in nuclear physics. As we will describe in later sections, a remarkable recent development in a related context is the “complementarity” of two descriptions in terms of hadrons and in terms of quark/gluon variables for both dilute matter and dense matter as discussed in a later section of this review. This suggests that the Cheshire Cat notion can be generalized to a wider class of phenomena, going beyond the “confinement size.”

2.2 The Chiral Bag Lagrangian

The Cheshire cat phenomenon in our view is a generic feature in *modeling* QCD or other gauge theories. One may therefore formulate it in various different ways. The use of the chiral bag is not the only way or maybe not even the best way to exploit it. Since we understand the chiral-bag structure better than others, however, we write here the explicit form of the Lagrangian that the chiral bag model takes and that should capture the essential physics of the nucleon. We shall do this for the flavor $SU(3)$ (with up, down and strange quarks) although the nucleon structure is mainly dictated by the non-strange quarks, with the strange quark playing a minor and as yet obscure role. It can be written generically in three terms,

$$S = S_V + S_{\bar{V}} + S_{\partial V}. \quad (2.1)$$

The first term defined in the volume V is the “bag” action that reflects the explicit QCD variables, quarks ψ and gluons G_μ^a :

$$S_V = \int_V d^4x \left(\bar{\psi} i \not{D} \psi - \frac{1}{2} \text{tr } G_{\mu\nu} G^{\mu\nu} \right) + \dots \quad (2.2)$$

where the trace goes over the color. Here ψ is the quark field with the color, flavor and Poincaré indices suppressed, $G_{\mu\nu}$ the gluon field tensor and D_μ the covariant derivative.

The ellipsis stands for quark mass terms that we will leave unspecified. The action for the outside sector occupying the volume \tilde{V} contains relevant physical hadronic fields of zero baryon charge representing color-singlet effective degrees of freedom. It includes the octet Goldstone bosons and non-Goldstone excitations as well as the singlet η' which acquires mass through $U(1)_A$ anomaly and takes the form

$$S_{\tilde{V}} = \frac{f^2}{4} \int_{\tilde{V}} d^4x \left(\text{Tr} \partial_\mu U^\dagger \partial^\mu U + \frac{1}{4N_F} m_{\eta'}^2 [\text{Tr}(\ln U - \ln U^\dagger)]^2 \right) + \dots + S_{WZW} \quad (2.3)$$

where $N_F = 3$ is the number of flavors, Tr goes over the flavor index and

$$\begin{aligned} U &= e^{i\eta'/f_0} e^{2i\pi/f}, \\ f_0 &\equiv \sqrt{N_F/2}f. \end{aligned} \quad (2.4)$$

Here the ellipsis stands for mass terms and heavy-mass fields or higher derivative terms etc. The S_{WZW} is the Wess-Zumino-Witten term [19] that encodes chiral anomalies present in QCD:

$$S_{WZW} = -N_c \frac{i}{240\pi^2} \int_{D_5[\partial D_5 = V \times [0,1]]} \epsilon_{\mu\nu\lambda\rho\sigma} \text{Tr}(L^\mu L^\nu L^\lambda L^\rho L^\sigma) \quad (2.5)$$

with $L = g^\dagger(x, s)dg(x, s)$ defined as $g(x, s = 0) = 1$ and $g(x, s = 1) = U(x)$. The inside QCD sector and the outside hadronic sector must be connected by an action that “translates” them. This is the role of the surface term. It has two terms,

$$S_{\partial V} = S_{\partial V}^{(n)} + S_{\partial V}^{(an)} \quad (2.6)$$

with the “normal” boundary term

$$S_{\partial V}^{(n)} = \frac{1}{2} \int_{\partial V} d\Sigma^\mu (n_\mu \bar{\psi} U^{\gamma_5} \psi) + \dots \quad (2.7)$$

with

$$U^{\gamma_5} = e^{i\eta'\gamma_5/f_0} e^{2i\pi\gamma_5/f} \quad (2.8)$$

and the “anomalous” boundary term

$$S_{\partial V}^{(an)} = i \frac{g^2}{32\pi^2} \int_{\partial V} d\Sigma^\mu K_{5\mu} (\text{Tr} \ln U^\dagger - \text{Tr} \ln U) + \dots \quad (2.9)$$

where K_5^μ is the “Chern-Simons current”

$$K_5^\mu = \epsilon^{\mu\nu\alpha\beta} (G_\nu^a G_{\alpha\beta}^a - \frac{2}{3} g f^{abc} G_\nu^a G_\alpha^b G_\beta^c). \quad (2.10)$$

Again irrelevant terms are subsumed in the ellipses. The “normal” term (2.7) assures chiral invariance of the model as well as color confinement at the classical level. The

“anomalous” term – which is not gauge invariant – takes care of the quantum anomaly (Casimir) induced inside the bag that would violate color confinement [24, 11] if left uneliminated ³.

Up to date, nobody has been able to extract the full content of this model. There are some unresolved technical difficulties that frustrate its solvability. Even so, whatever we have been able to learn from it so far has been found to be fully consistent with Nature. We believe that physics of any other viable chiral model, solitonic or non-solitonic (e.g., [27]), is essentially – though perhaps not in detail – captured in the model (2.1).

Since there have been extensive reviews on the matter [11], we shall simply summarize the salient features obtained from the model:

- Due to a Casimir effect in the bag controlled by the surface term (2.7), the baryon charge is fractioned as a function of the bag radius into the V and \tilde{V} sectors such that the conserved integer baryon charge is recovered. The baryon charge fractionization was first noticed in 1980 by Vento et al. [28] with a reasoning based on an analogy to the monopole-isodoublet system studied by Jackiw and Rebbi [29] and established later [30] for the special chiral angle (“magic angle”) of the pionic hedgehog field and then generalized in [31] for arbitrary chiral angle. The result is that the confinement size or the bag radius has no physical meaning although the baryon size does. The “cloudy bag” model [18] ignores the hedgehog component of the pion field, so in that picture, the baryon charge will be entirely lodged by fiat inside the bag. This implies, in the framework of the chiral bag, that the cloudy bag is *forced to be big* to be consistent with Nature. The real question here is whether or not such a big bag can capture the essential physics involved. This does not address the question of consistency. On the other hand, the limit where the bag radius is shrunk to zero with the totality of the baryon charge “leaked” into the “pion cloud” describes the skyrmion, with the pion cloud picking up the topological charge. The only issue here is whether or not the point-bag description captures the essential physics involved. There is no inconsistency in this description of the baryon.

That the physics should not depend upon the bag radius is an aspect of the “Cheshire Cat Principle” (CCP) [16]. It is the trading between the topological character of the skyrmion configuration and the explicit fermionic charge of the quarks that makes it satisfy exactly the CCP. It is possible to formulate this notion as a gauge symmetry. Formulated as a gauge symmetry, picking a particular bag radius R is equivalent to fixing the gauge as formulated by Damgaard, Nielsen and Sollacher [21]. We will call this “Cheshire-cat gauge symmetry.”

³This form of bulk action plus a surface Chern-Simons term for the bag structure has recently been seen to arise from non-perturbative string theory [25]. It turns out that in four dimensions, the interior of the hadronic bag can be identified as the 3-brane and the boundary of the bag as the world-volume of the Chern-Simons 2-brane in which the dynamics is entirely lodged. This theory does not contain quarks as in the model we are considering but the topological term that is added carries the information on the anomaly present in the theory.

We should also point out that the chiral bag structure of the sort we are discussing arises from QCD proper in the large N_c limit [26].

- While the topological nature of the baryon charge implies an *exact* Cheshire-Cat, the flavor quantum numbers such as isospin, strangeness etc. are not directly linked to topology. Therefore their conservation is not directly connected with topology. They are quantum variables given in terms of collective coordinates. This means that while conserved flavor quantum numbers in QCD remain conserved after collective quantization (unlike the classically conserved baryon charge in the skyrmion limit), various static quantities such as axial charges g_A (both singlet and non-singlet), magnetic moments as well as energies and form factors may not necessarily manifest the *perfect* CC property. They must depend more or less on the details of the parameters and dynamics taken into account.

A good illustration of this feature is the N_c dependence of the theory (where N_c is the number of colors). While the skyrmion sector is strictly valid in the large N_c limit, the bag sector containing the QCD variables encompasses all orders of $1/N_c$. This means that in order to assure the CC for the quantities that depend on N_c , the skyrmion sector would have to have appropriate $1/N_c$ corrections that map to the quark-gluon sector. In practice this means that other hadronic (massive) degrees of freedom than pionic must be introduced into the outside of the bag. What enters will depend on the processes involved.

Most remarkably, however, extensive studies carried out in the field, chiefly by Park [32], confirmed that *all* nucleon properties, be they static or non-static, topological or non-topological, can be satisfactorily and consistently described in terms of the Cheshire-Cat picture. Even more surprisingly, the so-called “proton-spin problem” can also be resolved in a simple way within the model (2.1) [33]. For this, the anomalous surface term (2.9) associated with the $U(1)_A$ anomaly and the η' mass figures importantly. As in other Cheshire Cat phenomena (e.g., the baryon charge), various radius dependent terms conspire to give a more or less radius independent result: Here the cancellation is between the “matter” contribution (from both the quark and η') and the “gauge field” (gluon) contribution, each of which is individually bag-radius dependent and grows in magnitude with bag radius. The resulting flavor-singlet axial charge a^0 for the proton shown in Fig. 1 comes out to be small as observed in the EMC/SMC experiments. We should stress that this is not the only explanation for the small a^0 . There are several seemingly alternative explanations but our point here is that the Cheshire Cat emerges even in a case where QCD aspects are highly non-trivial and subtle involving quantum anomalies of the chiral symmetry.

- So far we have been dealing with long-distance phenomena only. What about shorter-distance physics? Can Cheshire Cat for instance address such short-distance problems as nucleon structure functions seen in deep inelastic lepton scattering where asymptotic freedom is operative and hence QCD should be “visible”? The answer to this is that as one probes shorter distances, the model (2.1) should be modified with more and more higher-dimension operators implied by the ellipsis in the action. There is nothing that suggests that the skyrmion picture when suitably

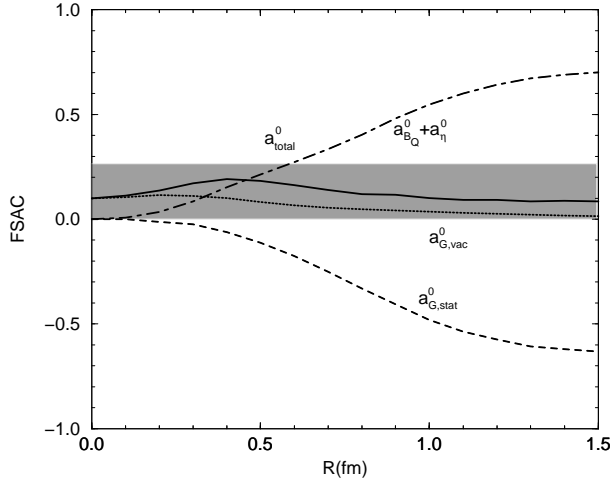


Figure 1: Various contributions to the flavor singlet axial current of the proton as a function of bag radius and comparison with the experiment: (a) the “matter” (quark plus η) contribution ($a_{B_Q}^0 + a_\eta^0$), (b) the gauge field: the static gluon contribution due to quark source ($a_{G,stat}^0$) and the gluon vacuum contribution ($a_{G,vac}^0$), and (c) the total (a_{total}^0). The shaded area corresponds to the range admitted by experiments.

extended should fail if one works hard enough. It is simply that the calculation will get harder and harder and it will be more economical to switch over to the “big bag” or partonic (quark/gluon) picture. Logically, therefore, a hybrid description that exploits both regimes would have a more predictive power. Thus it is easy to understand that the chiral quark-soliton model, a variation on the model (2.1) formulated in a relativistically invariant form [27], has been successfully applied to the problem. We will see later that even at asymptotic density where the QCD variables are the correct variables, the notion of effective fields is applicable.

3 EFFECTIVE FIELD THEORIES IN NUCLEAR PHYSICS

3.1 Chiral Symmetry in Nuclear Processes

The next question we wish to address is: Given the Cheshire Cat freedom, how does one treat nuclei, namely, two- -or more-nucleon systems? That is, how is nuclear physics formulated in QCD?

For this, it is clear that the most efficient and economical way would be to adopt the “point-bag” description ⁴. Once we adopt the zero-radius bag surrounded by meson cloud

⁴In accordance with the Cheshire-Cat principle, one could continue using the hybrid bag-meson de-

as a nucleon, we can represent it as a local field interacting with pions. How to do nuclear physics in terms of *local* nucleon and meson fields and still do QCD is encoded in what is called “Weinberg theorem” [35]. In the present context, the theorem states that doing *in a consistent way* an effective field theory with the nucleon, pion and other meson fields is no more and no less than doing the gauge field theory QCD in terms of quarks and gluons.⁵ What is required is that such an approach preserve the necessary symmetries – Lorentz invariance, unitarity, cluster decomposition etc. – and is quantum mechanical. We are simply to write down the most general such local Lagrangian with all possible terms consistent with the symmetries involved. This strategy is powerfully illustrated in the description of the baryon (octet and decaplet baryon) structure in terms of an effective chiral Lagrangian constructed of baryon and Goldstone boson fields [36]⁶. An initial attempt to implement Weinberg theorem in nuclear physics was made in 1981 [37] (it was incomplete in the chiral counting at the time but was completed in 1991 as mentioned later) but the major development came after Weinberg’s paper in 1990 [38].

3.2 Objectives of EFTs in Nuclear Physics

There are two major roles of EFT in nuclear physics. One is to establish that nuclei as strongly interacting systems – that have been accurately described in the past in what one would call “standard nuclear physics approach (SNPA)” or alternatively “potential model (PM)” based on phenomenological potentials – can *also* be understood from the point of view of a fundamental theory, QCD, and the other is to be able to make nontrivial and precise predictions that are important not only for nuclear physics *per se* but also for other areas of physics such as astrophysics and condensed matter physics. The former renders the impressively rich variety of nuclear processes a respectable domain of research. The latter is to provide an invaluable tool for progress in related areas of physics. In this review some recent developments that are relevant to the general theme of this review

scription by incorporating relevant (hadron) degrees of freedom [34]. One advantage of this approach might be that the quark-bag introduction can implement more readily short-range physics that enters in many-body systems, albeit at a subleading level.

⁵To quote Weinberg [35]: “*We have come to understand that particles may be described at sufficiently low energies by fields appearing in so-called effective quantum field theories, whether or not these particles are truly elementary. For instance, even though nucleon and pion fields do not appear in the Standard Model, we can calculate the rates for processes involving low-energy pions and nucleons by using an effective quantum field theory of pion and nucleon fields rather than of quark and gluon fields.... When we use a field theory in this way, we are simply invoking the general principles of relativistic quantum theories, together with any relevant symmetries; we are not making any assumption about the fundamental structure of physics.*”

⁶While the Lagrangian (2.1) is a *model* of QCD, the baryon chiral Lagrangian used here is an effective *theory* of QCD. It is therefore reasonable to expect that being a theory, the more judiciously organized and the more terms computed, the more accurate the calculation will become. There is of course the question of convergence but applied within appropriate kinematics, the theory should work out better the more one works. This is indeed what is being found in baryon chiral perturbation calculations for which the strategy is fairly well formulated. This is not the case with “nuclear chiral perturbation theory” where no systematic strategy has yet been fully worked out as we will stress below.

will be discussed.

The examples of remarkable success are the $n + p \rightarrow d + \gamma$ at threshold [39] – a classic nuclear physics process – and the inverse $\gamma + d \rightarrow n + p$ [40] – a process relevant to cosmological baryosynthesis. Going beyond the simplest nuclear systems involving two nucleons, the method can be applied to processes that involve n nucleons where $n > 2$, such as for instance the solar “hep” process [41, 42] $^3\text{He} + p \rightarrow ^4\text{He} + e^+ + \nu_e$ which figures in the solar neutrino problem and the axial charge transitions in heavy nuclei (to be discussed later) which provide evidence for BR scaling.

An exhaustive and beautiful review on the subject with a somewhat different emphasis has recently been given by Beane et al [44] where a comprehensive list of references is found.

In addressing nuclear EFT, there are currently two complementary – and *not different* as one might be led to believe – ways of organizing the expansion, one based on Weinberg’s strategy [38] and the other based on Seattle-Pasadena strategy [45]. We will loosely refer to the former as “Weinberg scheme” and to the latter as “KSW (Kaplan-Savage-Wise) scheme.” The Weinberg scheme contains the SNPA/PM (standard nuclear approach/potential model) as a legitimate and essential component of the theory whereas the KSW scheme by-passes it, although the latter can be effectively exploited to justify the former in certain kinematic domains that we are interested in. We will focus on the former as we find it more natural and straightforward from nuclear physicists’ point of view and for the processes we will discuss, sometimes considerably more predictive.

The Weinberg scheme [38, 46] that we will use here is the version that has been formulated by Park et al [47, 48] (this will be referred to hereafter as PKMR) and uses the following basic strategy. It starts by recognizing that the SNPA/PM (e.g., [49, 50]) based on solutions of the Schrödinger equation with the “most realistic” potential available in the market fine-tuned to a large number of experimental data on one and two nucleon systems, captures most accurately the essential physics of, and hence describes, when implemented by many-body forces, the bulk of properties of few-nucleon systems, in some cases (e.g., low-energy scattering) within $\sim 1\%$ accuracy ⁷. We will therefore consider the SNPA/PM results as *input* (e.g., “counter terms”) in lieu of attempting to compute them from first principles. Our aim is *not* to recalculate them from a *more fundamental theory* but to correctly interpret and incorporate them as a legitimate leading term in a systematic expansion of a more fundamental framework [51, 47], namely, an effective theory of QCD. This, we believe, is completely in line with the notion of effective theory,

⁷There is a well-known caveat in carrying out this program in general and in assessing the “accuracy” of approximations in particular for n -body systems with $n > 2$. While there are useful constraints that help in organizing, in Weinberg’s terminology, the “reducible” and “irreducible” terms for two-body systems, this is not usually the case for many-body systems. Together with many-body forces in the potential which are difficult to pin down precisely although numerically small, there can be a variety of organizational ambiguities in classifying “reducible” and “irreducible” contributions, e.g., off-shell effects, that could contaminate the calculations resorting to a variety of approximations one is compelled to make, even though a full consistent field theoretic approach should in principle be free from such ambiguities. This is an issue that will require considerable effort to sort out. We are grateful to Kuniharu Kubodera for stressing this point in the context of the PKMR approach.

e.g., the one à la Wilson. Our key point is that *it is in how to do embed, and how to systematically calculate the quantities that are missing from, the SNPA/PM results into a fundamental theory that EFT has its true power*. Since the standard nuclear physics approach/potential model (SNPA/PM) results are to be inputs to the more fundamental theory, it is clearly more profitable look at the *response functions* to external fields rather than at scattering amplitudes (which the SNPA/PM can address accurately) to make meaningful predictions. Our thesis is that this is where chiral symmetry and its broken mode can play their primary role in nuclear physics, in both quantitatively describing and accurately predicting nuclear phenomena.

3.3 Effective Chiral Lagrangians

For very low-energy processes that we are dealing with, the nucleons can be considered “heavy,” i.e., nonrelativistic while the pions are relativistic. We shall therefore use the heavy-baryon formalism although a relativistic formulation can be made, particularly for the case where the nucleon mass drops as in BR scaling that we will discuss below. The leading-order chiral Lagrangian that consists only of local nucleon and pion fields – with other heavy fields integrated out – takes the form

$$\begin{aligned}\mathcal{L}_0 = & \bar{N} [iv \cdot D + 2ig_A S \cdot \Delta] N - \frac{1}{2} \sum_A C_A (\bar{N} \Gamma_A N)^2 \\ & + f_\pi^2 \text{Tr} (i\Delta^\mu i\Delta_\mu) + \frac{f_\pi^2}{4} \text{Tr}(\chi_+)\end{aligned}\quad (3.1)$$

with

$$\begin{aligned}D_\mu N &= (\partial_\mu + \Gamma_\mu) N, \\ \Gamma_\mu &= \frac{1}{2} [\xi^\dagger, \partial_\mu \xi] - \frac{i}{2} \xi^\dagger \mathcal{R}_\mu \xi - \frac{i}{2} \xi \mathcal{L}_\mu \xi^\dagger, \\ \Delta_\mu &= \frac{1}{2} [\xi^\dagger, \partial_\mu \xi] + \frac{i}{2} \xi^\dagger \mathcal{R}_\mu \xi - \frac{i}{2} \xi \mathcal{L}_\mu \xi^\dagger, \\ \chi_+ &= \xi^\dagger \chi \xi^\dagger + \xi \chi^\dagger \xi\end{aligned}\quad (3.2)$$

where $\mathcal{R}_\mu = \frac{\tau^a}{2} (\mathcal{V}_\mu^a + \mathcal{A}_\nu^a)$ and $\mathcal{L}_\mu = \frac{\tau^a}{2} (\mathcal{V}_\mu^a - \mathcal{A}_\nu^a)$ denote, respectively, the left and right external gauge fields, χ is proportional to the quark mass matrix and if we ignore the small isospin-symmetry breaking, becomes $\chi = m_\pi^2$ in the absence of the external scalar and pseudo-scalar gauge fields, and

$$\xi = \sqrt{\Sigma} = \exp \left(i \frac{\vec{\tau} \cdot \vec{\pi}}{2f_\pi} \right) \quad (3.3)$$

is the chiral field for the Goldstone bosons. The \mathcal{L}_0 is the leading order chiral Lagrangian in the sense that it is leading order in derivatives, in pion mass and in “ $1/M$ ” where M is the free-space nucleon mass. This is a suitable Lagrangian for (chiral) perturbation near the medium-free vacuum described by the so-called “irreducible graphs.” However

for nuclear processes in general, certain “reducible graphs” involve propagators that are infra-red enhanced and require terms higher order in $1/M$, namely, nucleon kinetic energy term. For the KSW approach, the *ab initio* account of this “correction” term is essential. For the PKMR where the reducible graphs are accounted for via Schrödinger equation or Lippman-Schwinger equation, the chiral expansion is all that matters, so this Lagrangian plays a key role.

The second term in (3.1) is the leading four-fermion interaction and contains no derivatives. We will specify the explicit form later. For convenience, we will work in a reference frame in which the four velocity v^μ and the spin operator S^μ are

$$v^\mu = (1, \vec{0}) \quad \text{and} \quad S^\mu = \left(0, \frac{\vec{\sigma}}{2} \right). \quad (3.4)$$

The next-to-leading order Lagrangian including four-fermion contact terms can be written as

$$\begin{aligned} \mathcal{L}_1 = & \bar{N} \left(\frac{v^\mu v^\nu - g^{\mu\nu}}{2m_N} D_\mu D_\nu + \frac{g_A}{m_N} \{S \cdot D, v \cdot D\} + c_1 \text{Tr} \chi_+ + 4 \left(c_2 - \frac{g_A^2}{8m_N} \right) (v \cdot i\Delta) \right. \\ & + 4c_3 i\Delta \cdot i\Delta + \left(2c_4 + \frac{1}{2m_N} \right) [S^\mu, S^\nu] [i\Delta_\nu, i\Delta_\mu] \Big) N \\ & - 4id_1 \bar{N} S \cdot \Delta N \bar{N} N + 2id_2 \epsilon^{abc} \epsilon_{\mu\nu\lambda\delta} v^\mu \Delta^{\nu,a} \bar{N} S^\lambda \tau^b N \bar{N} S^\delta \tau^c N + \dots, \end{aligned} \quad (3.5)$$

where $\epsilon_{0123} = 1$, $\Delta_\mu = \frac{\tau^a}{2} \Delta_\mu^a$. Terms that are not relevant for the present discussion are implied in the ellipses.

3.4 Nucleon-Nucleon Scattering

Although the genuine predictivity of the EFT is in response functions, we start with nucleon-nucleon scattering at very low energies as this issue has been the focus of the recent activity in the field. If the energy scale involved is much less than the pion mass, $m_\pi \sim 140$ MeV, then we might integrate out the pion field and work with an effective theory containing only the nucleon field. We will reinstate the pions later since the PKMR strategy relies on the pion degree of freedom explicitly. Since the pionless theory has interesting aspects on its own that merits study, we will consider this before putting the pion field into the picture.

When the pions are integrated out, the Lagrangian (3.1) further simplifies to

$$\begin{aligned} \mathcal{L} = & N^\dagger \left(i\partial_t + \frac{\vec{\nabla}^2}{2M} \right) N + \dots \\ & - \frac{1}{2} [C^s (N^\dagger N)^2 + C^t (N^\dagger \boldsymbol{\sigma} N)^2 + \dots] \end{aligned} \quad (3.6)$$

where the nucleon kinetic energy term (which is formally higher order from the heavy-baryon chiral counting) is reinstated. With the pion fields removed from the theory, this

Lagrangian has no remnant of chiral symmetry. The nucleon field is just a matter field and does not know anything about the symmetry. This does not mean that the theory is inconsistent with the symmetry of QCD. We shall consider the S-wave channels 1S_0 and 3S_1 (in the notation of $^{2S+1}S_J$). The C coefficients for these channels are related to the C coefficients in (3.6) by

$$C^{(1S_0)} = C^s - 3C^t, \quad C^{(3S_1)} = C^s + C^t. \quad (3.7)$$

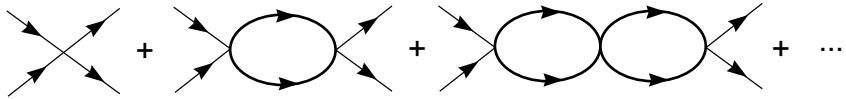


Figure 2: Graphs contributing to the scattering amplitude

The scattering amplitude is \mathcal{A} given by the sum of the Feynman diagrams given in Fig.2:

$$\mathcal{A} = -\frac{C}{1 - C(GG)} \quad (3.8)$$

where C is the four-fermion interaction constant in (3.6) and (GG) is the two-nucleon propagator connecting the two vertices, both written symbolically. In the center-of-mass (CM) frame, this propagator has a linear divergence in dimension $D = 4$ as one can see from a naive dimensional counting of

$$\begin{aligned} (GG) &= -i \int \frac{d^4 q}{(2\pi)^4} \left(\frac{i}{E + q_0 - \mathbf{q}^2/2M + i\epsilon} \right) \left(\frac{i}{-q_0 - \mathbf{q}^2/2M + i\epsilon} \right) \\ &= \int \frac{d^3 q}{(2\pi)^3} \left(\frac{1}{E - \mathbf{q}^2/2M + i\epsilon} \right) \end{aligned} \quad (3.9)$$

with $|\mathbf{k}| = \sqrt{ME}$. To make the integral meaningful, let us put a momentum cutoff at say at $\Lambda/2$. Then (3.9) is given by

$$(GG)_\Lambda = -\frac{M}{4\pi} \left(\frac{\Lambda}{\pi} + i|\mathbf{k}| \right). \quad (3.10)$$

This linear divergence poses no fundamental problem here since the theory is an effective one with the degrees of freedom above a certain cutoff having been integrated out. On the contrary, in the Wilsonian sense, this cutoff dependence has a physical meaning: It delineates the onset of “new physics”. Substituting this into the amplitude formula (3.8), we have

$$\mathcal{A} = \frac{-C}{1 + \frac{CM}{4\pi} \left(\frac{\Lambda}{\pi} + i|\mathbf{k}| \right)}. \quad (3.11)$$

Next, we trade in the theoretical constant C for a physical quantity. To do this, the scattering amplitude (for S wave) is written in terms of the phase shift $\delta \equiv \delta_S$ as

$$\mathcal{A} = \frac{4\pi}{M} \frac{1}{|\mathbf{k}| \cot \delta - i|\mathbf{k}|}. \quad (3.12)$$

Now using the effective range formula

$$|\mathbf{k}| \cot \delta = -\frac{1}{a} + \frac{1}{2} r_0 |\mathbf{k}|^2 + \mathcal{O}(|\mathbf{k}|^4) \quad (3.13)$$

where a is the scattering length and r_0 the effective range, we have, to the lowest order in momentum,

$$\mathcal{A} = -\frac{4\pi}{M} \frac{1}{1/a + i|\mathbf{k}|}. \quad (3.14)$$

So from (3.11) and (3.14), we find

$$C(\Lambda) = \frac{4\pi}{M} \left(\frac{1}{-\frac{\Lambda}{\pi} + 1/a} \right) \quad (3.15)$$

where we have explicated the cutoff dependence of the effective Lagragian which shows how an effective theory carries the “memory” of the degrees of freedom that have been integrated out. Obviously physical observables should not depend upon what value one takes for the cutoff Λ , since the cutoff can be chosen arbitrarily. This is a statement of renormalization group (RG) invariance of the physical quantities, which reads for the amplitude as

$$\Lambda \frac{d\mathcal{A}}{d\Lambda} = 0. \quad (3.16)$$

One can easily verify that (3.15) is the solution of this renormalization group equation (RGE).

In standard field theory calculations in particle physics, one uses dimensional regularization (DR) instead of cutoff. This is because the DR has the advantage that it preserves symmetries, e.g., chiral symmetry in our case, order by order. In the case we are concerned with, with no pions, no symmetry is spolied by the cutoff regularization at least up to the order considered. In general when one does higher order calculations, however, it is not a straightforward matter to preserve chiral symmetry with the cutoff regularization since it requires judicious inclusion of symmetry breaking counter terms so as to restore symmetry. This is why some authors (e.g., the KSW collaboration) prefer using DR. Now what does the above linear divergence mean in DR?

For this we go back to the propagator (GG), Eq.(3.9), and work out the integral using DR:

$$(GG)_\mu = -i \left(\frac{\mu}{2} \right)^{4-D} \int \frac{d^D q}{(2\pi)^4} \left(\frac{i}{E + q_0 - \mathbf{q}^2/2M + i\epsilon} \right) \left(\frac{i}{-q_0 - \mathbf{q}^2/2M + i\epsilon} \right)$$

$$\begin{aligned}
&= \left(\frac{\mu}{2}\right)^{4-D} \int \frac{d^{D-1}q}{(2\pi)^{D-1}} \left(\frac{1}{E - \mathbf{q}^2/2M + i\epsilon} \right) \\
&= -M(-|\mathbf{k}|^2)^{(D-3)/2} \Gamma\left(\frac{3-D}{2}\right) \frac{\left(\frac{\mu}{2}\right)^{4-D}}{(4\pi)^{\frac{D-1}{2}}}
\end{aligned} \tag{3.17}$$

This is regular for $D \neq 3$ but singular for $D = 3$. In renormalizable field theories where power divergences are absent in principle, it is legitimate to simply set $D = 4$, thereby dropping power divergences. But in non-renormalizable theories, one cannot sweep under the rug the singularities that lurk behind the physical dimension. This is because in the Wilsonian renormalization scheme to which our EFT belongs, there are no true singularities and as mentioned, the power divergence structure instead carries physical information. As mentioned, the situation here is quite analogous to the quadratic divergence that needs to be included in hidden local symmetry (HLS) theory discussed above⁸. The physics behind may be the same. In fact, this must be a generic feature of all effective field theories of the sort we are dealing with here, that is, the theories that have fixed points nearby. To do a correct regularization with DR in the present case, the linear power divergence – the only power divergence there is in this theory at one loop – has to be subtracted. In this sense, the “power divergence subtraction (PDS)” scheme used by KSW is a proper implementation of Wilsonian effective field theory in nucleon-nucleon scattering, the unnatural length scale associated with the large scattering length signaling the presence nearby of an infrared fixed point and conformal invariance.

Subtracting the linear divergence, we have the power-divergence-subtracted (PDS) propagator

$$(GG)_\mu^{PDS} = (GG)_\mu - \frac{M\mu}{4\pi(D-3)} = -\frac{M}{4\pi}(\mu + i|\mathbf{k}|). \tag{3.18}$$

Comparing with (3.10), we see that the scale parameter μ in DR is equal to the cutoff Λ/π .

As noted by [52], the large scattering length for the S -wave scattering, i.e., $a^{(1S_0)} = -23.714\text{fm} \sim (1/(8\text{ MeV}))$ reflects that nature is close to a fixed point and conformal invariance. This is seen in (3.15) in the limit $1/a \rightarrow 0$:

$$\Lambda \frac{d}{d\Lambda}(\Lambda C)|_{1/a \rightarrow 0} = 0. \tag{3.19}$$

In view of the length scale involved, $a \rightarrow \infty$ is close to nature, signaling a quasi-bound state. Note that the linear divergence subtraction plays a crucial role here, a feature analogous to the conformal invariance of hidden local symmetry (HLS) theory at chiral restoration with the quadratic divergence playing a crucial role [12].

The discussion made up to this point is general, clarifying the essential feature of effective field theories in two-body nuclear systems. The KSW approach has been

⁸Taking into account the power divergence (i.e., quadratic divergence) in HLS is crucial in arriving at the vector manifestation of chiral symmetry of Harada and Yamawaki [12] discussed in Section 4 and also in Section 11.2.

developed further, including pions as perturbation [44]. As we will show below, the PKMR strategy, while faithful to the EFT strategy, departs from this point in that the rigorous counting rule is sacrificed *somewhat* in favor of predictivity.

3.5 The PKMR Approach: *More Effective EFT*

The faithful adherence to the counting rule has the short-coming in that while postdictions are feasible provided enough experimental information is available, it is hard if not impossible to make accurate predictions. The reason is that as one goes to higher orders to achieve accuracy, one encounters increasing number of counter terms that remain as unknown parameters and these parameters can at best be fixed by the *very process* one would like to predict. This is just a fitting, and not a prediction. Thus instead of adhering strictly to the counting rule that requires by-passing wave functions, we shall develop a scheme along the line originally proposed by Weinberg that would allow us to exploit the wave functions that are “accurately” determined from the standard nuclear physics/PM procedure.

The key observation that we will exploit is the following. All nuclear processes involve two sorts of graphs: “reducible” and “irreducible.” In the case of two-body systems, they will be two-particle reducible and two-particle irreducible (2PI). Instead of summing the two classes of graphs order-by-order in strict accordance with a given counting scheme as in KSW, one computes irreducible graphs to a given order in chiral perturbation theory (χ PT) and then account for reducible graphs by solving Schrödinger equation or Lippman-Schwinger equation with the irreducible vertex injected into the equation. This procedure accords to potentials and wave functions a special role as in the standard nuclear physics calculations. What we hope to do is then to combine the accuracy of the standard nuclear physics/potential model approach with the power of χ PT. We might call this *more effective* effective field theory (MEEFT). The advantage of working with wavefunctions is that one can make *predictions* in nuclear electro-weak response functions that are difficult to make in an order-by-order calculation because of un-fixed counter terms. The disadvantage is of course that one is forced to sacrifice the strict adherence to a counting rule. It turns out however that in the processes so far studied with controlled approximations, this sacrifice is minor numerically. A clear explanation as to how this comes about in two-body systems was given by Cohen and Phillips [53].

3.5.1 *NN scattering*

To justify the method that we will apply to response functions, we first discuss how the method works out in nucleon-nucleon scattering which is well understood in various different ways, field theoretical or non-field theoretical. Compared with the KSW approach, the present scheme is a bit less elegant but the point of our exercise is to show that it can be at least as accurate as the KSW scheme [53].

For simplicity consider proton-neutron scattering in the 1S_0 channel ⁹. Since we

⁹The proton-proton interaction as in the solar proton fusion process requires the Coulomb interaction

are to account for the reducible graphs by Lippman-Schwinger equation, we only need to compute the potential as the sum of irreducible graphs to a certain chiral order in the Weinberg counting. For this we can work directly with the heavy-baryon chiral Lagrangian (3.1) with the pion exchange put on the same footing as the contact four-fermion interaction. The potential calculated to the next-to-leading order (NLO) is of the form

$$\mathcal{V}(\mathbf{q}) = -\tau_1 \cdot \tau_2 \frac{g_A^2}{4f_\pi^2} \frac{\sigma_1 \cdot \mathbf{q} \sigma_2 \cdot \mathbf{q}}{\mathbf{q}^2 + m_\pi^2} + \frac{4\pi}{M} [C_0 + (C_2 \delta^{ij} + D_2 \sigma^{ij}) q^i q^j] + \dots \quad (3.20)$$

with

$$\sigma^{ij} = \frac{3}{\sqrt{8}} \left(\frac{\sigma_1^i \sigma_2^j + \sigma_1^j \sigma_2^i}{2} - \frac{\delta^{ij}}{3} \sigma_1 \cdot \sigma_2 \right), \quad (3.21)$$

where \mathbf{q} is the momentum transferred. The C_2 and D_2 terms containing quadratic derivatives are NLO contributions that are added to (3.6) since we will work to that order. There are one-loop corrections involving two-pion exchange that appear at the NLO and that can be taken into account but as shown by Hyun, Park and Min [54], in the kinematic regime we are considering here, they are not important for the key point we want to discuss here. As it stands, the potential (3.20) is not regularized, so it has to be regularized just as the Feynman propagator (GG), Eq.(3.9), had to be. One can do this in various different ways; they should all give the same result. A particularly convenient one for solving differential equations in coordinate space is to take the following form when one goes to coordinate space

$$V(\mathbf{r}) \equiv \int \frac{d^3 \mathbf{q}}{(2\pi)^3} e^{i\mathbf{q} \cdot \mathbf{r}} S_\Lambda(\mathbf{q}^2) \mathcal{V}(\mathbf{q}), \quad (3.22)$$

with a smooth regulator $S_\Lambda(\mathbf{q}^2)$ with a cutoff Λ . For our purpose it is convenient to take the Gaussian regulator,

$$S_\Lambda(\mathbf{q}^2) = \exp \left(-\frac{\mathbf{q}^2}{\Lambda^2} \right). \quad (3.23)$$

In the PKMR formalism, pions play a special role due to what is called “chiral filter mechanism” (to be defined below) but we can illustrate our essential point without the pions, so let us drop the pion exchange term for the moment. Given the Fourier-transformed potential properly regulated as mentioned, the Lippman-Schwinger equation for the S -wave can be solved in a standard way. The resulting wave function can be explicitly written down:

$$\begin{aligned} \psi(\mathbf{r}) = & \varphi(\mathbf{r}) + \frac{S(\frac{ME}{\Lambda^2}) C_E}{1 - \Gamma_E C_E} \left[1 - \frac{\sqrt{Z} C_2}{C_E} (\nabla^2 + ME) \right. \\ & \left. - \frac{\sqrt{Z} D_2}{C_E} \frac{S_{12}(\hat{r})}{\sqrt{8}} r \frac{\partial}{\partial r} \frac{1}{r} \frac{\partial}{\partial r} \right] \tilde{\Gamma}_\Lambda(\mathbf{r}) \end{aligned} \quad (3.24)$$

in addition to the QCD interaction. Although technically delicate, this part is known, so we will not go into the detail. We shall also restrict to the 1S_0 channel. The 3S_1 channel is slightly complicated because of the coupling to the D -wave but involves no new ingredient.

where φ is the free wave function and

$$\Gamma_E = 4\pi \int \frac{d^3\mathbf{p}}{(2\pi)^3} \frac{S_\Lambda^2(\mathbf{p})}{ME - \mathbf{p}^2 + i0^+}, \quad (3.25)$$

$$\tilde{\Gamma}_\Lambda(\mathbf{r}) = 4\pi \int \frac{d^3\mathbf{p}}{(2\pi)^3} \frac{S_\Lambda(\mathbf{p})}{ME - \mathbf{p}^2 + i0^+} e^{i\mathbf{p}\cdot\mathbf{r}}, \quad (3.26)$$

$$Z = (1 - C_2 I_2)^{-2}, \quad (3.27)$$

$$C_E = a_\Lambda \left(1 + \frac{1}{2} a_\Lambda r_\Lambda ME \right) + (\sqrt{Z} D_2 ME)^2 \Gamma_E, \quad (3.28)$$

with

$$a_\Lambda \equiv Z \left[C_0 + (C_2^2 + \delta_{S,1} D_2^2) I_4 \right], \quad (3.29)$$

$$r_\Lambda \equiv \frac{2Z}{a_\Lambda^2} \left[2C_2 - (C_2^2 - \delta_{S,1} D_2^2) I_2 \right] \quad (3.30)$$

where I_n ($n = 2, 4$) are defined by

$$I_n \equiv -\frac{\Lambda^{n+1}}{\pi} \int_{-\infty}^{\infty} dx x^n S^2(x^2). \quad (3.31)$$

The phase shift can be calculated by looking at the large- r behavior of the wavefunction,

$$p \cot \delta = \frac{1}{S^2(\frac{ME}{\Lambda^2})} \left[I_\Lambda(E) - \frac{1 - \eta^2(E)}{a_\Lambda(1 + \frac{1}{2} a_\Lambda r_\Lambda ME)} \right], \quad (3.32)$$

where the $\eta(E)$ is the D/S ratio, which vanishes for the 1S_0 channel and $I_\Lambda(E) = \Gamma_E + i\sqrt{ME}S^2(ME/\Lambda^2) \equiv \Lambda I(\frac{ME}{\Lambda^2})$. The expression for the phase shift contains a lot more than what was considered above even at LO since the wavefunction is computed to all orders in the potential and we are using a Gaussian cutoff. As such it is not obvious that the renormalization group invariance, i.e., the Λ independence, is preserved. This may appear to be a shortcoming of the approach and would constitute a defect if the Λ dependence were non-negligible.

Let us see how this works out with the present pionless example. As before, we use the effective range formula (3.13) to fix the coefficients $C_{0,2}$. We have

$$\frac{1}{a_\Lambda} = \frac{1}{a} + \Lambda I(0) = \frac{1}{a} - \frac{\Lambda}{\sqrt{\pi}}, \quad (3.33)$$

$$r_\Lambda = r_e - \frac{2I'(0)}{\Lambda} - \frac{4S'(0)}{a\Lambda^2} = r_e - \frac{4}{\sqrt{\pi}\Lambda} + \frac{2}{a\Lambda^2}. \quad (3.34)$$

At threshold, it can be easily verified that the renormalization-group (RG) invariant form for C_0 , (3.15), is recovered. What happens away from the threshold is less trivial. For illustration we take the CM momentum $p = 68.5$ MeV corresponding to $\sim m_\pi/2$. The result for the 1S_0 channel is given in Fig.3; here the phase shift δ (in degree) is plotted vs.

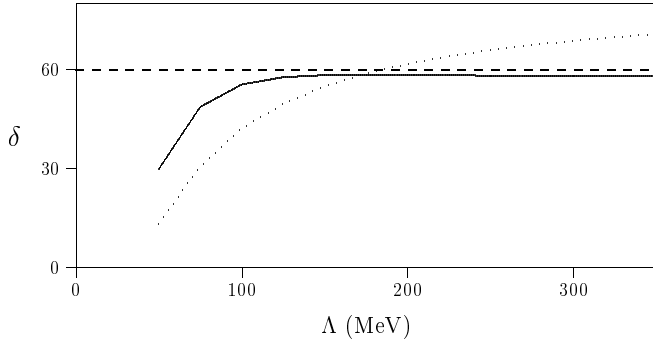


Figure 3: Cutoff dependence/independence in pionless theory: $np\ 1S_0$ phase shift (degrees) vs. the cut-off Λ for a fixed CM momentum $p = 68.5$ MeV. The solid curve represents the NLO result, the dotted curve the LO result and the horizontal dashed line represents the experimental value.

Λ . We learn from this exercise that within the present scheme it is clearly inconsistent with the renormalization group invariance if the potential is calculated only up to LO. It is at NLO and $\Lambda \gtrsim m_\pi$ that the cutoff independence is recovered. We see that $\Lambda \sim m_\pi$ is the scale at which a “new degree of freedom” enters into the pionless theory, an obvious but important fact.

Next we incorporate pions. Once pions are included, the cutoff should be put above m_π . Furthermore the pion presence should reduce the Λ dependence – if any – for given CM momenta. This feature is seen in Fig.4. We see clearly that the pion presence improves markedly the ability to describe scattering. The interplay between the probe momentum, the pion presence, the cutoff and the chiral order becomes transparent: The more refined the potential and the higher the chiral order, the more consistent and more accurate becomes the prediction. This will be the key point of our next consideration when we look at response functions.

3.5.2 Electroweak response functions: Accurate postdictions and predictions

We now turn to our principal assertion that it is in calculating nuclear response functions to the electroweak (EW) external fields that the PKMR approach has its power. We will first discuss two-body systems and then make predictions for n -body systems with $n \geq 2$. In doing this, we will put pions to start with since we will exploit what is known as “chiral filter mechanism” first introduced in [51] and elaborated further in [48]. The chiral filter mechanism which has been verified in χ PT states that whenever allowed by symmetry and kinematics, one-soft-pion exchange in the electroweak currents dominates, with the corrections to which are in principle controllable by χ PT and, conversely, whenever forbidden by symmetry or suppressed by kinematics, the corrections to the leading order current are uncontrolled by chiral expansion and require going beyond standard low-order χ PT. We will refer to these two phenomena as “two sides of the same coin.” In this formalism, therefore, pions play a prominent role. At a momentum scale $p \ll m_\pi$,

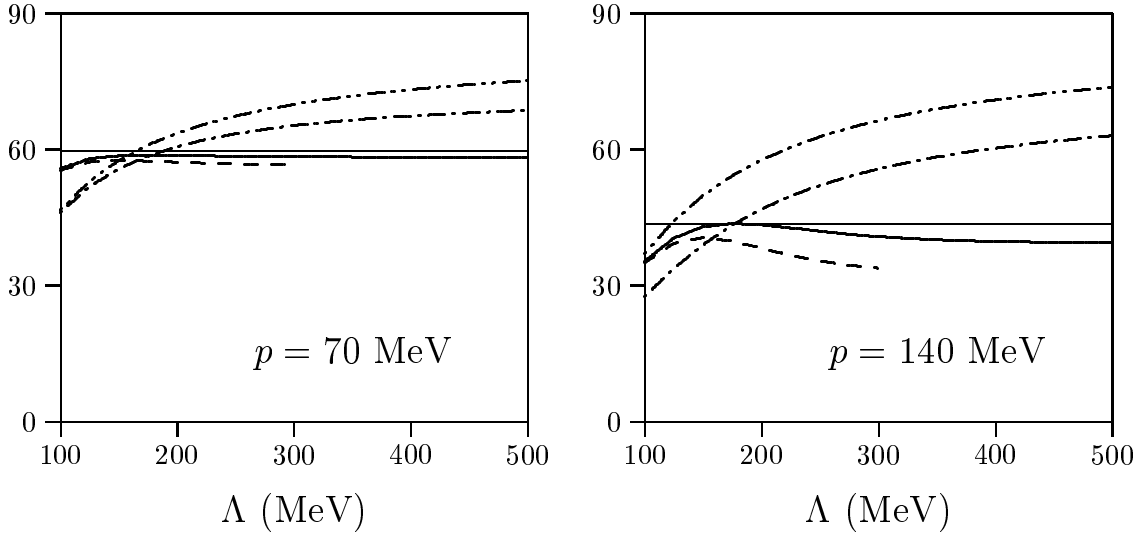


Figure 4: The $np\ 1S_0$ phase shift (degrees) vs. the cutoff Λ for fixed CM momenta $p = 70$ MeV (left) and $p = 140$ MeV (right). The next-to-leading order (NLO) results are given by the solid (with pions) and dashed (without pions) curves, and the leading-order (LO) results by the dot-dashed (with pion) and dot-dot-dashed (without pion) curves. The horizontal line represents the experimental data obtained from the Nijmegen multi-energy analysis. The NLO result without pions is drawn only up to $\Lambda \gtrsim 300$ MeV, above which the theory becomes meaningless, that is, unnatural as well as inconsistent.

one can work with a pionless EFT as described in [44] in which the role of the chiral filter would of course be moot. However in this case, one loses the predictive power since one would be left with one or more counter terms that are left undetermined by theory or experiments. The PKMR strategy circumvents this difficulty.

The PKMR strategy is quite simple. We take the most sophisticated wavefunctions from the SNP (standard nuclear physics)/PM (potential model) approach with the potential fit to an ensemble of empirical data on two-body systems and compute the EW currents using the chiral Lagrangian (3.1) to as high an order as possible in the chiral counting. Such realistic potentials – which have been extensively studied and confirmed empirically – can then be interpreted as resulting from high-order χ PT calculations. For two-body systems, we use as the input the most “sophisticated” potential available in the literature, i.e., the Argonne $v18$ potential – and the resulting wavefunctions [50]. For making predictions in n -body systems with $n > 2$, we rely on Ref.[49]. The power of these wavefunctions in confronting few-body nuclei is well documented in the literature. In all cases, the scattering and static properties of the nuclei involved are extremely accurately given and more or less justified within χ PT whenever many-body corrections are unimportant. Whenever many-body corrections are important, on the other hand, they can in turn be calculated by χ PT as we shall show using the chiral filter argument. In all cases studied up to date, it is possible to make error estimates by assessing the deviation from the RG invariance, that is, the Λ dependence.

Before calculating the full amplitudes to confront nature, we first verify that using

the “realistic wavefunction” is *indeed* consistent with actually calculating the wavefunctions systematically in the chiral counting starting with (3.1) or (3.6). For this purpose, it suffices to look at the *single-particle* $M1$ matrix elements for the process

$$n + p \rightarrow d + \gamma \quad (3.35)$$

and the *single-particle* Gamow-Teller matrix element in the solar proton fusion process

$$p + p \rightarrow d + e^+ + \nu_e \quad (3.36)$$

and verify that there is a matching between a bona-fide EFT and the hybrid scheme we are using. We are interested ¹⁰ in $\mathcal{E}(M1)$ and $\mathcal{E}(GT)$ defined by

$$\mathcal{E}(M1) \equiv \frac{\mathcal{M}_{M1}^{\text{th}} - \mathcal{M}_{M1}^{v18}}{\mathcal{M}_{M1}^{v18}}, \quad \mathcal{E}(GT) \equiv \frac{\mathcal{M}_{GT}^{\text{th}} - \mathcal{M}_{GT}^{v18}}{\mathcal{M}_{GT}^{v18}}, \quad (3.37)$$

where $\mathcal{M}_{M1}^{\text{th}}$ and \mathcal{M}_{M1}^{v18} denote, respectively, the *single-particle* $M1$ transition matrix element of our NLO calculation considered above for the np scattering and that of the Argonne potential, and similarly for $\mathcal{E}(GT)$. Here we are taking the Argonne potential as the most accurate and closest to “experiment.” In Fig.5 are plotted the deviations from the Argonne result as a function of the cutoff. We see that as in the case of the phase shift for $p \sim m_\pi$, the inclusion of the pion degree of freedom markedly reduces the cutoff dependence, in conformity with the stated requirement for a viable effective theory.

Leaving the details to the literature [48, 39], we merely summarize a few concrete results, both postdictions and predictions, of full calculations to NLO or NNLO including pions. Some technical details including precise definitions of the quantities involved can be found in the next subsection immediately following this where we address the question of “hard-core correlations” invoked extensively in standard calculations dealing with short-distance nuclear interactions.

- *POSTDICTION*

The most celebrated case of postdiction is the thermal np capture process (3.35). The unpolarized cross section is dominated by the $M1$ operator – defined below – that is protected by the “chiral filter” and has been calculated in the PKMR approach with the Argonne $v18$ to the accuracy of $\sim 1\%$ [39],

$$\sigma_{th} = 334 \pm 3 \text{ mb} \quad (3.38)$$

to be compared with the experimental value $\sigma_{exp} = 334.2 \pm 0.5 \text{ mb}$. The error bar on the theoretical value represents the range of uncertainty in the short-distance physics unaccounted for in the NNLO chiral perturbation series that is reflected in the cutoff dependence. Here the correction to the single-particle $M1$ matrix element is dominated by the soft-pion contribution with the remaining corrections

¹⁰These are of course not the whole story since there are two-body corrections known as “meson-exchange currents” that we will consider shortly.

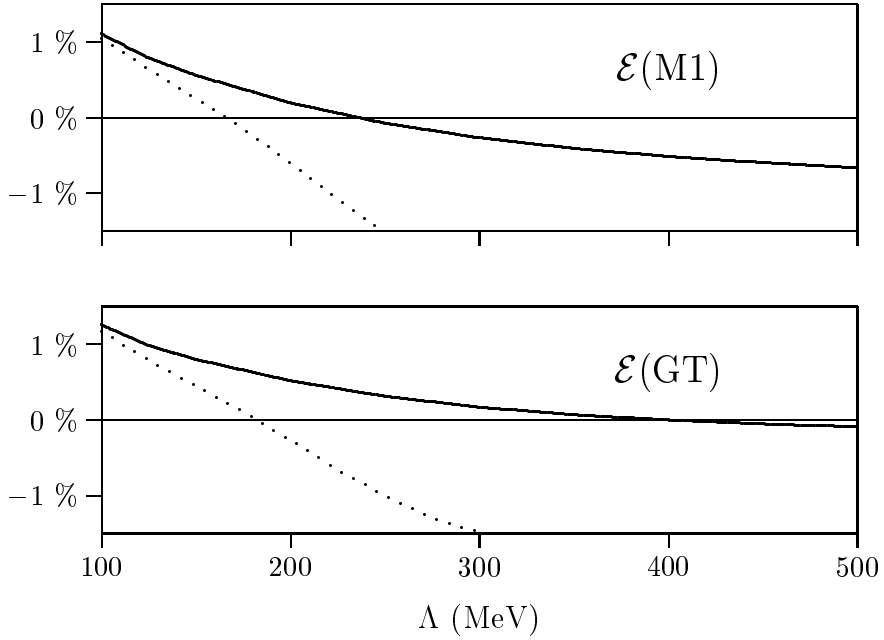


Figure 5: $\mathcal{E}(M1)$ (upper) and $\mathcal{E}(GT)$ (lower) vs. the cutoff Λ . The solid curves represent the NLO results with pions and the dotted curves without pions. When pions are included, the physically relevant cutoff must lie between the pion mass m_π and the lowest resonance, say, $m_\sigma \sim 450$ MeV.

amounting to less than 10% of the *unsuppressed* soft-pion term in conformity with the chiral filter argument. Since this calculation has *no free parameters*, it is actually a prediction whereas the KSW calculation without pions has one unknown counter term as the leading correction term [55] ¹¹. The upshot of the χ PT result à la PKMR is that it confirms the result of Riska and Brown [5] *and in addition* supplies the corrections to their result with an error estimate, which is the ultimate power of the approach as far as postdictions are concerned. Now having explained accurately the threshold np capture, one can then proceed to make predictions for the inverse process $d + \gamma \rightarrow n + p$ for which cross section data are available as well as for the process $e+d \rightarrow n+p+e$ as a function of momentum transfer. A good agreement with experiments is obtained [56] for the photodisintegration of the deuteron $d+\gamma \rightarrow n+p$. Remarkably the simple theory seems to work also for the latter to a momentum transfer much greater than justified by the cutoff involved [6].

• PREDICTIONS

To bring our point home, we cite a few cases of predictions that precede experiments. For these predictions, the χ PT Lagrangian (3.1) is used for calculating the

¹¹In order to explain the experimental value in this calculation, the counter term turns out to require to be considerably bigger in magnitude than, and to have a sign opposite to that of, the soft-pion correction of [39]. This seems to imply that the counter term that appears in this pionless theory describes a different physics than the chiral-filter protected mechanism.

irreducible graphs entering in the electroweak currents.

1. While the unpolarized cross section for the np capture process is dominated by the isovector $M1$ operator that is protected by the chiral filter mechanism, the process

$$\vec{n} + \vec{p} \rightarrow d + \gamma \quad (3.39)$$

with polarized neutron and proton can provide information of the suppressed isoscalar $M1$ and $E2$ matrix elements. The isoscalar $M1$ matrix element turns out to be particularly interesting because a precise calculation of this matrix element requires implementing “hard-core correlations” of standard nuclear physics in terms of regularization in field theory. Although the understanding is still poor, the issue presents a first indication of how the short-distance prescription encoded in the hard core may be understood in a more systematic way.

As noted more precisely below, the matrix elements involved are suppressed by three orders of magnitude with respect to the isovector $M1$ matrix element – due to the fact that these are unprotected by the chiral filter mechanism, so cannot be “seen” directly in the cross section but can be singled out by polarization and anisotropy measurements. The ratios with respect to the isovector $M1$ are predicted to be

$$\mathcal{R}_{M1} = (-0.49 \pm 0.01) \times 10^{-3}, \quad \mathcal{R}_{E2} = (0.24 \pm 0.01) \times 10^{-3}. \quad (3.40)$$

There are no data available at the moment; in this sense these are true predictions. The error bars represent the possible uncertainty in the cutoff dependence, indicating the uncertainty in the short-distance physics. We should mention that the identical results were obtained in the KSW scheme, with however, somewhat bigger error estimates [44].

2. The next prediction is on the proton fusion process (3.36). Here the dominant matrix element involved, i.e., Gamow-Teller, is unprotected by the chiral filter but it turns out that the single-particle matrix element which can be precisely calculated in the standard nuclear physics/PM approach dominates with only small correction terms although the latter are not accurately and systematically controlled by low-order χ PT. The uncertainty in the correction terms is manifested in the error bar that we quote in the result. The quantity that carries information on nuclear dynamics is the astrophysical S factor, $S_{pp} = \sigma(E)EE^{2\pi\eta}$ where σ is the cross section for the process (3.36) and $\eta = M\alpha/(2p)$. The prediction is [57]

$$S_{pp}(0) = (4.05 \times 10^{-25})(1 \pm 0.0015 \pm 0.0048)^2 \text{ MeV barn} \quad (3.41)$$

where the first error is due to the uncertainty in the one-body matrix element and the second due to the uncertainty in the two-body matrix element that

is truncated at the NLO. Since the major contribution is given by the single-particle term that is accurately described by the standard nuclear physics/PM theory, it is in the error estimate that the EFT has its value here.

In the solar neutrino problem, the S factor is an input as a Standard Model property. This means that the measurement of the solar neutrino flux cannot be used to check this prediction. The import of this χ PT calculation is to supply as accurate an S factor as possible.

3. So far we have been concerned with two-nucleon systems that can be equally well treated by both the Kaplan-Savage-Wise (KSW) approach and the Park-Kubodera-Min-Rho (PKMR) approach. We now turn to a case where the PKMR can make a possible prediction [41, 42] whereas a strict adherence to the counting rule would frustrate the feat due to too many unknown parameters. This is the solar “hep” problem



This process produces neutrinos of the maximum energy $E_\nu \approx 19.8$ MeV; for this lepton momentum, not only the S wave but also the P wave need to be taken into account. Computing the neutrino flux as needed for the solar neutrino problem requires both vector and axial-vector matrix elements. While the vector matrix element involves no subtleties – and hence is straightforwardly calculated (including two-body currents), the principal matrix element of the axial-vector current turns out to be extremely intricate. Since the P wave enters non-negligibly, the time component of the axial current cannot be ignored. However this part of the current is under theoretical control since the axial charge operator is chiral-filter protected [51, 47]: the corrections to the known single-particle axial-charge matrix element are dominated by one-soft-pion-exchange two-body matrix elements (with three-body operators absent to the order considered) and are accurately calculable, given “accurate” wave functions that we suppose are available in the literature. The principal difficulty is in the matrix element of the space component of the axial current, the most important of which is the Gamow-Teller operator. Three-body contributions are higher-order than those coming from one-body and two-body terms and can be ignored. Normally the matrix element of the single-particle Gamow-Teller operator $g_A \sum_i \tau^\pm(i) \sigma^a(i)$ is of order 1 if the symmetries of the initial and final nuclear states are normal since the operator just flips spin and isospin. However in the “hep” case, the dominant components of the initial state $|p^3\text{He}\rangle$ and the final state $|{}^4\text{He}\rangle$ have different spatial symmetries so the overlap is largely suppressed. One finds, numerically, that to the chiral order that is free of unknown parameters (e.g., next-to-next-to leading order, NNLO, or $\mathcal{O}(Q^3)$), the single-particle GT matrix element comes out to be ~ -0.4 in unit of g_A . The suppression factor is 2 or 3 relative to the normal matrix element. Now main corrections to the one-body Gamow-Teller are expected to be

from two-body terms. However these corrections are chiral-filter-unprotected as we have explained and hence cannot in general be calculated accurately in chiral perturbation theory unlike the corrections to the single-particle axial charge matrix elements. To make the situation even worse, the two-body corrections come with a sign opposite to the single-particle one with a size comparable to the main term, typically $\sim +0.2$, thus leading to a significant further suppression. This shows why it is *essential* to be able to calculate in a controlled fashion higher chiral order corrections to the GT matrix element.

Such a calculation looks infeasible at first sight. Fortunately it turns out that the calculation of this chiral-filter-unprotected term parallels closely the calculation of the suppressed isoscalar $M1$ and $E2$ matrix elements in the polarized np capture mentioned above, thereby enabling the PKMR approach to pin down the most problematic part of the “hep” process within a narrow range of uncertainty dictated by the range of the cutoff involved. Since the S factor needed for the solar neutrino “hep” process requires (many) other terms (that are calculable without any serious difficulties), we feel it is not meaningful in the context of this article to quote specific numbers. We refer to the literature [41, 42] for details. Here we merely stress that within the PKMR scheme, such a calculation is indeed feasible, parameter-free to next-to-next-to-leading order (NNLO or $\mathcal{O}(Q^3)$) in chiral perturbation theory. As explained below, this comes about thanks to a renormalization-cutoff interpretation of what is known in nuclear physics as “hard-core correlation.” A similar calculation in a standard nuclear physics approach based on the traditional treatment of exchange currents [4] has been performed by Marcucci et al [43]. This approach uses the same accurate wave functions as in PKMR, without however resorting to a systematic chiral counting. The results turn out to be similar hinting that the standard approach of [43] may well be consistent with the EFT approach to the order considered.

3.5.3 The chiral filter: Two sides of the same coin

While the processes protected by the chiral filter, such as the $M1$ operator and the axial charge operator [51], are accurately calculable since one-soft-pion exchange dominates with correction terms usually suppressed by an order of magnitude relative to the dominant soft-pion exchange, the situation is not the same for those processes that have no chiral-filter protection. Even so, the PKMR approach can still make a meaningful statement on such processes. That is the story of the other side of the same coin.

If the chiral filter does not apply, then the role of the pion is considerably diminished and, compounded with higher order effects, clean and reliable low-order calculations will no longer be feasible. A prime example of this situation is the process $p + p \rightarrow p + p + \pi^0$. Here one-soft-pion exchange is suppressed by symmetry and a variety of correction terms of comparable importance compete in such a way that no simple χ PT description can be obtained. Both the PKMR and the KSW are unsuccessful for this process.

The proton fusion process (3.36) presents a different situation at least in the PKMR approach [57]. Since the process is essentially dominated by the Gamow-Teller operator with no accidental suppression, the single particle matrix element in the standard nuclear physics (SNP)/potential model (PM) approach simply dominates. On the other hand, since one is dealing with low-energy (or momentum) probes with the relevant scale much less than the pion mass, one may simply integrate out the pion and work with a pionless effective Lagrangian as in [58]. However the price to pay here is to face higher-order counter terms. We learn from the chiral filter that these corrections cannot be computed in a low-order expansion. This is because those terms reflect the physics of a distance scale shorter than that that can be captured in a few perturbative expansion. While in the PKMR approach, the counter terms of high order that are required are numerically small compared with the leading single-particle term given in the SNP/PM approach, with no help of the chiral filter, there is nothing that says that subleading corrections are necessarily small compared with the leading-order correction that one may be able to calculate. For example in high-order KSW calculations in the “pionless EFT” for the proton fusion (see [58]), the corrections occur at fifth order. Now even if the counter terms that appear at that order are – eventually – fixed by the inverse neutrino processes that may be measurable in the laboratories, the error incurred in this fifth order calculation will not be any smaller than what the PKMR approach can obtain at a lower order.

3.5.4 An interpretation of hard-core correlation in an effective field theory

The isoscalar matrix elements of the polarized neutron and proton capture process (3.39),

$$\vec{n} + \vec{p} \rightarrow d + \gamma \quad (3.43)$$

are *not* chiral-filter-protected. Nonetheless it was possible to make the predictions (3.40). How this comes about is interesting from the point of view of learning something about short-range correlations in nuclei. We elaborate on this point in the rest of this section.

At threshold, the initial nuclear state in (3.43) is in either the ${}^1S_0(T = 1)$ or ${}^3S_1(T = 0)$ channel, where T is the isospin. The process therefore receives contributions from the isovector M1 matrix element (M1V) between the initial ${}^1S_0(T = 1)$ and the final deuteron ($T = 0$) state, along with the isoscalar M1 matrix element (M1S) and the isoscalar E2 (E2S) matrix element between the initial ${}^3S_1(T = 0)$ and the final deuteron ${}^3S_1 - {}^3D_1$ states. Since M1V is by far the largest amplitude, the spin-averaged cross section $\sigma_{unpol}(np \rightarrow d\gamma)$ is totally dominated by M1V. Meanwhile, since the initial 1S_0 state has $J = 0$, the M1V cannot yield spin-dependent effects, whereas M1S and E2S can.

The T matrix for the process can be written as

$$\langle \psi_d, \gamma(\hat{k}, \lambda) | \mathcal{T} | \psi_{np} \rangle = \chi_d^\dagger \mathcal{M}(\hat{k}, \lambda) \chi_{np} \quad (3.44)$$

with

$$\mathcal{M}(\hat{k}, \lambda) = \sqrt{4\pi} \frac{\sqrt{v_n}}{2\sqrt{\omega} A_s} [i(\hat{k} \times \hat{\epsilon}_\lambda^*) \cdot (\boldsymbol{\sigma}_1 - \boldsymbol{\sigma}_2) \text{ M1V}$$

$$-i(\hat{k} \times \hat{\epsilon}_\lambda^*) \cdot (\boldsymbol{\sigma}_1 + \boldsymbol{\sigma}_2) \frac{M1S}{\sqrt{2}} + (\boldsymbol{\sigma}_1 \cdot \hat{k} \boldsymbol{\sigma}_2 \cdot \hat{\epsilon}_\lambda^* + \boldsymbol{\sigma}_2 \cdot \hat{k} \boldsymbol{\sigma}_1 \cdot \hat{\epsilon}_\lambda^*) \frac{E2S}{\sqrt{2}} \Big] \quad (3.45)$$

where v_n is the velocity of the projectile neutron, A_s is the deuteron normalization factor $A_s \simeq 0.8850 \text{ fm}^{-1/2}$, and χ_d (χ_{np}) denotes the spin wave function of the final deuteron (initial np) state. The emitted photon is characterized by the unit momentum vector \hat{k} , the energy ω and the helicity λ , and its polarization vector is denoted by $\hat{\epsilon}_\lambda \equiv \hat{\epsilon}_\lambda(\hat{k})$. The amplitudes, M1V, M1S and E2S, represent the isovector M1, isoscalar M1 and isoscalar E2 contributions, respectively, all of which are real at threshold. These quantities are defined in such a manner that they all have the dimension of length, and the cross section for the unpolarized np system takes the form

$$\sigma_{unpol} = |M1V|^2 + |M1S|^2 + |E2S|^2. \quad (3.46)$$

The isoscalar terms ($|M1S|^2$ and $|E2S|^2$) are strongly suppressed relative to $|M1V|^2$ — approximately by a factor of $\sim O(10^{-6})$ — so the unpolarized cross section is practically unaffected by the isoscalar terms. As mentioned above, the isovector M1 amplitude was calculated [39] very accurately up to $\mathcal{O}(Q^3)$ relative to the single-particle operator. The result expressed in terms of M1V is: $M1V = 5.78 \pm 0.03 \text{ fm}$, which should be compared to the empirical value $\sqrt{\sigma_{unpol}^{exp}} = 5.781 \pm 0.004 \text{ fm}$. Here, we will focus on the isoscalar amplitudes.

Now the isoscalar matrix elements can be isolated by spin-dependent observables, namely by the photon circular polarization $P_\gamma \equiv \frac{I_{+1}(0^\circ) - I_{-1}(0^\circ)}{I_{+1}(0^\circ) + I_{-1}(0^\circ)}$ and the anisotropy $\eta_\gamma \equiv \frac{I(90^\circ) - I(0^\circ)}{I(90^\circ) + I(0^\circ)}$ where $I_\lambda(\theta)$ is the angular distribution of photons with helicity $\lambda = \pm 1$, with θ the angle between \hat{k} (direction of photon emission) and a quantization axis of nucleon polarization ¹². Measurement of P_γ and η_γ can determine the empirical values of the ratios

$$\mathcal{R}_{M1} \equiv \frac{M1S}{M1V}, \quad \mathcal{R}_{E2} \equiv \frac{E2S}{M1V}. \quad (3.47)$$

Both M1S and E2S are suppressed relative to the isovector M1 matrix element (M1V) due to mismatch in symmetries of the wave functions etc. We will however take the single-particle matrix elements of M1S and E2S as the leading order (LO) in chiral counting of the higher order terms in calculating the ratios \mathcal{R}_{M1} and \mathcal{R}_{E2} . Radiative corrections to these leading-order terms come at N^1LO and are calculated easily given

¹²Explicit forms are not needed for our discussion but we write them down for completeness:

$$\begin{aligned} P_\gamma &= |\vec{P}_n| \frac{\sqrt{2}(\mathcal{R}_{M1} - \mathcal{R}_{E2}) + \frac{1}{2}(\mathcal{R}_{M1} + \mathcal{R}_{E2})^2}{1 + \mathcal{R}_{M1}^2 + \mathcal{R}_{E2}^2}, \\ \eta_\gamma &= pP \frac{\mathcal{R}_{M1}^2 + \mathcal{R}_{E2}^2 - 6\mathcal{R}_{M1}\mathcal{R}_{E2}}{4(1 - pP) + (4 + pP)(\mathcal{R}_{M1}^2 + \mathcal{R}_{E2}^2) + 2pP\mathcal{R}_{M1}\mathcal{R}_{E2}} \end{aligned}$$

where $pP \equiv \vec{P}_p \cdot \vec{P}_n$ and \vec{P} is the polarization three-vector.

the wave functions ¹³. Relative to the leading order (LO) terms, corrections will then be classified by N^n NO for $\mathcal{O}(Q^n)$. For the chiral-filter protected M1V, the leading two-body correction appears at N^1 LO and the one-loops and the counter-terms appear at N^3 LO. For the isoscalar current, not protected by the chiral filter, the counting rules are quite different. While the E2S receives only negligible contributions from higher order (N^3 LO and N^4 LO) corrections, the situation with M1S is quite different. The corrections are quite large even though the leading two-body corrections for the M1S turn out to appear in tree order at N^3 LO while the loop corrections come at N^4 LO and are finite.

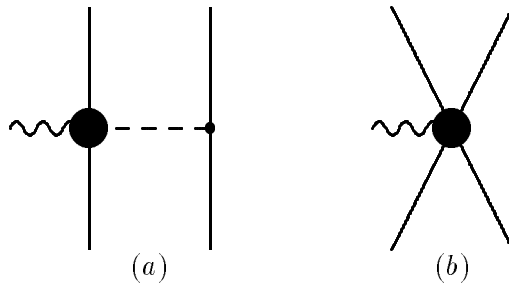


Figure 6: Generalized tree diagrams for the two-body isoscalar current. The solid circles include counter-term insertions and (one-particle irreducible) loop corrections. The wiggly line stands for the external field (current) and the dashed line the pion.

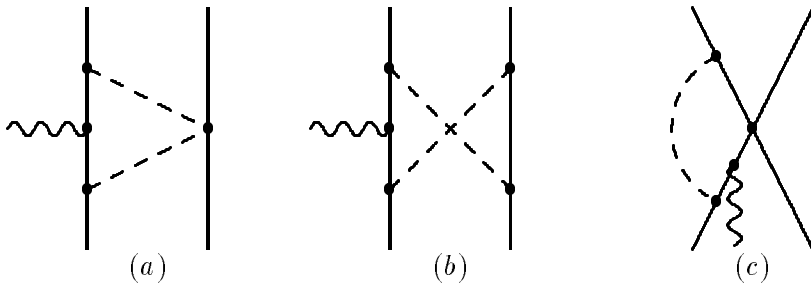


Figure 7: One-loop graphs contributing to the two-body currents. They come at $\mathcal{O}(Q^4)$ and higher orders relative to the LO one-body term. All possible insertions on the external line are understood.

Given that the higher corrections *separately* are quite large as expected from the chiral-filter argument, there is a problem which does not arise in chiral-filter-protected

¹³Although not in the main line of discussion, we quote as an aside the numbers to give an idea of the size we are dealing with. With the realistic Av18 wavefunctions, the numerical results for the sum of the LO and NLO come out to be

$$\begin{aligned} M1S_{1B}(\text{fm}) &= (-4.192 - 0.105) \times 10^{-3} = -4.297 \times 10^{-3}, \\ E2S_{1B}(\text{fm}) &= (1.401 - 0.007) \times 10^{-3} = 1.394 \times 10^{-3}. \end{aligned}$$

processes. It has to do with the zero-range interactions that come as radiative corrections involving the four-Fermi contact interactions (proportional to C_A) in Eq.(3.1) (see Fig.7c) and as four-Fermi counter terms (see Fig.6b). It turns out that there is only one term of the latter type that contributes, i.e., a term in the Lagrangian of the form

$$\Delta\mathcal{L} \sim -ig_4(\partial_\mu\mathcal{B}_\nu - \partial_\nu\mathcal{B}_\mu)\bar{N}[S^\mu, S^\nu]N\bar{N}N \quad (3.48)$$

where \mathcal{B}_μ is the isoscalar external field and g_4 is an undetermined coefficient. When the chiral-filter mechanism is operative, these zero-range interactions appear at higher order and are expected to be suppressed by “naturalness” conditions and more importantly by “hard-core” correlation functions that are incorporated in the wave functions. In the present case, the chiral filter is not effective and hence it is not a good approximation to let hard-correlation functions “kill” the contact interactions. One way to resolve this problem is to exploit the cutoff regularization that was used above in Section 3.4 for NN scattering. Operationally, we can achieve this goal by replacing the delta function in coordinate space attached to zero-range terms by the delta-shell with hard core r_c ,

$$\delta^3(\vec{r}) \rightarrow \frac{\delta(r - r_c)}{4\pi r_c^2}. \quad (3.49)$$

We then have to assure that the *total contribution* we compute be independent of r_c within a reasonable range. This requirement corresponds to the renormalization-group invariance. When the chiral filter mechanism is operative, dropping the zero-range terms is justified since the r_c independence is not spoiled. If this requirement is not satisfied, the effective theory is not reliable and the result cannot be trusted. The present case belongs to this class.

It turns out fortunately that for M1S, there enters only one particular linear combination of four-Fermi terms involving g_4 and C_A ’s and that it is this combination – call it X – that figures in the magnetic moment of the deuteron. Fitting to the deuteron magnetic moment allows the constant X to be uniquely determined for any given value of r_c . The result for the total M1S for wide-ranging values of r_c is given for illustration in Table 1. The remarkable insensitivity to r_c may be taken as a sign of RG invariance and

r_c (fm)	0.01	0.2	0.4	0.6	0.8
M1S	-2.849	-2.850	-2.852	-2.856	-2.861

Table 1: The total contributions to M1S in unit of 10^{-3} fm vs. r_c in fm. Recall the single-particle contribution: $M1S_{1B} \approx -4.30 \times 10^{-3}$ fm.

a support for the procedure. This is more remarkable considering that the series in the chiral order does not appear to be converging. To exhibit this, we quote how each term of N^nLO for $n \geq 3$ contributes to the ratio \mathcal{R}_{M1} in the range of r_c

$$r_c^{min} \equiv 0.01 \text{ fm} \leq r_c \leq r_c^{max} \equiv 0.8 \text{ fm}. \quad (3.50)$$

Expressed in the chiral order and in the range (r_c^{max}, r_c^{min}) , the \mathcal{R}_{M1} comes out to be

$$\begin{aligned}\mathcal{R}_{M1} \times 10^3 &= \text{“LO”} + \text{“N}^3\text{LO”} + \text{“N}^4\text{LO”} + \text{“(N}^3\text{LO + N}^4\text{LO)}_X\text{”} \\ &= -0.74 + (-0.48, -0.74) + (0.23, 0.46) + (0.49, 0.54) \\ &= (-0.50, -0.49)\end{aligned}\tag{3.51}$$

where the contribution that depends on the single parameter X fixed by the deuteron magnetic moment is indicated by the subscript X . This is how the value given in (3.40) has been arrived at. The crucial observation which applies also to the *hep* process discussed above is that the final result cannot be arrived at by any partial sum of the terms. Also note the importance of the X -dependent term. Needless to say, an experimental check of the result obtained here would be highly desirable.

4 “VECTOR MANIFESTATION” OF CHIRAL SYMMETRY

The major problem that we have to face in going to many-body systems is how the structure of the ground state, i.e., “vacuum” is to be described and how the properties of hadronic degrees of freedom get modified in the changed background. This question will be addressed more specifically in the next section in terms of an effective in-medium field theory. Here we address the generic aspects based on symmetries involved in the problem. We will discuss the problem in terms of density but we believe the general argument applies as well to temperature at least up to the chiral restoration point. Possible differences that appear after the critical point will be mentioned in Section 11.

To discuss how the vacuum changes as matter density increases and how the properties of baryonic matter are affected by the vacuum change, we need to first address how chiral symmetry is affected by the medium. While it is generally accepted that chiral symmetry endowed with N_F -flavor massless quarks breaks spontaneously in the (zero-density) vacuum as $SU(N_F)_L \times SU(N_F)_R \rightarrow SU(N_F)_{L+R}$, it is not fully known how the broken symmetry gets restored in medium under extreme conditions, that is, at high temperature and/or at high density. There are several different scenarios with which the broken symmetry can get restored as temperature and/or density are/is dialed. As we will argue, what happens in nuclei and nuclear matter where matter density is non-zero depends rather crucially on what scenario the chiral symmetry restoration adopts.

For concreteness and simplicity, take the two-flavor case with up and down quarks ($N_F = 2$). The argument is the same – except possibly for the order of phase transition – for the case $N_F = 3$ that holds when the strangeness flavor is included.

The “standard scenario” is the σ model one where the broken Nambu-Goldstone mode gets restored to the Wigner-Weyl mode wherein the triplet of pions π^i with $i = \pm, 0$ and the scalar σ (in the chiral limit) merge to an $O(4)$ massless degenerate multiplet at the phase transition. At the phase transition, other hadrons such as nucleons, vector mesons etc. could be either massless or massive as long as they appear in chiral multiplet

structure. Now in zero density, the scalar σ need not be the fourth component of $O(4)$ as in linear σ model. It could for instance be a chiral singlet but what is required is that at the phase transition it joins the pions into the $O(4)$ as described by Weinberg in his “mended symmetry” scenario [59, 60]. One should note that the σ -model scenario is moot on the latter spectra, so, e.g., the vector meson ρ (which will figure importantly in later discussions) could become either lighter or heavier as one approaches the chiral restoration. This model belongs to the $O(4)$ universality class and has been extensively discussed in the literature [61]. At present, it is not inconsistent with lattice measurements with temperature but it is not the only viable scheme either.

There is an alternative scenario to the above standard one recently proposed by Harada and Yamawaki [12] which we believe provides support to the BR scaling to be elaborated below as well as connects with the color-flavor locking scenario of QCD discussed in Section 11.2. The distinguishing feature of Harada-Yamawaki’s “vector manifestation” is that chiral symmetry with two flavors (u and d) is restored by the triplet of pions merging with a triplet of the longitudinal components of vector mesons to the representation $(3, 1) \oplus (1, 3)$. At the chiral point, the vector coupling g_V flows to the fixed point $g_V = 0, a = 1$ corresponding to what Georgi called vector symmetry limit [62] *together with* the pion decay constant f_π going to zero. In this case, the vector ρ will become massless together with other matter fields, i.e., constituent quarks and the vector coupling will vanish, a feature which is an important factor in our discussions to follow.

Limiting ourselves to the two-flavor case (the three-flavor case can be similarly treated), we consider specifically the hidden local symmetry (HLS) theory of Bando et al [63] with the symmetry group $[U(2)_L \times U(2)_R]_{global} \times [U(2)_V]_{local}$ consisting of a triplet of pions, a triplet of ρ -mesons and an ω -meson. Motivated by the observation that in the vacuum, the ρ and ω mesons are nearly degenerate and the quartet symmetry is fairly good phenomenologically, we put them into a $U(2)$ multiplet. In this theory, baryons (proton and neutron) do not appear explicitly. They can be considered as having been integrated out. If needed, they can be recovered as solitons (skyrmions) of the theory.

The relevant degrees of freedom in the HLS theory are the left and right chiral fields denoted by $\xi_{L,R}$,

$$\xi_{L,R} = e^{i\sigma/f} e^{\mp i\pi/f} \quad (4.1)$$

with $\sigma(x) = \sigma^a T^a$ and $\pi = \pi^a T^a$ and the hidden local gauge fields denoted by

$$V_\mu \equiv V_\mu^\alpha T^\alpha = \frac{\tau^a}{2} \rho_\mu^a + \frac{1}{2} \omega_\mu \quad (4.2)$$

with $\text{Tr}(T^\alpha T^\beta) = \frac{1}{2} \delta^{\alpha\beta}$. If we denote the $[U(2)_L \times U(2)_R]_{global} \times [U(2)_V]_{local}$ unitary transformations by (g_L, g_R, h) , then the fields transform $\xi_{L,R} \mapsto h(x) \xi_{L,R} g_{L,R}^\dagger$ and $V_\mu \mapsto h(x) (V_\mu - i\partial_\mu) h^\dagger(x)$. Harada and Yamawaki discuss chiral symmetry restoration driven by large N_F . However their arguments are quite general, so here we shall apply them to high temperature and/or high density although no rigorous proof for the applicability has yet been given in the literature.

Following the reasoning of [64, 65], we take the HLS Lagrangian as an effective Lagrangian that results when high-energy degrees of freedom above the chiral scale Λ taken to be higher than the vector meson mass m_V are integrated out. Now the scale Λ will in general depend on the number of flavors N_F , density n or temperature T depending upon what system is being considered. This is to be taken as a *bare* Lagrangian in the Wilsonian sense with the parameters $g_V(\Lambda)$ which is the hidden gauge coupling constant, $a(\Lambda)$ which signals that chiral $U(2) \times U(2)$ symmetry is spontaneously broken by taking the value $a \neq 1$ and $f_\pi(\Lambda)$ which is the pion decay constant playing the role of order parameter for chiral symmetry with $f_\pi = 0$ signaling the onset of the Wigner-Weyl phase. Reference [65] describes how these parameters can be determined in terms of QCD condensates by matching – à la Wilson – the vector and axial-vector correlators with the ones of QCD at the chiral scale Λ and how by following renormalization group (RG) flows to low energy scales, one can determine low-energy parameters that can be related to those that figure in chiral perturbation theory (for, e.g., $\pi\pi$ scattering). An important observation here is that *independently of how the transition is triggered*, the (assumed) equality at chiral restoration (where $\langle \bar{q}q \rangle = 0$) of the vector and axial-vector correlators, i.e.,

$$\Pi_V|_{\langle \bar{q}q \rangle = 0} = \Pi_A|_{\langle \bar{q}q \rangle = 0} \quad (4.3)$$

where

$$\begin{aligned} i \int d^4x e^{iq \cdot x} \langle 0 | T J_\mu^a(x) J_\nu^b(0) | 0 \rangle &= \delta^{ab} (q_\mu q_\nu - g_{\mu\nu} q^2) \Pi_V(-q^2), \\ i \int d^4x e^{iq \cdot x} \langle 0 | T J_{5\mu}^a(x) J_{5\nu}^b(0) | 0 \rangle &= \delta^{ab} (q_\mu q_\nu - g_{\mu\nu} q^2) \Pi_A(-q^2) \end{aligned} \quad (4.4)$$

implies that the HLS theory approaches the Georgi vector limit, namely, $g_V = 0$ and $a = 1$, in addition to the vanishing of f_π . That chiral symmetry is restored with $f_\pi = 0$ at the Georgi vector limit follows from a proper account of quadratic divergence in the renormalization group flow equation for f_π and a .¹⁴ In terms of baryon density which we shall denote n (reserving ρ for the ρ meson here), we interpret this to imply that at the

¹⁴The quadratic divergence is present when the cutoff regularization is used whereas it is absent at four dimensions $D = 4$ when the dimensional regularization is used. The quadratic divergence present in the cutoff regularization corresponds to a singularity at $D = 2$ in the dimensionally regularized integral from one-loop graphs which comes out to be proportional to the Γ function

$$\sim \Gamma(1 - D/2) = \frac{\Gamma(3 - D/2)}{1 - D/2} - \Gamma(2 - D/3).$$

In a renormalizable theory, this singularity (or any other power divergence) does not figure at $D = 4$ but in an effective (nonrenormalizable) theory like HLS, this singularity present at $D = 2$ – which is absent at $D = 4$ – has to be subtracted. This procedure is quite similar to the subtraction of the singularity at $D = 3$ that was required in the KSW scheme for two-nucleon scattering discussed in Section 3.4 and we suspect that a similar physics is at work here. Note that were it not for this quadratic divergence, the f_π would not run and hence would not go to zero at the point where the Georgi vector limit is reached. Thus the quadratic term plays a crucial role in specifying the symmetry structure of the chiral restoration phase transition.

critical density $n = n_c$, we must have

$$g_V(\Lambda(n_c); n_c) = f_\pi(\Lambda(n_c); n_c) = 0, \quad a(\Lambda(n_c); n_c) = 1 \quad (4.5)$$

where we have indicated the density dependence of the cutoff Λ . The same argument should hold with temperature with T_c replacing n_c .

In HLS theory, the vector mass is given by the Higgs mechanism. In free space, it is of the form

$$m_V \equiv m_\rho = m_\omega = \sqrt{a(m_V)} g_V(m_V) f_\pi(m_V) \quad (4.6)$$

where the cutoff dependence is understood. Here the parameter $a(m_V)$ etc means that it is the value at the scale m_V determined by an RG flow from the *bare* quantity $a(\Lambda)$. Note that (4.6) is similar, but not identical, to the KSRF relation $m_{\rho(KSRF)} = \sqrt{2} g_{\rho\pi\pi} f_\pi(0)$ ¹⁵. Now in medium with $n \neq 0$, this mass formula will remain the same except that it will depend upon density,

$$m_V^* \equiv m_\rho^* = m_\omega^* = \sqrt{a(m_V^*)} g_V(m_V^*) f_\pi(m_V^*). \quad (4.7)$$

The density dependence is indicated by the star. As in the case of N_F discussed in [12], the cutoff Λ will depend upon density, say, Λ^* implicit in (4.7).

The Harada-Yamawaki argument (or theorem) suggests that at $n = n_c$ where $\langle \bar{q}q \rangle = 0$ and hence $\Pi_V^*(n_c) = \Pi_A^*(n_c)$, the Georgi's vector limit $g_V = 0$, $a = 1$ is reached together with $f_\pi = 0$. This means that

$$m_V^*(n_c) = 0. \quad (4.8)$$

¹⁵However numerically they are very close. We explain as a side remark how this comes about. While Eq.(4.6) for $m_V = M_V(Q = m_V)$ is approximate with numerically small corrections of order $g_V^2/(4\pi)^2$ ignored there, the corresponding formula for $Q = 0$, i.e., $M_V^2(0) = a(0)g^2(0)f_\pi^2(0)$ is an exact low-energy theorem [66]. The small corrections arise in going from the off-shell point $Q = 0$ to the on-shell point $Q = m_\rho$. Noting that the KSRF relation is given in terms of the ρ on-shell constant $g_{\rho\pi\pi}$ and the pion on-shell constant $f_\pi(0)$, we first extract the former from HLS Lagrangian given in terms of on-shell quantities:

$$g_{\rho\pi\pi} = \frac{g(m_\rho)}{2} \frac{f_\sigma^2(m_\rho)}{f_\pi^2(0)}$$

where f_σ is the decay constant of the scalar that goes into the longitudinal component of the ρ by Higgs mechanism (which becomes equal to f_π at the Georgi vector limit). The pion decay constant f_π runs with pion loops below the ρ scale but f_σ does not run below m_ρ since the ρ decouples. Using $f_\sigma^2(m_\rho) = a(m_\rho)f_\pi^2(m_\rho)$, we can rewrite the KSRF mass formula as

$$m_{\rho(KSRF)}^2 = M_\rho^2(m_\rho) \frac{a(m_\rho)}{2} \frac{f_\pi^2(m_\rho)}{f_\pi^2(0)}.$$

By the renormalization group equations given by Harada and Yamawaki, we have $a(m_\rho) \simeq 1$ and $\frac{f_\pi^2 m_\rho}{f_\pi^2(0)} \simeq 2$. Thus, we get

$$m_{\rho(KSRF)}^2 \simeq M_\rho(m_\rho) \equiv m_\rho^2.$$

At this point, the quartet scalars will be “de-Higgsed” from the vector mesons and form a degenerate multiplet with the triplet of massless pions (and “ η ”¹⁶) with the massless vectors decoupled. This assures that the vector correlator is equal to the axial-vector correlator in the HLS sector matching with the QCD sector. This is the “vector manifesation” of chiral symmetry. In this scenario, *dictated by the renormalization group equations, the vector meson masses drop as density increases*. Note that this scenario is distinct from the “standard” (as yet to-be-established) picture in which the ρ and a_1 come together as do the pions and a scalar σ . In the standard scenario, there is nothing which forces the vector mesons to become massless and decouple. They can even become more massive at chiral restoration than in the vacuum [67]. Thus the vanishing of the vector-meson mass is a *prima facie* signal for the phase transition in the Harada-Yamawaki picture.

Harada and Yamawaki showed that the chiral restoration in the vector manifestation can occur at some large number of flavors $N_F \gtrsim 4$, as expected in large N_F QCD. Here using the same reasoning, we have arrived at the conclusion that the same vector manifestation can take place at the critical density (or temperature)¹⁷.

The “running” of the parameters g_V , a and f_π implies that away from the critical point, the vector meson masses drop as a function of density as density is increased. In the next section we will discuss the same phenomenon in terms of BR scaling. The scaling that we will encounter below will correspond to (4.7) with $a^*g_V^*/(ag_V) \approx 1$. It will be suggested that this ratio stays more less constant up to near the transition point and drops rapidly afterwards, so the vector meson mass must fall faster than f_π^* .

5 LANDAU FERMI LIQUID FROM CHIRAL LAGRANGIANS

5.1 Fluctuating Around Zero-Density Vacuum

We have developed the thesis that chiral symmetry can be suitably implemented into nuclear problems involving a few nucleons. Furthermore EFT can be formulated in such a way that the traditional nuclear physics approach with realistic potentials (i.e., PM) can be identified as a *legitimate* part of a consistent EFT supplying the leading term in the expansion. This means that what nuclear physicists have been doing up to today – and their highly successful results – can be considered as an essential part of the modern structure of strong interactions based on QCD. For the few-nucleon processes we have been dealing with, e.g., NN scattering, $n + p \leftrightarrow d + \gamma$, solar $p + p \rightarrow d + e^+ + \nu_e$

¹⁶We assume that the fourth pseudoscalar “ η ” gets a mass by $U(1)_A$ anomaly, so can be excluded from our consideration.

¹⁷We must emphasize that this conclusion makes an implicit assumption that the same reasoning applies to temperature and/or density. The analysis of [68] for the N_F -driven phase transition is that the top-down phase transition from $N_F > N_{Fc}$ to $N_F < N_{Fc}$ is neither first-order nor second-order. The order parameter is found to be continuous at the phase transition, so it is not first-order. However the correlation length does not diverge at the phase transition, so it is not second-order either. If correct, this phase transition may appear to be different from that expected in temperature or density.

etc., what enters into the theory is the chiral symmetric Lagrangian determined in free space, that is, at zero density. The starting point there is an effective chiral Lagrangian that describes QCD in the matter-free vacuum, with masses and coupling constants all determined in particle experiments in medium-free space. The few-nucleon problems are then treated by fluctuating around the matter-free vacuum near a “fixed point” (at infinite scattering length) discussed above. The machinery for doing this is the well-established chiral perturbation theory (χ PT) involving baryons. Since the processes involved occur near the fixed point of the theory, one can successfully do the perturbation.

Now how do we go to heavier nuclei, nuclear matter and denser matter which must live at a different fixed point, say, the Fermi-liquid fixed point to be described below which is not necessarily near the above fixed point? This is the principal question that we wish to answer in this review. If there are no phase changes along the way, one may attempt to build many-nucleon systems in a perturbative scheme starting with the free-space Lagrangian mentioned above. Indeed there have been several such attempts in χ PT to reach at nuclear matter [70, 71]. It is not obvious though that this can be done beyond the normal matter density since a strong-coupling expansion is involved and large anomalous dimensions arise. This means that it may be simply too hard if not impossible to handle various phase changes (kaon condensation, chiral restoration, color superconductivity etc.) that are conjectured to occur as one increases density toward chiral restoration as demanded for relativistic heavy-ion processes and for describing compact stars. A different but perhaps more precise way of saying the same thing is in terms of the skyrmion picture for dense matter which is closest to QCD if N_c is taken to be large. In the skyrmion description, a lump of baryonic matter with a given baryon number B is characterized by a “topological vacuum” associated with a conserved winding number B . A system with density $\rho'_B \gg \rho_B$ means that $B' \gg B$ for a given volume. Now the point is that the B' vacuum cannot be connected to the B vacuum by a small perturbation. In what follows, therefore, we shall take a different route and formulate a chiral Lagrangian field theory using a “sliding” vacuum with parameters of the Lagrangian running with matter density. This leads to the notion of Brown-Rho scaling and in-medium effective field theory for a system with Fermi seas, i.e., Landau Fermi-liquid theory.

5.2 Skyrmion vs. Q-Ball

Consider bound many-nucleon systems corresponding to nuclei. If the number of colors can be taken to be very large, then one may approach them starting with a skyrmion-type Lagrangian constructed of Goldstone boson fields (and heavy mesons) and looking for solutions of the winding number W equal to the baryon number B or the mass number A in a nucleus. The Skyrme Lagrangian which consists of the current algebra term and the quartic term

$$\mathcal{L}_{sk} = \frac{f^2}{4} \text{Tr}(\partial_\mu U \partial^\mu U^\dagger) + \frac{1}{32e^2} \text{Tr}[U \partial_\mu U^\dagger, U \partial_\nu U^\dagger]^2 + \dots \quad (5.1)$$

which may be viewed as an approximate zero bag size limit of the Lagrangian (2.1) has been extensively studied mathematically for baryon number up to $B = 22$ with a

fascinating result [69]. (The ellipsis stands for higher derivative and/or heavy-meson and chiral-symmetry breaking terms that are to be added as needed.) The Lagrangian of the type (5.1) suitably extended with higher derivatives and/or massive boson fields is accurate only at large- N_c limit, so it is not clear what the classical solution of this Lagrangian for $B \geq 2$ represents since in nature $N_c \ll \infty$. Nonetheless this development is quite exciting since it is closest to QCD at least for $N_c = \infty$. As stated above, the ground states with baryons numbers B and B' with $B \gg B'$ cannot be connected by small perturbation because they represent different topological “vacua.”

A direction we will adopt here is not as ambitious as the above but we will attempt to account for the different vacuum structure for dense systems (heavy nuclei) than for dilute systems (light nuclei). We shall start with a theory for a system with a Fermi sea. It is possible that such a system emerges as a sort of nontopological soliton or “Q-ball” from a theory based on chiral perturbation theory defined at zero density as suggested first by Lynn [70] and recently refined by Lutz et al [71]. Although there is no proof, we believe that the Q-ball system which is non-topological is essentially equivalent to the skyrmion system which is topological. This equivalence is somewhat like in the nucleon structure where the two pictures work equally well. The essential point we shall accept here is that a non-topological soliton solution exists possessing the liquid structure that is supposed to be present in nuclear matter. We will later identify this with what we do know but for the moment let us assume that we have a Fermi sea filled with nucleons. It is fortunate for our purpose that such a system is accessible to an elegant and powerful effective field theory treatment as shown by various authors [72] that leads to Landau’s Fermi liquid theory applied to nuclear systems [73].

5.3 Effective Chiral Lagrangian for Many-Nucleon Systems

What we wish to do in our case is to arrive, following the developments in [74, 75, 76], at the Landau Fermi liquid theory starting from an effective chiral Lagrangian that we have been discussing above. Treating the nucleon in terms of a local field denoted by N and the Goldstone boson field by $\xi = \sqrt{U} = e^{i\pi\cdot\tau/2f_\pi^*}$, we can write a simple Lagrangian of the form

$$\mathcal{L} = \bar{N} [i\gamma_\mu(\partial^\mu + iv^\mu + g_A^* \gamma_5 a^\mu) - M^*] N - \sum_i C_i^* (\bar{N} \Gamma_i N)^2 + \dots \quad (5.2)$$

where the ellipsis stands for higher dimension nucleon operators and the Γ_i ’s Dirac and flavor matrices as well as derivatives consistent with chiral symmetry. The star affixed on the masses and coupling constants will be defined precisely below. The induced vector and axial vector “fields” are given by $v_\mu = -\frac{i}{2}(\xi^\dagger \partial_\mu \xi + \xi \partial_\mu \xi^\dagger)$ and $a_\mu = -\frac{i}{2}(\xi^\dagger \partial_\mu \xi - \xi \partial_\mu \xi^\dagger)$.¹⁸ In (5.2) only the pion (π) and nucleon (N) fields appear explicitly: all other fields have been integrated out. The effect of massive degrees of freedom will be lodged in higher-

¹⁸The ξ field appearing here is the “gauge-fixed” one, $\xi_L = \xi_R^\dagger = \xi$. Here we are dealing with the matter far away from the chiral phase transition point, so we are taking the unitary gauge.

dimension and/or higher-derivative interactions. The external electro-weak fields if needed are straightforwardly incorporated by suitable gauging.

When applied to symmetric nuclear matter in the mean field approximation, the Lagrangian (5.2) is known to be equivalent [77, 78] to the Lagrangian that contains just the degrees of freedom that figure in a linear model of the Walecka-type [79] ¹⁹

$$\begin{aligned}\mathcal{L} = & \bar{N}(i\gamma_\mu(\partial^\mu + ig_v^\star\omega^\mu) - M^\star + h^\star\sigma)N \\ & -\frac{1}{4}F_{\mu\nu}^2 + \frac{1}{2}(\partial_\mu\sigma)^2 + \frac{m_\omega^{\star 2}}{2}\omega^2 - \frac{m_\sigma^{\star 2}}{2}\sigma^2 + \dots\end{aligned}\quad (5.3)$$

where the ellipsis denotes higher-dimension operators. We should stress that (5.3) is consistent with chiral symmetry since here both the ω and σ fields are *chiral singlets*. In fact the σ here has nothing to do with the chiral fourth-component scalar field of the linear sigma model except near the chiral phase transition density; it is a “dilaton” connected with the trace anomaly of QCD and is supposed to approach the chiral fourth component in the “mended symmetry” way à la Weinberg [59, 60] near chiral restoration. In practice, depending upon the problem, one form is more convenient than the other. In what follows, both (5.2) and (5.3) will be used interchangeably.

In (5.2) and (5.3), the mass and coupling parameters affixed with stars depend upon the “sliding” vacuum defined at a given “density.” (Putting density into the parameters of a Lagrangian is subtle because of chiral symmetry and thermodynamic consistency. We will specify more precisely how the “density” is to be defined.) We are thinking of the situation where an external pressure (e.g., gravity for compact stars) is exerted and hence we can think of the parameters of the Lagrangian varying as a function of density. They need not be associated with quantities defined at a *minimum* of an effective potential of the theory without the external pressure.

The next important observation we shall exploit is that by Matsui [80] that a Lagrangian of the type (5.2) can give in the mean field the result of Landau Fermi liquid. This means that in the same approximation, the chiral Lagrangian (5.2) can be mapped to Landau Fermi liquid. From the works in [72] which tell us that Landau theory is a fixed-point theory with a *Fermi-liquid fixed point* which is distinct from that of the effective Lagrangian used for two-nucleon systems discussed above, we learn that the theory (5.2) in the mean field has two fixed-point quantities, viz, the effective quasiparticle (or Landau) mass m_N^* and the Landau parameters \mathcal{F} for quasiparticle interactions. The full interaction between two quasiparticles \mathbf{p}_1 and \mathbf{p}_2 at the Fermi surface of symmetric nuclear matter written in terms of spin and isospin invariants is defined by

$$\begin{aligned}\mathcal{F}_{\mathbf{p}_1\sigma_1\tau_1,\mathbf{p}_2\sigma_2\tau_2} = & \frac{1}{N(0)} \left[F(\cos\theta_{12}) + F'(\cos\theta_{12})\boldsymbol{\tau}_1 \cdot \boldsymbol{\tau}_2 + G(\cos\theta_{12})\boldsymbol{\sigma}_1 \cdot \boldsymbol{\sigma}_2 \right. \\ & \left. + G'(\cos\theta_{12})\boldsymbol{\sigma}_1 \cdot \boldsymbol{\sigma}_2 \boldsymbol{\tau}_1 \cdot \boldsymbol{\tau}_2 + \frac{\mathbf{q}^2}{k_F^2} H(\cos\theta_{12})S_{12}(\hat{\mathbf{q}}) \right]\end{aligned}$$

¹⁹For asymmetric nuclear matter, isovector fields (e.g., ρ , a_1 etc.) must be included in a chirally symmetric way.

$$+ \frac{\mathbf{q}^2}{k_F^2} H'(\cos \theta_{12}) S_{12}(\hat{\mathbf{q}}) \boldsymbol{\tau}_1 \cdot \boldsymbol{\tau}_2 \Big] \quad (5.4)$$

where θ_{12} is the angle between \mathbf{p}_1 and \mathbf{p}_2 and $N(0) = \frac{4k_F^2}{(2\pi^2)} \left(\frac{dp}{d\varepsilon} \right)_F$ is the density of states at the Fermi surface. Also, $\mathbf{q} = \mathbf{p}_1 - \mathbf{p}_2$ and $S_{12}(\hat{\mathbf{q}}) = 3\boldsymbol{\sigma}_1 \cdot \hat{\mathbf{q}} \boldsymbol{\sigma}_2 \cdot \hat{\mathbf{q}} - \boldsymbol{\sigma}_1 \cdot \boldsymbol{\sigma}_2$, where $\hat{\mathbf{q}} = \mathbf{q}/|\mathbf{q}|$. The tensor interactions H and H' are important for the axial charge to be considered later. The functions F, F', \dots are expanded in Legendre polynomials, $F(\cos \theta_{12}) = \sum_\ell F_\ell P_\ell(\cos \theta_{12})$, with analogous expansion for the spin- and isospin-dependent interactions.

The fixed point m_N^* is associated with a given Fermi momentum k_F or density ρ of the given system, so that there will be a set of fixed points \mathcal{F} for each (given) k_F or ρ . Thus we will have the Landau parameters that depend upon density once we accept that the Landau mass depends on density as is obvious from the Landau mass formula

$$\frac{m_N^*}{M} = 1 + \frac{1}{3} F_1 = (1 - \frac{1}{3} \tilde{F}_1)^{-1} \quad (5.5)$$

where $\tilde{F}_1 \equiv (M/m_N^*) F_1$ and F_1 is the $l = 1$ component of the interaction F in (5.4).

5.4 Brown-Rho Scaling

How the fixed point quantities vary with density cannot be determined from the effective Lagrangian alone. It must be tied to the vacuum property characterized by the chiral condensate $\langle \bar{\psi} \psi \rangle$ where ψ is the quark field. The dependence must therefore be derived from the fundamental theory, QCD. In the past QCD sum rules have been used to extract information on this matter. For our purpose, it is more convenient to take the Skyrme Lagrangian (5.1) as a starting point and try to deduce the necessary information. We expect it to give the leading behavior corresponding to a mean field theory in the sense to be defined more precisely later. This is the argument presented in the original BR paper [2]. Implementing the scalar dilaton field χ associated with the trace anomaly of QCD to the Lagrangian extended to take explicitly into account the vector mesons $V_\mu = \rho_\mu, \omega_\mu$, it has been found that in the mean field the following scaling holds, e.g., in the Lagrangian (5.3) ²⁰:

$$\Phi(\rho) \approx \frac{f_\pi^*(\rho)}{f_\pi} \approx \frac{m_\sigma^*(\rho)}{m_\sigma} \approx \frac{m_V^*(\rho)}{m_V} \approx \frac{M^*(\rho)}{M}. \quad (5.6)$$

Here f_π is the pion decay constant, the f_π^* being the in-medium one ²¹. We caution that the M^* is the nucleon in-medium mass (or BR scaling mass) which is *not* the same as

²⁰The scalar σ as well as the vector V are absent in (5.2) since they have been integrated out. Their scaling will appear therefore in the coefficients representing those degrees of freedom, namely, C_i^* 's. The connections between the two are given in [74, 75, 76].

²¹Since Lorentz invariance is lost in medium, the constants f_π^* , g_A^* etc. contain two components, space part and time part, that are in general different. The parameters that appear in BR scaling are mean-field quantities and are defined more precisely in the sense described above for a generalized Walecka model (5.3). The same remark applies to the in-medium vector coupling we will discuss in later sections.

the Landau mass m_N^* as we will see shortly. The quantity $\Phi(\rho)$, related to the quark condensate $\Phi \approx (\langle \bar{q}q \rangle^*/\langle \bar{q}q \rangle)^a$ where a is a constant which we will find in Section 8 equals ~ 1 , is the scaling factor that needs to be determined from (fundamental) theory or experiments.

Let us now examine more closely what the “density dependence” in general (not necessarily in the context of BR scaling) means in the Lagrangian (5.2) or (5.3). For this, let us take (5.3) and introduce the chirally invariant operator

$$\check{\rho}u^\mu \equiv \bar{N}\gamma^\mu N \quad (5.7)$$

where $u^\mu = (\sqrt{1 - \mathbf{v}^2})^{-1}(1, \mathbf{v}) = (\sqrt{\rho^2 - \mathbf{j}^2})^{-1}(\rho, \mathbf{j})$ is the fluid 4-velocity. Here $\mathbf{j} = \langle \bar{N}\gamma N \rangle$ is the baryon current density and $\rho = \langle N^\dagger N \rangle = \sum_i n_i$ the baryon number density. The expectation value of $\check{\rho}$ yields the baryon density in the rest-frame of the fluid. Using $\check{\rho}$ it is easy to construct a Lorentz invariant, chirally invariant Lagrangian with density dependent parameters.

Now a density dependent mass parameter in the Lagrangian should be interpreted as $m^* = m^*(\check{\rho})$. This means that the model (5.3) is no longer linear. It is highly non-linear even at the mean field level.

The Euler-Lagrange equations of motion for the bosonic fields are the usual ones but the nucleon equation of motion is not. This is because of the functional dependence of the masses and coupling constants on the nucleon field:

$$[i\gamma^\mu(\partial_\mu + ig_v^*\omega_\mu - iu_\mu\check{\Sigma}) - M^* + h^*\sigma]N = 0 \quad (5.8)$$

with

$$\begin{aligned} \check{\Sigma} &= \frac{\partial \mathcal{L}}{\partial \check{\rho}} \\ &= m_\omega^* \omega^2 \frac{\partial m_\omega^*}{\partial \check{\rho}} - m_\sigma^* \sigma^2 \frac{\partial m_\sigma^*}{\partial \check{\rho}} - \bar{N} \omega^\mu \gamma_\mu N \frac{\partial g_v^*}{\partial \check{\rho}} - \bar{N} N \frac{\partial M^*}{\partial \check{\rho}}. \end{aligned} \quad (5.9)$$

Here we are assuming that $(\partial/\partial\check{\rho})h^* \approx 0$. This can be justified using NJL model [112] but we will simply assume it here ²². The additional term $\check{\Sigma}$, which may be related to what is referred to in many-body theory as “rearrangement terms”, is essential in making the theory consistent. This point has been overlooked in the literature.

The crucial observation is that when one computes the energy-momentum tensor with (5.3), one finds, in addition to the canonical term (which is obtained when the parameters are treated as constants), a new term proportional to $\check{\Sigma}$

$$T^{\mu\nu} = T_{can}^{\mu\nu} + \check{\Sigma}(\bar{N}u \cdot \gamma N)g^{\mu\nu}. \quad (5.10)$$

²²In fact apart from the phenomenological requirement, there is no reason to assume this. All our arguments that follow would go through without difficulty even if the coupling constant were to scale with density.

The pressure is then given by $\frac{1}{3}\langle T_{ii} \rangle_{\mathbf{v}=0}$. The additional term in (5.10) matches precisely the terms that arise when the derivative with respect to ρ acts on the density-dependent masses and coupling constants in the formula derived from T_{00} :

$$p = -\frac{\partial E}{\partial V} = \rho^2 \frac{\partial \mathcal{E}/\rho}{\partial \rho} = \mu\rho - \mathcal{E} \quad (5.11)$$

where

$$\mathcal{E} = \langle T^{00} \rangle. \quad (5.12)$$

This matching assures energy-momentum conservation and thermodynamic consistency. This verifies that interpreting “density-dependent” parameters in our Lagrangian as the dependence on $\check{\rho}$ with $\langle \check{\rho} \rangle$ being the density is consistent with both chiral symmetry and thermodynamics.

5.5 Landau Mass and BR Scaling

We end this section by writing down the relations between the parameters of the Lagrangian (5.2) or equivalently (5.3) and Landau parameters. We will use the former and take (including the isovector channel)

$$-\sum_i C_i^* (\bar{N}\Gamma_i N)^2 \approx -\frac{C_{\tilde{\omega}}^{*2}}{2} (\bar{N}\gamma_\mu N)^2 - \frac{C_{\tilde{\rho}}^{*2}}{2} (\bar{N}\gamma_\mu \tau N)^2 + \dots \quad (5.13)$$

This may be considered as the leading terms that result when the vectors ω and ρ are integrated out. But it is more than just that. In fact, the subscripts can be taken to represent not only the vector mesons ω and ρ that nuclear physicists are familiar with but also *all* vector mesons of the same quantum numbers (which account for the appearance of the tilde on the vector mesons), so the two “counter terms” on the right-hand side subsume the *full* short-distance physics of the given chiral order. Since the Lagrangian (5.2) in tree order must correspond to the mean field of (5.3), one can simply compute the relevant Feynman graphs with (5.2) and match them to the Landau Fermi liquid formula. One obtains [74]

$$\frac{m_N^*}{M} = \left(\Phi^{-1} - \frac{1}{3} \tilde{F}_1(\pi) \right)^{-1} \quad (5.14)$$

where $\tilde{F}_1(\pi)$ is the pion contribution to F_1 which is completely fixed by chiral symmetry so the only parameter that enters in (5.14) is the BR scaling $\Phi \approx M^*/M$.

Now using the Landau mass formula (5.5) and

$$\tilde{F}_1 = \tilde{F}_1(\tilde{\omega}) + \tilde{F}_1(\pi) \quad (5.15)$$

we find

$$\tilde{F}_1(\tilde{\omega}) = 3(1 - \Phi^{-1}). \quad (5.16)$$

This is the main result of the connection between the chiral Lagrangian with BR scaling and Landau Fermi liquid theory. This is a highly non-trivial relation which says that BR scaling – which in the context of the QCD vacuum reflects modification due to matter density – is tied to short-range quasiparticle interactions. This means that what may be considered to be a basic feature of QCD and nuclear interactions via nuclear forces are inter-related, indicating another level of the Cheshire Catism.

- *Determining $\Phi(\rho)$*

If one accepts the BR scaling (5.6), there are several sources to use for determining the scaling factor $\Phi(\rho)$. For instance, one can determine it from the QCD sum rule for the mass ratio m_ρ^*/m_ρ [81] or from the ratio f_π^*/f_π using the Gell-Mann-Oakes-Renner (GMOR) formula for pion mass in medium ²³ or a fit to nuclear matter properties [74]. The result comes out to be about the same at nuclear matter density

$$\Phi(\rho = \rho_0) \approx 0.78. \quad (5.17)$$

In terms of the parameterization of the form

$$\Phi(\rho) = (1 + y\rho/\rho_0)^{-1}, \quad (5.18)$$

the result corresponds to $y(\rho = \rho_0) \approx 0.28$. This gives the Landau mass $m_N^*/M \approx 0.70$ which is to be compared with the QCD sum-rule value $0.69_{-0.07}^{+0.14}$ and with the value 0.68 indicated from peripheral heavy-ion collisions. This provides a consistency check.

6 INDIRECT EVIDENCES FOR BR SCALING

6.1 Indications in Finite Nuclei

Before the publication on BR scaling in [2], Brown and Rho proposed [82, 83] that some of the missing strength in the longitudinal response function in nuclei could be explained by the dropping masses in medium $m_\rho^*/m_\rho \approx m_N^*/m_N \approx 0.75$. The same dropping masses (of both the nucleon and the ρ) could also explain that within certain range of kinematics relevant to experiments, the transverse response function does not scale in medium. This is essentially the picture that is confirmed by the Morgenstern-Meziani analysis mentioned in the introduction and described in detail in Section 7.

In addition to the electromagnetic response functions, there were further predictions in [83] that followed from the dropping masses. One was the anomalous gyromagnetic ratio δg_l in nuclei which gets enhanced by the scaling factor. This will be discussed below in terms of a more modern formulation with chiral Lagrangians and Landau Fermi liquid

²³Using the in-medium GMOR formula to arrive at the value (5.17), it is assumed that the pion mass remains unaffected by density up to nuclear matter density. This assumption may have to be re-examined in view of the “pion mass” measured in deeply bound pionic states which indicate a mild increase as a function of density as discussed in Section 8. This issue is not so simple to address since it is not clear that the mass that appears in the GMOR relation is the same quantity that has been “measured.”

theory although the physics is essentially the same as in this work. The second is that the dropping mass implies that as density increases, the tensor force in nuclei gets weakened. The reason is that the tensor force is given by two agencies, one-pion exchange and one- ρ exchange coming with opposite signs. At low density, the pion exchange dominates, so the net effect is more or less controlled by the pion tensor. However as density increases, the ρ tensor gets enhanced by the factor $(m_N/m_N^*)^2$ apart from the increased range of the ρ -exchange force. Therefore the ρ tensor tends to cancel more and more the pion tensor as density increases, thereby suppressing the net tensor force in the outer region where pion exchange dominates. There are some indications that the suppressed tensor force is consistent with nuclear spectra as well as with Gamow-Teller transitions in nuclei to which we shall return shortly.

There is, however, a possible caveat to this as we will see later and that has to do with the possibility that the vector coupling $g_{\rho NN}^*$ will also drop as density increases, eventually decoupling as dictated by the “vector manifestation” discussed above. It is not clear at what density this decoupling sets in but there are empirical indications that the tensor force weakening is operative at least up to nuclear matter density. The phenomenology in nuclei discussed above also indicates that at least at the low densities encountered in nuclei, the ratio $g_{\rho NN}^*/m_\rho^*$ does increase. It should be noted that even when the vector decoupling takes place, with the flavor symmetry in the hadronic sector yielding to the color gauge symmetry in the quark-gluon sector²⁴, some vector repulsion remains coming from (Fierzed) gluon exchange [13].

6.2 The Anomalous Gyromagnetic Ratio in Nuclei

The development given above in Section 5 of the effective chiral Lagrangians with BR scaling and Fermi liquid fixed point theory can provide a more sophisticated and rigorous explanation for the enhanced gyromagnetic ratio g_l in nuclei mentioned above. We discuss this as a strong, though indirect, evidence for BR scaling. The nuclear gyromagnetic moment g_l in the convection current for a particle sitting on top of the Fermi sea is defined as

$$\mathbf{J} = \frac{\mathbf{k}}{M} g_l. \quad (6.1)$$

We have defined $g_l \equiv 1 + \delta g_l$ such that the bare nucleon mass M , *not* the effective (Landau) mass m_N^* , appears in the formula. This is because we want to preserve charge conservation associated with the factor 1 in g_l , δg_l being purely isovector.

The δg_l has been determined from experiments. The measurement that is most relevant to our theory is the one on giant dipole resonances on heavy nuclei, in particular in the lead region. The result of [84] on ^{209}Bi gives the proton value

$$\delta g_l^p = 0.23 \pm 0.03. \quad (6.2)$$

²⁴The way this change-over takes place is discussed in Section 11.

This can also be determined from magnetic moment measurements but the analysis is somewhat more complex and hence less precise. We shall refer to (6.2).

Given the effective chiral Lagrangian (5.2), with the connections we have established so far, it is easy to compute in the mean field order the nuclear gyromagnetic ratio g_l . It suffices to calculate all terms of the same order to assure that charge is conserved or what is equivalent, “Kohn theorem” is satisfied. The result is the Migdal formula [73] given in terms of the parameters of the Lagrangian, that is, the BR scaling $\Phi(\rho)$,

$$g_l = \frac{1 + \tau_3}{2} + \delta g_l \quad (6.3)$$

with

$$\delta g_l = \frac{1}{6}(\tilde{F}'_1 - \tilde{F}_1)\tau_3 = \frac{4}{9} \left[\Phi^{-1} - 1 - \frac{1}{2}\tilde{F}_1(\pi) \right] \tau_3. \quad (6.4)$$

As mentioned above, $\tilde{F}_1(\pi)$ is completely fixed by chiral symmetry for any density – possibly up to chiral restoration – so the only quantity that appears here is the BR scaling factor. At nuclear matter density, we have $\frac{1}{3}\tilde{F}_1(\pi)|_{\rho=\rho_0} = -0.153$. Now taking $\Phi(\rho_0) \approx 0.78$ from (5.17), we predict from (6.4)

$$\delta g_l^{th} = 0.227\tau_3. \quad (6.5)$$

This agrees with the experiment (6.2) providing a quantitative check of the BR scaling.

6.3 Axial Charge Transitions in Heavy Nuclei

Another process where the Lagrangian (5.2) with BR scaling together with the PKMR’s EFT can make a prediction is in the axial charge beta transition of the type

$$A(J^\pm) \rightarrow A'(J^\mp) + e^-(e^+) + \bar{\nu}(\nu) \quad \Delta T = 1. \quad (6.6)$$

This process was studied by several experimentalists with the objective of exhibiting strong medium-enhancement of the matrix element of the axial charge operator A_0^a that governs the process (6.6) in heavy nuclei. Such an enhancement was first observed by Warburton in the lead region [85] and since then several authors confirmed Warburton’s finding in various other heavy nuclei. Warburton focused on the quantity (that we shall refer to as “Warburton ratio”)

$$\epsilon_{MEC} = M_{exp}/M_{sp} \quad (6.7)$$

where M_{exp} is the *measured* matrix element for the axial charge transition and M_{sp} is the *theoretical* single-particle matrix element for a nucleon *without* BR scaling. There are several theoretical uncertainties involved in extracting the Warburton ratio. First, one has to extract from given beta decay data what corresponds to the axial charge matrix element. This involves estimating accurately other terms than the axial charge that

contribute. The second is what one means precisely by M_{sp} which is a theoretical entity. For these reasons, an unambiguous conclusion is difficult to arrive at. However what is significant is Warburton's observation that in heavy nuclei, ϵ_{MEC} can be substantially larger than the possible uncertainties involved:

$$\epsilon_{MEC}^{HeavyNuclei} = 1.9 \sim 2.0. \quad (6.8)$$

Furthermore more recent measurements and their detailed analyses in different nuclei [86, 87, 88] as shown in Table 2 quantitatively confirm this result of Warburton.

The prediction from the Lagrangian (5.2) with BR scaling in the same approximation as in the gyromagnetic ratio case is [89, 74]

$$\epsilon_{MEC}^{\chi th} = \Phi^{-1}(1 + \tilde{\Delta}) \quad (6.9)$$

where $\tilde{\Delta}$ is, in accordance with the chiral filter mechanism, dominated by the pionic contribution with small controllable corrections from vector degrees of freedom ²⁵, the magnitude and the density dependence of which are again totally controlled by chiral symmetry, with the BR scaling Φ appearing as an overall factor. For $\rho = \rho_0/2$ and $\rho = \rho_0$, we find [74]

$$\epsilon_{MEC}^{\chi th}|_{\rho=\rho_0/2} \approx 1.63, \quad \epsilon_{MEC}^{\chi th}|_{\rho=\rho_0} \approx 2.06. \quad (6.10)$$

This is in an overall agreement with all the available Warburton ratios (see Table 2).

Table 2: “Empirical values” for ϵ_{MEC}

Mass number A	ϵ_{MEC}	Reference
12	1.64 ± 0.05	[86]
50	1.60 ± 0.05	[87]
205	1.95 ± 0.05	[88]
208	2.01 ± 0.10	[85]

6.4 Axial-Vector Coupling Constant g_A^* in Dense Matter

One can make a rather simple statement on how the axial-vector coupling constant g_A^* scales in dense matter on the basis of BR scaling and the Fermi liquid theory.

The story of g_A^* in nuclei is a long story and rather involved with nuclear structure effects compounded with strong nuclear tensor correlations, excitations of nucleon resonances and possible effects of the vacuum change [90, 91, 92, 93]. Gamow-Teller transitions in complex nuclei, particularly giant resonances thereof, play an important role in

²⁵In terms of the Landau-Migdal fixed-point parameters, $\tilde{\Delta} = G'_1/3 - 10H'_0/3 + 4H'_1/3 - 2H'_2/15$ with the dominant contribution coming from the soft pions [51].

presupernova stage of the collapsing stars and the effective coupling constant g_A^* figures importantly in their description [94].

What we will present here is probably not the unique explanation of what is going on but it is a version that is immediate from, and consistent, with the general theme of this review ²⁶.

We have arrived above at the Landau mass formula (5.14) given in terms of the BR scaling parameter Φ . The Landau mass differs from the BR scaling mass M^* due to the pion contribution. From the Skyrme-type Lagrangian from which we have deduced the scaling behavior, this means that there must be contributions from other than the property of f_π . The only other factor that enters in the skyrmion description is the coefficient of the Skyrme quartic term e or in terms of a physical quantity, g_A . When this is taken into account, the resulting expression is found to be [74] ²⁷

$$\frac{m_N^*}{M} = \sqrt{\frac{g_A^*}{g_A}} \Phi \quad (6.11)$$

from which we get

$$\frac{g_A^*}{g_A} = \left(1 + \frac{1}{3} F_1(\pi)\right)^2 = \left(1 - \frac{1}{3} \tilde{F}_1(\pi) \Phi\right)^{-2}. \quad (6.12)$$

At nuclear matter density, this predicts

$$g_A^*(\rho_0) \approx 1. \quad (6.13)$$

What does this mean physically? If we accept that the Landau mass is a fixed point of the Fermi liquid theory, then the g_A^* must be a constant *defined* at the fixed point. It therefore must correspond to decimating all the way down to the Fermi surface, that is to say, sending the infrared cutoff k_c in the renormalization-group equation to zero. In this limit, g_A^* must be proportional to the Landau parameter G'_0 . This connection in infinite (translationally invariant) matter is being investigated in [95]. What this means in practice in finite nuclei in which the transition is measured is not yet fully understood.

²⁶It is perhaps appropriate at this point to clarify how the absence of Lorentz symmetry manifests itself in our treatment of g_A^* , an issue we briefly alluded to earlier. As the two (preceding and this) subsections clearly show, the effective axial coupling constant g_A in matter is different for the space and time components of the axial current. We see that the time component of the axial charge (measured through axial-charge transitions) is enhanced in nuclear matter whereas the space component of the axial charge (measured through Gamow-Teller transitions as here) is quenched. Although we did not make the distinction in discussing BR scaling, it is evident that the g_A^* that appears in the relation between the BR scaling mass M^* and the Landau mass m_N^* involves the space component measured by Gamow-Teller transitions. A similar separation can be made for instance for the pion decay constant f_π^* which will be discussed in Section 8.

²⁷Since the middle expression of (6.12) involves the pionic contribution $F_1(\pi)$, one might think that g_A^* differs from g_A merely due to the presence of the pion. This interpretation is not correct. The Landau parameter $F_1(\pi)$ contains the density of states $N(0) = 2k_F m_N^*/\pi^2$ which carries the Landau mass m_N^* and hence does involve BR scaling. This is clearly seen in the last equality.

But it appears reasonable to suppose that applied to finite nuclei, what we obtained here is an effective constant that should be used *when the Gamow-Teller matrix element is computed within the valence shell with the single-particle states undergoing the Gamow-Teller transition restricted to the lowest-lying excitations on top of the Fermi sea*. In other words, the g_A^* so obtained is a fixed-point quantity.

An apt illustration of how this reasoning seems to be working is given by the complete $0f1p$ -shell Monte Carlo calculation of Gamow-Teller response functions by Radha et al [96] and also big shell-model diagonalization by Caurier et al [97]. Remarkably, it is found that $g_A^* \approx 1$ is universally needed in these calculations [96, 98, 94] which may be taken as a support for the fixed-point notion of the g_A^* .

6.5 Evidences from “On-Shell” Vector Mesons

The indirect evidences we have discussed above dealt with the properties of hadrons that are way off-shell, with $q_\mu^2 \approx 0$. The masses and coupling constants that are probed in such processes correspond to the *parameters* of the effective Lagrangian and they would be near their physical parameters only if the tree approximations were valid. One would of course like to confront with measurements of the “physical hardrons” propagating in dense matter. In order to do this quantitatively with a theory that implements BR scaling, one would have to compute to higher orders, say, in chiral perturbation suitably formulated to incorporate the “sliding” vacuum structure associated with BR scaling. This would of course give rise to widths of the hadrons involved and to a further shift in mass from that of BR scaling which is mean field. Such a program has not yet been clearly formulated. Hence there are no predictions in our approach. For low density, there are several calculations that start from the zero density vacuum [121, 99] that predict that while the ρ meson may or may not be shifted in mass, the ω will. The ρ will broaden in width in matter but the ω will remain narrow and may even be bound in nuclear matter [100]. The experimental finding of this property of ω will confirm unambiguously the observations made in the preceding and following sections.

Experiments are presently being performed to check all this at various laboratories, notably at GSI and Jefferson Lab. Specifically, the signals from heavy-ion collisions to be discussed below address this issue although with results that are compounded with temperature effects.

Here we briefly comment on some recent experiments that seem to indicate that the vector-meson masses do decrease with density in nuclear matter or that at least the dropping masses are compatible with the observations. One is the TAGX collaboration result [101] on the process ${}^3\text{He}(\gamma, \rho^0)ppn$ with the tagged photons in the range 800–1120 MeV. The mass shift of the ρ^0 meson reported was $\delta m_\rho = 160 \pm 35$ MeV. This is nearly the amount predicted for nuclear matter, i.e., $m_\rho(1 - \Phi) \approx 170$ MeV for $\Phi = 0.78$ used above. This seems to be a bit too much a shift for such a small nucleus. It seems to involve other than just BR scaling. The other experiment is a more recent measurement [102] at KEK on the invariant mass spectra of the e^+e^- pairs in the target rapidity region of 12 GeV $p + A$ reactions with the nucleus $A = \text{C}$ and Cu . The experimental result

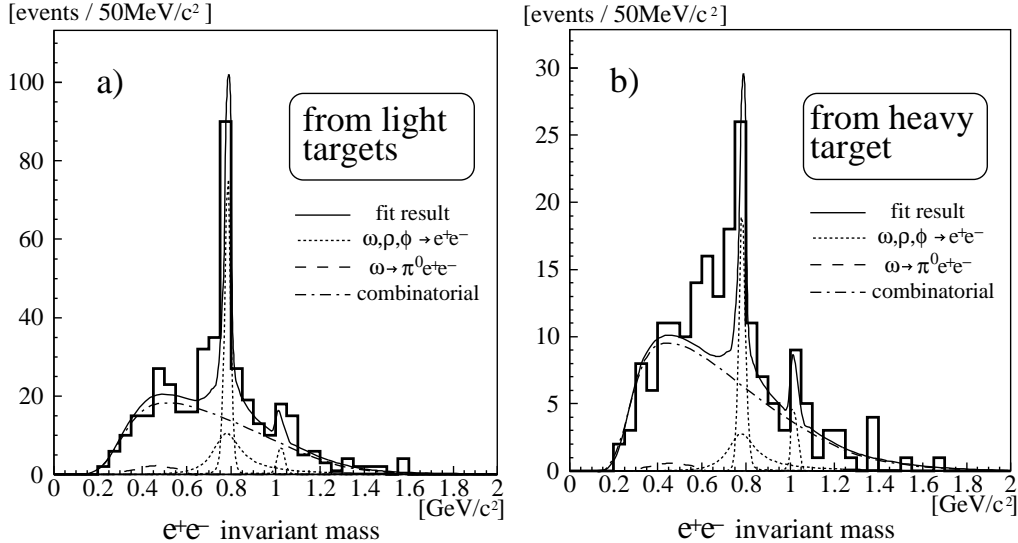


Figure 8: Distribution with invariant mass of e^+e^- pairs [102]: a) from a carbon target; b) from a copper target. The difference between histogram and thin solid line represents the effect of medium (density) on vector-meson mass, the e^+e^- invariant mass being determined by the in-medium vector-meson mass.

is given in Fig.8. This collaboration “sees” the mass shift of the vectors in the heavier nucleus indicative of a BR scaling. Although the precise value of the mass shift is not determined in this work, it is consistent with the expectation. We learned from private communication [103] that with their kinematic distribution, about 60% of the ρ mesons and about 10% of the ω mesons are estimated to decay inside Cu nucleus, so most of the excess on the low-mass side of the ω peak is from the ρ mesons. The authors of [102] considered the possibility of an in-medium increase in ω mass, but this did not give a statistically significant effect. More data and their analyses are forthcoming and will give a clearer insight into the properties of the hadrons on the “mass-shell,” thereby checking the BR scaled effective Lagrangian in more details.

7 DIRECT EVIDENCE FROM THE $(e, e'p)$ RESPONSE FUNCTIONS IN NUCLEI

The evidences for BR scaling given so far are more or less indirect. They are based on consistency with what we already know of nuclear interactions. In this section, we discuss what we consider to be the most direct evidence for BR scaling, namely, the longitudinal and transverse electromagnetic response functions in medium-heavy and heavy nuclei. Although the process involves off-shell properties of the vector meson, we believe that this evidence is cleaner and more direct than what we can extract from presently available heavy-ion data – including the celebrated CERES data – described below.

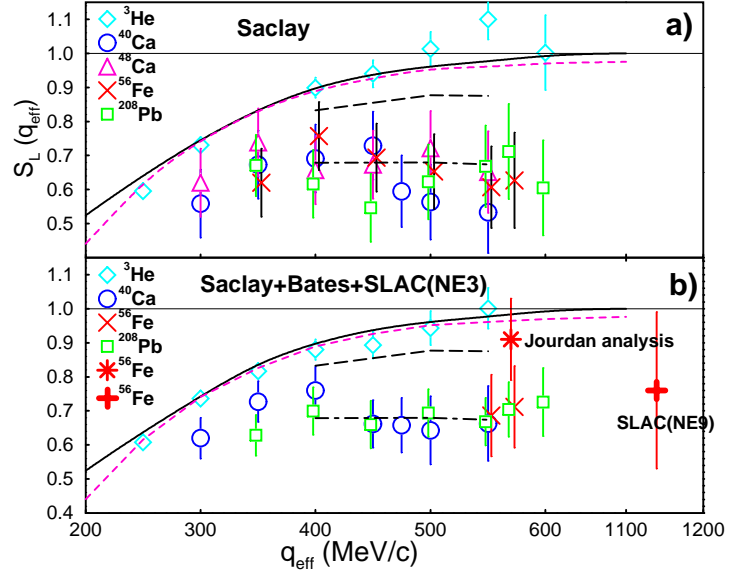


Figure 9: The longitudinal response function S_L as a function of q_{eff} using (a) Saclay data only and (b) Saclay data plus SLAC NE3 and Bates data. The SLAC NE9's ^{56}Fe result is shown by a cross and that of the Jourdan analysis by a star in (b). The theoretical curves are: the solid black curve for nuclear matter without BR scaling and the dashed curve for ^4He ; the long dashed curve is the same as the nuclear matter one integrated within the experimental limits of ω . The dot-dashed curve is with BR scaling. See Section 7 for details .

Electron scattering which knocks nucleons out of nuclei have been used for many years to tell us about the binding energy of protons in nuclei and also to pin down the effective mass that the proton has in the nucleus. To the extent that the electron couples through vector mesons to the nucleons, these experiments can also tell us about the *in-medium* properties of the vector mesons. This was worked out first in a paper by Soyeur, Brown and Rho [104] following the initial suggestion in [82, 83]. We follow here a more schematic treatment [105] which brings out the main ideas more clearly, and which is in semi-quantitative agreement with the more detailed calculation.

Before going further, let us remark that the experimental analysis has been thoroughly confused during the 1990's and only now is being clarified, chiefly due to efforts of Joseph Morgenstern. A global analysis by Jourdan [106] which relied on three-dimensional numerical calculation of Onley et al. [107] indicated that medium effects appeared to be absent, or at least the situation was unclear. The analyses involved therein were unnecessarily complicated in view of the fact that Yennie et al [108] had shown that the chief distortion by the Coulomb field could be reliably taken into account by shifting the momentum \mathbf{q} to an effective momentum

$$\mathbf{q}_{eff} = (\mathbf{1} - \mathbf{V}_c/|\mathbf{q}|) \quad (7.1)$$

where V_c is an effective Coulomb potential of the electron. This is a semiclassical correction

and had to be accompanied by higher order corrections for a quantitative description of the elastic electron scattering off nuclei [108] since the wavefunctions oscillate rapidly. Even there the \mathbf{q}_{eff} of eq.(7.1) gave a semiquantitative description of the distortion. Quasielastic scattering is very smooth as function of position in the integrand, and one would expect the introduction of \mathbf{q}_{eff} should be adequate there.

Before the linear accelerator was shut down in Saclay, quasielastic experiments were performed on ^{12}C and ^{208}Pb with a positron beam. In this case the sign of V_c changes, and the correction (7.1) to the momentum is of opposite sign. Using the effective momentum approximation of eq.(7.1), it has been shown [109] that both electron and positron scattering of ^{12}C and ^{208}Pb could be well described in a consistent way. Introduction of \mathbf{q}_{eff} handles what is called the lowest order focusing effect in the theory. Whereas Onley et al [107] found higher-order focusing effects to be important, introduction of these would ruin the consistency between the electron and positron scattering. Of course without substantial numerical work, it is not possible to check the Onley et al's results.

• Experimental Situation

Although as theorists we cannot go into the experimental situation in detail, we can see that the early disagreement between the MIT-Bates data and Saclay data changed when MIT replaced their old scattering chamber, where background was corrected for by simulation, by a new one. The updated MIT-Bates data and the Saclay data are now in substantial agreement. The analysis of the positron scattering introduced a new element. It could be straightforwardly explained by the effective momentum approximation (EMA). Kim et al [110] found that inclusion of higher order screening corrections in an approximate treatment of electron Coulomb distortion in quasi-elastic (e, e') reaction was important. Indeed for forward electron angles the low-energy side of the DWBA peak looks similar to the plane-wave result. The authors suggest that the phase factors effectively cancel the effect of the effective momentum on the low ω side of the quasielastic peak. However, if so, the next correction beyond the EMA would involve the square of the projectile charge which would be the same for electron and positron, negating the simple relation (7.1). This would also mean that the difference between plane wave and DWBA for positrons would be large. In any case, these matters can be only conjectured because the Ohio University collaborations have not been extended to positrons although it seems obvious that this should be done.

It is our belief that the whole situation, especially the theoretical analysis, has been a real shambles, for which we take partial responsibility. The Yennie, Boos and Ravenhall work was so convincing that theorists should have insisted that experiments were analyzed in the effective momentum approximation.

• Theory with BR Scaling

The mechanism for the change in quasielastic scattering can be quite simply understood by considering the vector dominance model in which the electron couples to the

nucleon through the vector meson. The vector mass enters into this coupling through

$$\mathcal{D}(m_V) = \frac{m_V^2}{m_V^2 + q^2} = \frac{1}{1 + q^2/m_V^2}. \quad (7.2)$$

Usually the numerator enters into the electron- ρ meson coupling and the denominator into the propagator, but the terms should be put together as in eq.(7.2) because $\mathcal{D}(m_V)$ must go to 1 as $q \rightarrow 0$ in order to conserve the electron charge. If now $m_V \rightarrow m_V^* \sim 0.8m_V$ then $\mathcal{D}(m_V^*) < \mathcal{D}(m_V)$.

The longitudinal response measures the charge density for which the operator is

$$\mathcal{O}^L = \frac{1}{2} + \frac{1}{2}\tau_3. \quad (7.3)$$

The ω -meson couples to the $\frac{1}{2}$ and the ρ -meson to the $\frac{1}{2}\tau_3$. The scattering via the ω -meson exchange will be chiefly longitudinal in nature, since the isoscalar magnetic moment, which gives the transverse response, is small. Thus, the suppression in the longitudinal response is essentially

$$F = \frac{1 + q^2/m_\omega^2}{1 + q^2/m_\omega^{*2}}. \quad (7.4)$$

Here what figures is the BR scaling in the ω meson mass.

For the transverse response the main operator is

$$\mathcal{O}^T = \mu_V \frac{\epsilon \cdot [\sigma \times q]}{2m_N} \tau_3, \quad (7.5)$$

this response coupling chiefly to the isovector magnetic moment. Now in medium $m_N \rightarrow m_N^*$ as well as the propagator changing, so the relevant factor is

$$F_T = \left(\frac{1 + q^2/m_\rho^2}{1 + q^2/m_\rho^{*2}} \right) \frac{m_N}{m_N^*}. \quad (7.6)$$

What enters here is the BR scaling in the nucleon mass. Now taking $m_\rho^*/m_\rho \sim m_N^*/m_N$ according to the BR scaling, one finds that the two factors in (7.6) nearly cancel each other in the range of momentum transfers $q \sim$ several hundred MeV in which the longitudinal and transverse responses have been measured.

In Fig.9, we show comparison of longitudinal data with the theory of Soyeur, Brown and Rho. Also a point from Jourdan's analysis using the Onley et al theory is shown. The drop of the dash-dot line, which included the Soyeur et al medium effects, below the Fabrocini and Fantoni solid line, which does not include these effects, is very clear, an $\sim 20\%$ effect.

Both predicted and experimental effects on the transverse scattering are small. This is an example where BR scaling has a visible effect. Clearly the separation of longitudinal and transverse components was essential to expose BR scaling.

• Comments

The Soyeur-Brown-Rho treatment in [104] was more complicated than our above schematic model because it built in the quark structure of the nucleon at short distances, essentially through inclusion of the chiral bag model. Since the latter was not scaled, the effect of scaling in our schematic model was somewhat diminished. Nonetheless they were quite large as seen from the difference between the dashed line and the stared point “Jourdan analysis” and Soyeur et al’s dash-dot line.

It should be noted that Saito, Tsushima and Thomas [111] obtained within the quark-meson (QMC) model results for the quasi-elastic electron scattering similar to those of Soyeur, Brown and Rho.

In the next Section, we will develop the evidence of medium-dependent vector-meson masses from the dilepton and photon experiments carried out at the SPS of CERN. Whereas the excess dilepton can be as simply produced in the Rapp-Wambach scenario as in the Brown-Rho scenario, the photons take us to higher densities and temperature, beyond the chiral restoration transition. We will develop a notion of complementarity between the BR dropping mass scenario and quark-gluon plasma (QGP) description for the photon treatment. As for quasielastic electron scattering we need not go into QGP since the hadron language is amply adequate. The dileptons we consider next fit in also quite simply with the quasielastic electron scattering. Our treatment in the next section will, however, allow us to unite the low-energy sector with the chiral restoration region of energies.

8 BR SCALING IN CHIRAL RESTORATION

One can approach the *phenomenology* of the chiral restoration from a variety of different angles. We define ours by introducing the role of BR scaling by a simple construction of the chiral restoration transition as mean field in the Nambu-Jona-Lasinio model. More precisely we consider the transition as mean field up to *both* ρ_c and T_c , the critical density and temperature, although there may well be a density discontinuity at the transition, making it first order. Most likely the transition is second order for $\rho = 0$, with a tri-critical point on the phase boundary going towards finite density. What is important for our discussion, however, is that masses of mesons other than the pion go smoothly to zero in the chiral limit. The simplest possible model for this is mean field NJL. We follow the construction of Brown, Buballa and Rho [112]. Relevant parts of this paper were reviewed in Brown and Rho [13]. The present description in NJL agrees with the vector manifestation scenario of Harada-Yamawaki’s hidden local symmetry theory (see Section 4) and with the quark-hadron complementarity picture given in Section 11.

8.1 Bag Constant and Scalar Field Energy

Brown, Buballa and Rho showed that the Walecka nuclear mean field theory at nuclear matter density could be connected with NJL mean field theory at higher densities;

e.g., the σ -field coupling the quarks in NJL can be taken to be 1/3 of that to nucleons in Walecka theory,

$$g_{\sigma QQ} = g_{\sigma NN}/3 \simeq 10/3. \quad (8.1)$$

Furthermore, the scalar field energy $\frac{1}{2}m_\sigma^2\sigma^2$ plays the role of the bag constant B in the chiral restoration transition. On the quark-gluon side of the transition the appearance of the bag constant corresponds to the disappearance of the scalar field energy going upwards from below through the transition. The magnitude of the effective bag constant is only $\sim 1/2$ of that that would be given by the trace anomaly:

$$B = -\frac{\beta(g)}{8g} \langle 0 | (G_{\mu\nu}^a)^2 | 0 \rangle \quad (8.2)$$

which to one loop (for $N_F = 3$) is

$$\begin{aligned} B &= \frac{9\alpha_s}{8\pi} \langle 0 | (G_{\mu\nu}^a)^2 | 0 \rangle = (245 \text{ MeV})^4 \\ &= 469 \text{ MeV/fm}^3 \simeq 2B_{eff} \end{aligned} \quad (8.3)$$

where $B_{eff} = \frac{1}{2}m_\sigma^2\sigma^2$. As found by Miller [113], only about 50% of the glue is “uncovered” in the chiral restoration transition. The other 50% remains as “covered” glue. In Shuryak et al [114], the soft glue disappears with the dynamically generated quark masses whereas the hard glue (“epoxy”) is made up of instanton molecules which do not break chiral symmetry. The amount of trace anomaly which disappears at the transition gives $B_{eff} \simeq 235 \text{ MeV/fm}^3$.

8.2 “Nambu Scaling” in Temperature

From the Gell-Mann-Oakes-Renner relation

$$m_\pi^2 = 2m_q \langle \bar{q}q \rangle / f_\pi^2 \quad (8.4)$$

and taking m_π not to scale with density, Brown and Rho [13] found hadron masses scaling as f_π^* with $f_\pi^* \propto |\langle \bar{q}q \rangle^*|^{1/2}$.²⁸ It was then with some surprise that Koch and Brown [115] found that the temperature dependence of the entropy in the many-body system as calculated in lattice gauge calculations [116] could be reproduced in the hadron sector best with the scaling

$$\frac{m^*}{m} \approx \frac{\langle \bar{q}q \rangle^*}{\langle \bar{q}q \rangle} \quad (8.5)$$

²⁸In [2], using Skyrme’s Lagrangian and looking at pions in medium, the scaling $f_\pi^* \propto |\langle \bar{q}q \rangle^*|^{1/3}$ was obtained. We now know that because of chiral symmetry broken only slightly in nature, the in-medium properties of a pion cannot be given correctly in the same mean field argument as used for other non-Goldstone bosons. Therefore it is safe to say that there is no accurate description of the pionic property based on model considerations. Future experiments will help in this direction.

for hadron masses other than the pion mass. In Fig.10 is shown how Nambu scaling behaves in the phase transition region. This scaling follows from the mean field NJL model and is referred to as “Nambu scaling” although it is a generic feature of the linear sigma model. The entropy is particularly suitable to study, since quark mean fields drop out so it tells us directly about the number of degrees of freedom.

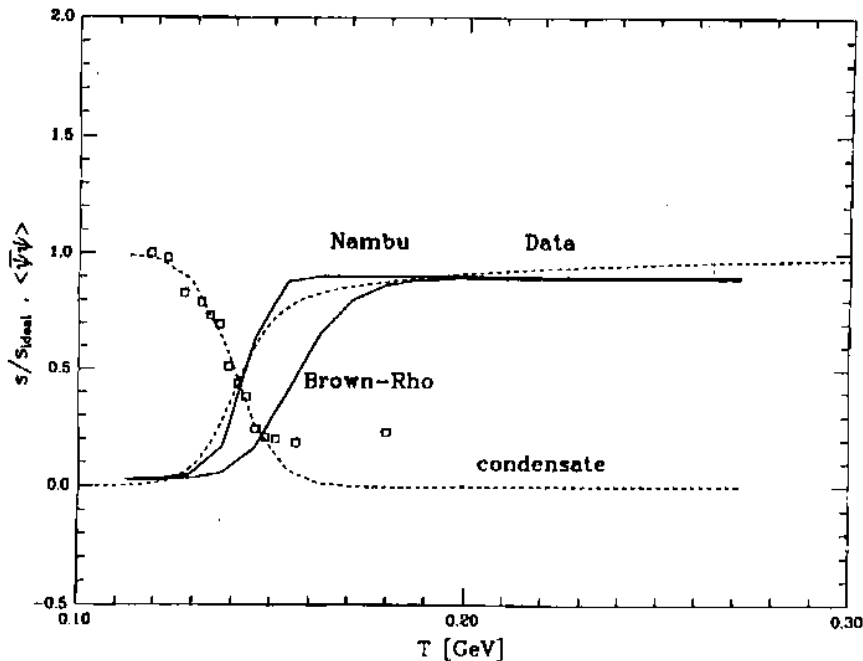


Figure 10: Comparison of entropy derived by Koch and Brown from the lattice data on energy density (dashed line) and from dropping masses (full lines) calculated in the Nambu scaling and in the naive Brown-Rho scaling. In the lower dashed line for $\langle\bar{\psi}\psi\rangle$ the bare quark mass has been taken out.

The hadron language is suitable for low temperatures. As stressed above and further elaborated later, we believe that our description is “dual” to a quark-gluon language as temperature moves towards the chiral restoration temperature. In particular, Koch and Brown limited their number of hadrons to 24, the number of light quarks. Rather than just cutting the number at this value, the same number can be consistently imposed by introducing excluded volume effects [117]. In any case the restriction that the hadronic description with dropping masses go over, in terms of the number of degrees of freedom, to the quark picture at higher temperature, must be built in. Otherwise it would not be possible to go beyond the Hagedorn temperature. The scale at which the change-over from hadron to quark language is made is one of convenience in accordance with the Cheshire Cat principle. Presumably it is in the region of the chiral restoration transition. This aspect becomes even more evident with the “hadron-quark continuity” discussed in

Section 11.

Finally note that the Nambu scaling that fits the entropy in the hadronic description comes from mean field, i.e., the coupling constant $g_{\sigma QQ}$ is not scaled. As long as we deal with the σ , the fluctuation field connected with chiral symmetry restoration, mean field seems to work very well, perhaps at least approximately up to the chiral restoration transition. In fact it was noticed in [74] that the mean field description of nuclear matter in terms of chiral Lagrangians implemented with BR scaling required that the scalar coupling be unscaled at least up to nuclear matter density. This will also be observed in the problem of “strangeness equilibration” discussed in Section 10.

8.3 “Nambu Scaling” in Density

Given that there is nothing which dictates that the scaling in temperature and that in density be the same, the question is whether the Nambu scaling also works in density, at variance with those found in [2, 13] which are different from the Nambu one. To answer this question let us first address the question: How must the pion mass m_π^* change with density in order to have Nambu scaling; i.e., hadron masses other than that of the pion to scale as

$$\frac{m^*}{m} = \frac{f_\pi^*}{f_\pi} = \frac{\langle \bar{q}q \rangle^*}{\langle \bar{q}q \rangle} ? \quad (8.6)$$

From Gell-Mann-Oakes-Renner equation

$$f_\pi^2 = 2m_q \langle \bar{q}q \rangle / m_\pi^2 \quad (8.7)$$

and since the quark mass does not change with density, we have

$$\frac{f_\pi^*}{f_\pi} = \left(\frac{\langle \bar{q}q \rangle^*}{\langle \bar{q}q \rangle} \right)^{1/2} \frac{m_\pi}{m_\pi^*}. \quad (8.8)$$

Now, to linear order in density we have

$$\frac{\langle \bar{q}q \rangle^*}{\langle \bar{q}q \rangle} = 1 - \frac{\rho \sigma_{\pi N}}{f_\pi^2 m_\pi^2} \approx 0.63 \quad \text{for } \rho = \rho_0. \quad (8.9)$$

Setting (8.6) equal to (8.7) at $\rho = \rho_0$ and using (8.8), we find that in order for the Nambu scaling to apply to density, the pion mass should scale up with density by a factor

$$\frac{m_\pi^*}{m_\pi} = \left(\frac{\langle \bar{q}q \rangle}{\langle \bar{q}q \rangle^*} \right)^{1/2} \approx 1.26 \quad \text{for } \rho = \rho_0. \quad (8.10)$$

It turns out that this increase seems to be supported empirically although it is not clear whether the “measured” mass is the same quantity that appears in the in-medium GMOR relation. Experiments which pinned down the increase in pion mass from bare mass by a factor of $1.20 \sim 1.24$ were performed recently at GSI [118] in the deeply bound states

of ^{207}Pb . Since the outer part of the pion wave functions is at the densities rather less than nuclear matter density, these factors may represent the lower limits and a factor of 1.26 for $\rho = \rho_0$ seems quite reasonable. Thus the Nambu scaling *may* hold at least near nuclear matter density.

We should mention however two caveats to this. One is that two-loop chiral perturbation calculations find smaller values for the mass shift. The calculation by Park et al [119] predicts the pion mass at nuclear matter density to be at most $6 \sim 7\%$ higher than that at zero density. This is a calculation where the off-shell ambiguity associated with the pion in medium being an off-shell quantity is minimized. For a pion field that contains substantial off-shell ambiguity, one can easily obtain the mass factor $1.20 \sim 1.24$ but this seems to be unreasonable. Another two-loop calculation by Kaiser and Weise [120] for the pion self-energy in asymmetric nuclear matter obtains about 10 % increase in mass of the pion which is consistent with the result of Park et al. The other caveat is that the scaling (8.6) with the value (8.9) at nuclear matter density would disagree with the value expected from the experimental value (6.2) for δg_l , Eq.(6.4), for which we have $\Phi(\rho_0) = 0.78$.

In the above we have established that NJL theory at mean field [112] works well in describing the scaling of masses. In ref.[78] it was shown that the Walecka mean field theory in terms of nucleons can be carried over with smooth change of parameters to a mean field theory of constituent quarks at higher densities. The constituent quark goes massless in the chiral limit with chiral restoration. In Section 11.2, we will suggest how this can be understood in terms of color-isospin locking and hidden local symmetry.

In low-energy nuclear physics we are used to introducing form factors with couplings. These decrease with increasing scale. In modern language, the form factors are there as a sort of regularization that plays an important role in effective field theories as discussed in Section 3. Why do we do so well here without form factors ? We believe that the reason lies in the special role that the scalar field σ has in chiral restoration. *A priori* it would seem reasonable to continue the linear approximation for σ -exchange between quarks

$$\overline{Q}(q^2 - m_\sigma^{\star 2})^{-1}Q \quad (8.11)$$

where Q is the constituent quark, down to small m_σ^{\star} where higher-order or nonlinear effects must enter. We believe that these effects must be counterbalanced, to a large extent, by form factors. As we develop in the next section, this does not seem to be so with vector mesons, where form factors really do not cut down the exchanges. As formulated more precisely in Section 11.2, the vector meson exchange at low densities (i.e., flavor symmetry) changes into gluon exchange at higher density (QCD symmetry) and asymptotic freedom assures that their effects go to zero with increasing scale.

9 SIGNALS FROM HEAVY-ION COLLISIONS

Extreme conditions of high temperature and/or high density are expected to be created in relativistic heavy-ion collisions being probed in RHIC at Brookhaven and to

be probed in CERN’s LHC. In this section, we discuss how BR scaling manifests itself in heavy-ion processes, leaving high-density zero-temperature situation to later sections. Before going into the details, we first define precisely the meaning of BR scaling in the context that we shall use in this section.

9.1 Top-Down and Bottom-Up and How They Connect

There are effectively two ways of approaching BR scaling. The BR scaling as first suggested in [2] is a “top-down” version starting, using quark mean field, from a high temperature/density regime wherein constituent quarks (or quasiquarks) are relevant degrees of freedom, i.e., near the chiral transition point and then extrapolating down to a low temperature/density regime wherein hadrons are appropriate degrees of freedom. In contrast, Rapp and Wambach and others [121] calculated medium dependent hadron properties in hadronic variables in a strong-coupling perturbation approach. We shall call this a “bottom-up” approach. The advantage of the latter approach is that one can resort to standard nuclear physics information using phenomenological Lagrangians at tree order with more or less known coupling constants. This approach has been found to be successful in reproducing the medium-dependent ρ -meson properties deduced from the CERN CERES dilepton experiments. In these experiments, most of the ρ -mesons come from densities less than nuclear matter density. In the low-density regime, the phenomenological approach is justified by *construction* in a well-prescribed way. The disadvantage of this approach is that as density increases beyond nuclear matter density, the possible vacuum change makes the tree order calculation unreliable because of the strong coupling or more precisely a large anomalous dimension which signals that one is fluctuating at a wrong ground state and that it is preferable to shift to a different vacuum even though no phase transitions are involved. This aspect was associated above with differences in topological vacua.

In [122, 123, 124], the top-down BR scaling and the bottom-up Rapp-Wambach approach were combined into a unified description. We will follow this description. We consider the most important component of the Rapp-Wambach theory, i.e., the introduction of the “ ρ -sobar” which is the excitation of the $I = 1, J = 3/2$ $N^*(1520)$ coupled together with the nucleon-hole to the quantum numbers of the ρ . There are of course other N^* -hole states of the same quantum numbers which would come in but here we shall focus on the dominant component only. At zero density this isobar-hole state is at 580 MeV. The phenomenological Lagrangian coupling the “elementary ρ ” and the isobar-hole $\hat{\rho}$ that we shall use²⁹ is

$$\mathcal{L}_{\rho N^* N}^{s-wave} = \frac{f_\rho}{m_\rho} \psi_{N^*}^\dagger (q_0 \vec{s} \cdot \vec{\rho}_a - \rho_a^0 \vec{s} \cdot \vec{q}) \tau_a \psi_N + h.c. , \quad (9.1)$$

where $f_{\rho N^* N}^2/4\pi \simeq 5.5$ from fits to photodisintegration data. Here (\vec{q}, q_0) are the ρ -meson momenta. we shall keep only the q_0 term in our dilepton discussion. The two branches

²⁹The non-covariant form of the Lagrangian is not unique as pointed out in [125].

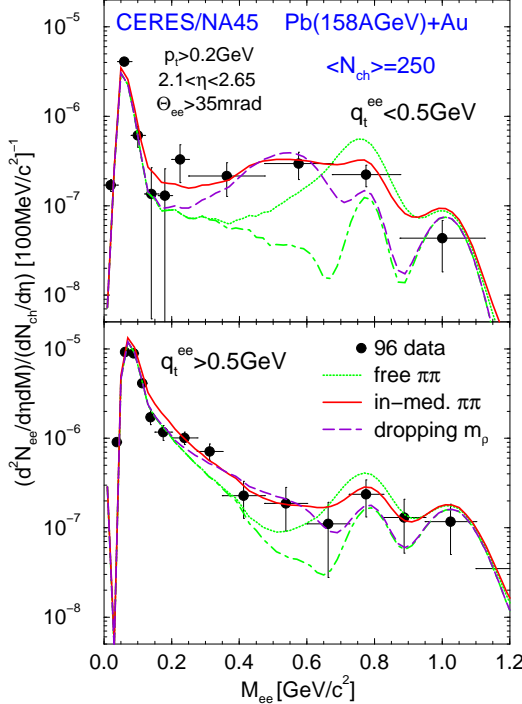


Figure 11: Dilepton data from central Pb (158 GeV/u)+Au collisions compared with Rapp/Wambach (labeled as “in-medium $\pi\pi$ ”) and Brown/Rho (labeled as “dropping m_ρ ”) for $q_t^{ee} < 0.5$ GeV (upper) and $q_t^{ee} > 0.5$ GeV (lower).

of the ρ spectral function can be located by solving self-consistently the real part of the ρ -meson dispersion relation (taking $\vec{q} = 0$)

$$q_0^2 = m_\rho^2 + \text{Re}\Sigma_{\rho N^* N}(q_0). \quad (9.2)$$

The natural width of the $N^*(1520)$ is supplemented at $\rho = \rho_0$ by an additional medium-dependent width of 250 MeV.

Including also the backward-going graph, the $N^*(1520)N^{-1}$ excitation contributes to the self-energy of the ρ -meson at nuclear matter density n_0 (in this section we denote density by n to avoid confusion with the ρ -meson))

$$\Sigma_{\rho N^* N}(q_0) = f_{\rho N^* N}^2 \frac{8}{3} \frac{q_0^2}{m_\rho^2} \frac{n_0}{4} \left(\frac{(\Delta E)^2}{(q_0 + i\Gamma_{tot}/2)^2 - (\Delta E)^2} \right), \quad (9.3)$$

where $\Delta E \simeq 1520 - 940 = 580$ MeV and $\Gamma_{tot} = \Gamma_0 + \Gamma_{med}$ is the total width of the $N^*(1520)$. If we neglect any in-medium correction to the width of the $N^*(1520)$ we find two solutions, located at $q_0^- \simeq 540$ MeV and $q_0^+ \simeq 895$ MeV. As n increases, Σ will become larger and initially the q_0 of the lower branch will go down. However, this downward movement will be halted once q_0 has decreased substantially. We note that already at $n = 0$, the $N^*(1520)$ decays $\sim 15\%$ of the time to $N\rho$ indicating that there is already mixing there. The mixing becomes stronger with increasing n .

As noted, the Rapp-Wambach theory works well for the low densities $n \lesssim n_0$ important for the CERES experiments. We show in Fig.11 fits to the CERES spectra with both Rapp-Wambach and Brown-Rho theories. In the BR approach, however, the vacuum is “sliding,” that is, for each new density, one has a new “vacuum” to fluctuate around. Recalling the skyrmion structure for given baryon number, we observe that “vacua” are solitonic in nature and cannot be connected by perturbation theory. Thus, the vacuum at $n \neq 0$ has no continuous connection with that at $n = 0$. This means that with the Lagrangian (9.1), the Rapp-Wambach theory can never approach the BR theory as density increases. One can see from (9.3) that the self-energy will stop bringing down the energy of the lower branch of the ρ as $(q_0/m_\rho)^2$ becomes smaller. This situation is somewhat like the usual Walecka mean field theory where the nucleon self-energy has a scalar density $\rho_s = \psi^\dagger \gamma_0 \psi$ in it. As ρ_s goes to zero, the self-energy which involves ρ_s linearly does likewise, so the nucleon mass can go to zero only at $n = \infty$. However with the introduction of negative energy states in Nambu-Jona-Lasinio theory, the mass of the constituent quark goes smoothly to zero at a density $n_c \sim 3n_0$ [112]. As argued in [123, 124], this can happen with (9.3) *only if* we replace there the factor $(q_0/m_\rho)^2$ by $\sim \epsilon (q_0/m_\rho^*)^2$. The unknown factor ϵ can be adjusted to give the same critical density as in NJL model. It is plausible that this change-over is related to the requirement in the Harada-Yamawaki scheme which is not present in few-order perturbation theory that the phase transition coincide with Georgi’s vector-limit fixed point. Once one accepts this, what follows turns out to be quite reasonable: with $\epsilon = 1$, m_ρ^* drops to zero at the same density as in the NJL model, $n_c \sim 3n_0$.

9.2 Distinguishing Rapp/Wambach and Brown/Rho

The modified sober picture obtained by replacing m_ρ by m_ρ^* as described above still differs in detail from the BR scaling picture of 1991 even though they describe more or less equally well the $m_\rho^* \rightarrow 0$ limit, because at any density less than n_c there are two branches of the ρ quantum number. However as $n \rightarrow n_c$ the width of the lower branch goes to zero and all of the spectral strength goes into it so we do recover the original BR scaling. We will encounter this feature once more in Section 11.2 from the consideration of hidden local symmetry and color-flavor-locking in QCD.

At densities $n \lesssim n_0$, the lower ρ branch most likely becomes very wide because of the large number of open channels that it couples to, which has led Rapp and Wambach to interpret their fit to the dilepton data from the broadening of the ρ , the lower parts of the spectral function contributing importantly to the dilepton production because of the greater Boltzmann factors.

So how do we distinguish between Rapp/Wambach and Brown/Rho; equivalently between broadening and movement towards chiral restoration? Formally we do not violate gauge invariance or any other invariance by using m_ρ^* rather than m_ρ . It is really up to nature to decide.

In a recent paper, Alam, Sarkar, Hatsuda, Nayak and Sinha [126] have suggested

that nature has decided for Brown/Rho³⁰. This work is extended in Alam et al [129]. In these papers, the calculations were based on mesonic processes such as $\pi\rho \rightarrow \pi\gamma$, $\pi\pi \rightarrow \rho\gamma$, etc. leading to thermal production of photons. The observation then was that when increasing the width of the ρ meson to ~ 1 GeV in order to take into account medium effects, the photon yield decreases as compared to the case using the free ρ width, thus underestimating the spectra. However these calculations neglect the contributions to the photons coming from some of the processes that increase the width, e.g., the $\rho \rightarrow N^*(1520)N^{-1}$ excitation (the collective “ ρ -sobar”) which provides the lower-mass ρ excitation in the Rapp/Wambach calculation. This contributes to the photon through the $N^*(1520) \rightarrow N\gamma$ decay. Calculations in progress (by C. Gale, M.A. Hadasz and R. Rapp) show that these baryonic processes contribute importantly so the conclusions of [126, 129] may be premature.

The bottom-up approach of Rapp and Wambach should be reliable at low density since it is based on phenomenological Lagrangians constructed in standard nuclear physics with known properties. Our principal argument is that this picture should cede to the Brown-Rho picture at higher densities replacing m_ρ by m_ρ^* in scaling the Lagrangian required to be consistent with Harada-Yamawaki’s vector manifestation. Of course much more detailed experiments will be needed to confirm this scenario.

³⁰In fact Alam et al suggest two scenarios that can describe the photons, one being the hadronic description with BR scaling and the other one in which quark-gluon-plasma (QGP) is initially produced at a temperature $T_i = 196$ MeV. One has a mixed phase of QGP and hadronic matter which persists down to a transition to hadronic matter at $T_c = 160$ MeV. In a later paper [127], Sarkar et al find that for relatively central collisions, the dilepton yield can be described by either of the two scenarios, BR scaling or one in which the QGP is originally produced as above. These authors find that “as of yet, it has not been possible to explain the observed low-mass enhancement of dileptons measured in the Pb+Au collisions as well as in the S+Au collisions at the CERN SPS in a scenario which does not incorporate in-medium effects in the vector meson mass.”

As noted earlier, we believe that two descriptions, BR scaling and the one in which the QGP is initially produced in a mixed phase, to be “dual” as long as the number of degrees of freedom in the former is constrained to equal that in the latter. The mixed phase in the scenario with the QGP formation could, however, be just the part of a second-order phase transition in the BR scaling scenario. In the latter the energy is used up, going down in temperature through the phase transition, in building up the scalar field energy as the hadrons gain back their masses. Most of the entropy decrease will come from the higher mass hadrons disappearing as their mass is increased, due to decreasing Boltzmann factors, rather than through expansion. It seems therefore reasonable that the various freeze-out species exhibit thermal equilibration at the chiral restoration temperature, the one at which hadron masses go to zero in the chiral limit in the BR scaling scenario, since the system spends a long time there.

Although the dropping masses with BR scaling and production of QGP in mixed phase at $T \sim 200$ MeV may be dual around the phase transition, it is excluded that the latter scenario describe the dropping masses found in ~ 300 MeV inelastic electron scattering, which we described in the previous section, or the many indirect evidences we described earlier in our review. In other words, the duality is useful only at higher scales, near and above the chiral restoration transition. One should remember the Bég-Shei theorem, that the nature of symmetry realization (i.e., Wigner-Weyl vs. Nambu-Goldstone) is irrelevant to discussing the short-distance symmetry [128].

10 “BROAD-BAND EQUILIBRATION” OF STRANGENESS IN HEAVY-ION COLLISIONS

10.1 Kaons and Chiral Symmetry

The strange quark is massive compared with the light (u, d) quarks, with $m_s \sim 150$ MeV. This gives the kaon a mass of $\sim 1/2$ GeV. This is a manifestation of both explicit and spontaneous chiral symmetry breaking. Unlike the previous cases where the decondensing of the condensate $\langle \bar{q}q \rangle$ – that is, restoring the spontaneously broken chiral symmetry – enters directly into the phenomena we were looking at, here it is the “rotating away” of the explicit chiral symmetry breaking intricately tied in with the decondensing of $\langle \bar{q}q \rangle$ that is principally manifested in the behavior of kaons in dense medium. This section deals with how this aspect is probed in the kaon production experiments at GSI. Based on work done recently [130], we will develop, in conjunction with BR scaling, the notion of “broadband equilibration” in heavy-ion processes and suggest the vector decoupling in dense medium.

10.2 Equilibration vs. Dropping Kaon Mass

Following work by Hagedorn [131] on production of anti- ${}^3\text{He}$, Cleymans et al [132] have shown that for low temperatures, such as found in systems produced at GSI, strangeness production is strongly suppressed. The abundance of K^+ mesons, in systems assumed to be equilibrated, is given by [133],

$$n_{K^+} \sim e^{-E_{K^+}/T} V \left\{ g_{\bar{K}} \int \frac{d^3 p}{(2\pi)^3} e^{-E_{\bar{K}}/T} + g_{\Lambda} \int \frac{d^3 p}{(2\pi)^3} e^{-(E_{\Lambda} - \mu_B)/T} \right\}. \quad (10.1)$$

Here the g 's are the degeneracies. Because strangeness must be conserved in the interaction volume V , assumed to be that of the equilibrated system for each K^+ which is produced, a particle of “negative strangeness”³¹ containing s , say, \bar{K} or Λ , must also be produced, bringing in the \bar{K} or Λ phase space and Boltzmann factors. The K^+ production is very small at GSI energies because of the low temperatures which give small Boltzmann factors for the \bar{K} and Λ in addition to the small Boltzmann factor for the K^+ . Note the linear dependence on interaction volume which follows from the necessity to include \bar{K} or Λ phase space.

In an extensive and careful analysis, Cleymans, Oeschler and Redlich [133] show that measured particle multiplicity ratios π^+/p , π^-/π^+ , d/p , K^+/π^+ , and K^+/K^- – but not η/π^0 – in central Au-Au and Ni-Ni collisions at (0.8-2.0)A GeV are explained in terms of a thermal model with a common freeze-out temperature and chemical potential, if collective flow is included in the description. In other words, a scenario in which the kaons and anti-kaons are equilibrated appears to work well. This result is puzzling in view of a recent

³¹By “negative strangeness” we are referring to the negatively charged strange quark flavor. The positively charged anti-strange quark will be referred to as “positive strangeness.”

study by Bratkovskaya et al [134] that shows that the K^+ mesons in the energy range considered would take a time of ~ 40 fm/c to equilibrate. We remark that this is roughly consistent with the estimate for higher energies in the classic paper by Koch, Müller and Rafelski [135] that strangeness equilibration should take ~ 80 fm/c. Such estimates have been applied at CERN energies and the fact that emergent particle abundances are described by Boltzmann factors with a common temperature ~ 165 MeV [136] has been used as part of an argument that the quark/gluon plasma has been observed.

We interpret the result of [133] as follows. Since free-space masses are used for the hadrons involved, Cleymans et al [133] are forced to employ a μ_B substantially less than the nucleon mass m_N in order to cut down Λ production as compared with K^- production, the sum of the two being equal to K^+ production. This brings them to a diffuse system with density of only $\sim \rho_0/4$ at chemical freeze-out. But this is much too low a density for equilibration.

We shall first show how this situation can be improved by replacing the K^- mass by the K^- energy at rest $\omega_{K^-}^* \equiv \omega_-(k=0) < m_K$. (The explicit formula for ω_{\pm} is given later, see eq. (10.25).) In doing this, we first have to reproduce the K^+ to K^- ratio found in the Ni + Ni experiments [137]:

$$n_{K^+}/n_{K^-} \simeq 30. \quad (10.2)$$

Cleymans et al reproduce the earlier smaller ratio of 21 ± 9 with $\mu_B = 750$ MeV and $T = 70$ MeV. How this or rather (10.2) comes out is easy to see. The ratio of the second term on the RHS of eq.(10.1) to the first term is roughly the ratio of the exponential factors multiplied by the phase space volume

$$R = \frac{g_\Lambda}{g_{\bar{K}}} \left(\frac{\bar{p}_\Lambda}{\bar{p}_{\bar{K}}} \right)^3 \frac{e^{-(E_\Lambda - \mu_B)/T}}{e^{-E_{K^-}/T}} \approx \left(\frac{m_\Lambda}{m_{\bar{K}}} \right)^{3/2} \frac{e^{-(m_\Lambda - \mu_B)/T}}{e^{-m_{K^-}/T}} \approx 21 \quad (10.3)$$

where we have used $g_\Lambda \approx g_{\bar{K}} \simeq 2$, $(\bar{p})^2/2m \simeq \frac{3}{2}T$, $E_\Lambda = 1115$ MeV and $E_{\bar{K}} = 495$ MeV. Inclusion of the Σ and Ξ hyperons would roughly increase this number by 50% with the result that the ratio of K^- to Λ, Σ, Ξ production is ³²

$$\frac{n_{K^-}}{n_{\Lambda+\Sigma+\Xi}} \simeq 1/32. \quad (10.4)$$

Since a K^+ must be produced to accompany each particle of one unit of strangeness (to conserve strangeness flavor), we then have

$$n_{K^+}/n_{K^-} \sim 33. \quad (10.5)$$

³²In order to reproduce this result with $\mu_B = 750$ MeV and $T = 70$ Mev within our approximation, we have assumed only the Σ^- and Σ^0 hyperons to equilibrate with the Λ . This may be correct because the Σ^+ and Ξ couple more weakly. Inclusion of the latter could change our result slightly. Probably they should be included in analysis of the AGS experiments at higher energies where they would be more copiously produced.

This is consistent with the empirical ratio (10.2). It should be noted that had we set μ_B equal to m_N , we would have had the K^+ to K^- ratio to be ~ 280 because it costs so much less energy to make a Λ (or Σ) rather than K^- in this case. In other words the chemical potential μ_B is forced to lie well below m_N in order to penalize the hyperon production relative to that of the K^- 's.

One can see from Fig.5 in Li and Brown [138] that without medium effects in the K^- mass, the K^+/K^- ratio is ~ 100 , whereas the medium effect decreases the ratio to about 23. This suggests how to correctly redo the Cleymans et al's analysis, namely, by introducing the dropping K^- mass into it.

In the next subsection we show that positive strangeness production takes place chiefly at densities greater than $2\rho_0$. As the fireball expands to lower densities the amount of positive strangeness remains roughly constant. The number of K^+ 's is such as to be in equilibrium ratio K^+/π^+ with the equilibrated number density of pions at $T = 70$ MeV, $n_\pi \approx 0.37 T_{197}^3 \text{ fm}^{-3}$. Only in this sense do the K^+ 's equilibrate. It will be noted, however, that with the T of 70 MeV, μ_B is chosen so that the empirical number of hyperons are produced. Since the number of K^+ is one greater than that of the hyperons (including the K^- in the negative strangeness), it will also be the apparent equilibrated ratio for this μ_B and T . Thus, with these two latter parameters the π , K^+ and K^- can be put into apparent equilibration. It is fairly easy for the nucleons to equilibrate with the pions at the given temperature because of the strong interaction.

It is amusing to note that the “equilibrated ratio” of ~ 30 for the n_{K^+}/n_{K^-} holds over a large range of densities for $T = 70$ MeV, once density-dependent K^- masses are introduced, in that the ratio R of (10.3) is insensitive to density. (Remember that because of the small number of K^- 's, the number of K^+ 's must be nearly equal to the number of hyperons, Λ , Σ^- and Ξ , in order to conserve strangeness.) This insensitivity results because $\omega_{K^-}^*$ decreases with density at roughly the same rate as μ_B increases. We can write R of (10.3), neglecting possible changes in T and $m_{\bar{K}}$ in our lowest approximation, as³³

$$R = \left(\frac{m_\Lambda}{m_{\bar{K}}} \right)^{3/2} e^{(\mu_B + \omega_{K^-}^*)/T} e^{-m_\Lambda/T}. \quad (10.6)$$

As will be further stressed later, the most important point in our arguments is that *the $\mu_B + \omega_{K^-}^*$ is nearly constant with density*. This is because whereas μ_B increases from 860 MeV to 905 MeV as ρ goes from $1.2\rho_0$ to $2.1\rho_0$, $\omega_{K^-}^*$ decreases from 380 MeV to 332 MeV, the sum $\mu_B + m_{K^-}^*$ decreasing very slightly from 1240 MeV to 1237 MeV. Indeed, even at $\rho = \rho_0/4$, $\mu_B + m_{K^-}^* \sim 1218$ MeV, not much smaller.

We believe that the temperature will change only little in the region of dropping masses because in a consistent evolution (which we do not carry out here) the scalar field energy $m_\sigma^2 \sigma^2/2$ in a mean field theory plays the role of an effective bag constant. In ref.[112] (which was reviewed in Section 8) this is phrased in terms of a modified Walecka

³³To be fully consistent, we would also have to consider the medium modifications of the Λ and K^+ properties. These and other improvements are left out for our rough calculation.

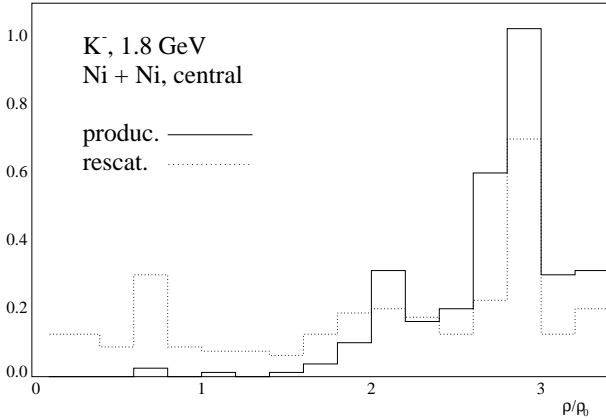


Figure 12: Calculations by Bratkovskaya and Cassing (private communication) which show the density of origin and that of the last interaction of the K^- mesons.

theory,

$$B_{eff} = \frac{1}{2} m_\sigma^2 \sigma^2 \Rightarrow \frac{1}{2} m_\sigma^2 (M_N/g_{\sigma NN})^2, \quad (10.7)$$

the σ going to $M_N/g_{\sigma NN}$ as the nucleon effective mass goes to zero with chiral restoration. Most of the energy with compression to higher densities goes with this effective bag constant, estimated [112] to be ~ 240 MeV/fm 3 , rather than heat, mocking up the behavior of a mixed phase with constant temperature. Moreover at $\rho = 2\rho_0$ where m_N^* may be $\sim 0.5m_N$, only about 25% of the bag constant B may have been achieved, so there may be some increase in temperature. We shall, at the same level of accuracy, have to replace $m_{\bar{K}}$ in the prefactor of eq.(10.6) by $\omega_{K^-}^*$. We adjust the increase in temperature so that it exactly compensates for the decrease in prefactor so that the K^+/K^- ratio is kept the same, as required by experiment [137]. We then find that the temperature at $\rho = 2\rho_0$ must be increased from 70 to 95 MeV. This is roughly the change given by that in inverse slopes of K^- and K^+ transverse momentum distributions found in going from low multiplicities to high multiplicities [137].

In any case, we see that R will depend but little on density. This near cancellation of changes in the factors is fortunate because the $K^- + p \leftrightarrow \Lambda$ reaction, operating in the negative strangeness sector, is much stronger than the positive strangeness reactions, so the former should equilibrate to densities well below $2\rho_0$ and we can see that the “apparent equilibration” might extend all the way down to $\rho \sim \rho_0/4$.

The near constancy of R with density also explains the fact the K^+/K^- ratio does not vary with centrality³⁴. Although R is the ratio of Λ ’s to K^- ’s, both of which are in the negative strangeness sector, nonetheless, the number of K^+ ’s must be equal to the sum of the two and since the Λ ’s are much more abundant than the K^- ’s, R essentially represents the K^+/K^- ratio.

³⁴We are grateful to Helmut Oeschler for pointing this out to us.

Detailed transport results of Bratkovskaya and Cassing (see Fig.12) show the last scattering of the detected K^- to be spread over all densities from $\rho_0/2$ to $3\rho_0$, somewhat more of the last scatterings to come from the higher density. This seems difficult to reconcile with a scenario of the K^- numbers being decided at one definite density and temperature, but given our picture of dropping masses, one can see that the K^+/K^- ratio depends little on density, that is, on μ_B at which the K^- last interacts. In any case we understand from our above argument that the apparent density of equilibration can be chosen to be very low in a thermal description and still get more or less correct K^+/K^- ratio.

10.3 The Equilibrium K^+/π^+ Ratio

We show here how our argument that gives a correct K^+/K^- ratio can reproduce the K^+/π^+ ratio. Let us leave $T = 70$ MeV and choose $\rho \sim 2\rho_0$ as educated guesses. We are thereby increasing the equilibration density by a factor ~ 8 . We then calculate the baryon density for this μ_B and $T = 70$ MeV and find $\rho = 2\rho_0$ which checks the consistency.

According to Brown et al [139] the K^+ production under these conditions will come chiefly from $BB \rightarrow N\Lambda K$, with excited baryon states giving most of the production. From the solid curve for $\rho/\rho_0 = 2$ in fig.9 of [139] we find $\langle\sigma v\rangle \sim 2 \times 10^{-3}$ mb = 2×10^{-4} fm 2 . The rate equation reads

$$\delta\Psi_K = \frac{1}{2}(\sigma_{BB}^{BYK} v_{BB})n_B^2 \simeq \frac{1}{2}(2 \times 10^{-4} \text{ fm}^2)\rho_B^2 = dn/dt = \frac{1}{9} \times 10^{-4} \text{ fm}^{-4} \quad (10.8)$$

where B , Y and K stand, respectively, for baryon, hyperon and kaon. For this, we have taken $\langle\sigma_{BB}^{BYK} v_{BB}\rangle$ from fig.9 of [139] and $\rho = 2\rho_0 = \frac{1}{3}$ fm $^{-3}$. Choosing a time $t = 10$ fm/ c we obtain

$$n_{K^+} \simeq \delta\Psi_K t = \frac{2}{9} \times 10^{-3} \text{ fm}^{-3}. \quad (10.9)$$

Now equilibrated pions have a density

$$n_\pi = 0.37(T/197\text{MeV})^3 \text{ fm}^{-3} = 0.016 \text{ fm}^{-3} \quad (10.10)$$

for $T = 70$ MeV. From (10.9) and (10.10) we get

$$n_{K^+}/n_{\pi^+} \simeq 0.0069 \quad (10.11)$$

which is slightly below the ‘‘equilibrated value’’ of 0.0084 of Table 1 of Cleymans et al [133]. Production of K^+ by pions may increase our number by $\sim 25\%$ [140].

Our discussion of K^+ production is in general agreement with earlier works by Ko and collaborators [140, 141]. In fact, if applied at the quark level, the vector mean field is conserved through the production process in heavy-ion collisions, so it affects only the strangeness condensation in which there is time for strangeness non-conservation. These

earlier works establish that at the GSI energies the K^+ content remains roughly constant once the fireball has expanded to $\sim 2\rho_0$, so that in this sense one can consider this as a chemical freeze-out density.

It should be noted that in the papers [142, 139, 140, 141] and others, the net potential – scalar plus vector – on the K^+ -meson is slightly attractive at $\rho \sim 2\rho_0$ even though the repulsive vector interaction is not decoupled. A hint for such change-over was noted already at nuclear matter density by Friedman, Gal and Mares [143]. Since in our top-down description the vector interaction can be thought of as applied to the quark (matter) field in the K^+ , the total vector field on the initial components of a collision is then the same as on the final ones, so the vector mean fields have effectively no effect on the threshold energy of that process. Our proposal here is that the vector mean field on the K^+ should be below the values used by the workers in [142, 139, 140, 141] due to the decoupling. However, in comparison with [142], our total potential on the K^+ at $\rho = 2\rho_0$ is ~ -85 MeV, as compared with their ~ -30 MeV. We have not redone the calculation of [139] to take into account this difference.

10.4 The Top-Down Scenario of K^\pm Production

Brown and Rho [78] discussed fluctuations in the kaon sector in terms of a simple Lagrangian

$$\delta\mathcal{L}_{KN} = \frac{-6i}{8f^{*2}}(\overline{N}\gamma_0 N)\overline{K}\partial_t K + \frac{\Sigma_{KN}}{f^{*2}}(\overline{N}N)\overline{K}K + \dots \equiv \mathcal{L}_\omega + \mathcal{L}_\sigma + \dots \quad (10.12)$$

It was suggested there that at high densities, the constituent quark or quasi-quark description can be used with the ω -meson coupling to the kaon viewed as a *matter field* (rather than as a Goldstone boson). Such a description suggests that the ω coupling to the kaon which has one non-strange quark is $1/3$ of the ω coupling to the nucleon which has three non-strange quarks. The \mathcal{L}_ω in the Lagrangian was obtained by integrating out the ω -meson as in the baryon sector. We may therefore replace it by the interaction

$$V_{K^\pm} \approx \pm \frac{1}{3}V_N. \quad (10.13)$$

In isospin asymmetric matter, we shall have to include also the ρ -meson exchange [78] with the vector-meson coupling treated in the top-down approach.

For the top-down scenario, we should replace the chiral Lagrangian (10.12) by one in which the “heavy” degrees of freedom figure explicitly. This means that $\frac{1}{2f^{*2}}$ in the first term of (10.12) should be replaced by g^{*2}/m_ω^{*2} and $\frac{\Sigma_{KN}}{f^{*2}}$ in the second term by $\frac{2}{3}m_K\frac{g_\sigma^{*2}}{m_\sigma^{*2}}$ assuming that both ω and σ are still massive. We will argue below that while the ω mass drops, the ratio g^{*2}/m_ω^{*2} should stay constant or more likely decrease with density and that beyond certain density above nuclear matter, the vector fields should decouple. On the other hand, g_σ is not scaled in the mean field that we are working with; the motivation for this is given in Brown, Buballa and Rho [112] who construct the chiral restoration

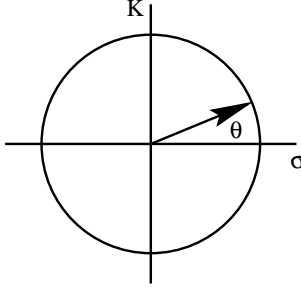


Figure 13: Projection onto the σ, K plane. The angular variable θ represents fluctuation toward kaon mean field.

transition in the mean field in the Nambu-Jona-Lasinio model. Thus

$$\frac{\Sigma_{KN}}{f^{*2}} \approx \frac{2}{3} m_K \frac{g_\sigma^2}{m_\sigma^{*2}}. \quad (10.14)$$

In this framework, m_σ^* is the order parameter for chiral restoration which drops à la BR scaling [2]:

$$\frac{m_\sigma^*}{m_\sigma} \equiv \Phi(\rho) \simeq \frac{1}{1 + y\rho/\rho_0} \quad (10.15)$$

with $y \simeq 0.28$, at least for $\rho \lesssim \rho_0$ ³⁵.

Once the vector is decoupled, a simple way to calculate the in-medium kaon effective mass, equivalent to using the \mathcal{L}_σ , is to consider the kaon as fluctuation about the “ σ ”-axis in the V-spin formalism [144] as depicted pictorially in Fig.13. The Hamiltonian for explicit chiral symmetry breaking is

$$\begin{aligned} H_{\chi SB} &= \Sigma_{KN} \langle \bar{N}N \rangle \cos(\theta) + \frac{1}{2} m_K^2 f^{*2} \sin^2(\theta) \\ &\simeq \Sigma_{KN} \langle \bar{N}N \rangle \left(1 - \frac{\theta^2}{2}\right) + \frac{1}{2} m_K^2 f^{*2} \theta^2 \end{aligned} \quad (10.16)$$

where the last expression is obtained for small fluctuation θ . Dropping the term independent of θ , we find

$$m_K^{*2} = m_K^2 \left(1 - \frac{\Sigma_{KN} \langle \bar{N}N \rangle}{f^{*2} m_K^2}\right). \quad (10.17)$$

Using eq. (10.14) we obtain

$$m_K^{*2} = m_K^2 \left(1 - \frac{2 g_\sigma^2 \langle \bar{N}N \rangle}{3 m_\sigma^{*2} m_K}\right). \quad (10.18)$$

³⁵ y may well be different from this value for $\rho > \rho_0$. In fact the denominator of $\Phi(\rho)$ could even be significantly modified from this linear form. At present there is no way to calculate this quantity from first principles.

In accord with Brown and Rho [78] we are proposing that eq.(10.17) should be used for low densities, in the Goldstone description of the K^\pm , and that we should switch over to eq.(10.18) for higher densities. It is possible that the m_K appearing in (10.18) should be replaced by m_K^* for self-consistency but the dropping of m_σ^{*2} makes the m_K^* of (10.18) decrease more rapidly than that of (10.17) so that eq.(10.17) with $\langle \bar{N}N \rangle$ set equal to the vector density ρ ³⁶, a much used formula valid to linear order in density

$$m_K^{*2} \approx m_K^2 \left(1 - \frac{\rho \Sigma_{KN}}{f^2 m_K^2} \right) \quad (10.19)$$

obviously gives too slow a decrease of m_K^* with density.

Although the above are our chief points, there are two further points to remark. One, even without scaling, our vector interaction on the kaon is still too large. Two, more importantly, there is reason to believe in the large Σ_{KN} term,

$$\Sigma_{KN} \sim 400 \text{ MeV.} \quad (10.20)$$

This comes from scaling of the pion sigma term

$$\Sigma_{KN} \equiv \frac{(m_u + m_s) \langle N | \bar{u}u + \bar{s}s | N \rangle}{(m_u + m_d) \langle N | \bar{u}u + \bar{d}d | N \rangle} \Sigma_{\pi N}. \quad (10.21)$$

Taking $m_s \sim 150$ MeV, $m_u + m_d \sim 12$ MeV, $\Sigma_{\pi N} = 46$ MeV and $\langle N | \bar{s}s | N \rangle \sim \frac{1}{3} \langle N | \bar{d}d | N \rangle$ from lattice calculations [145], one arrives at (10.20).

Other authors, in adjusting the Σ term to fit the kaon-nucleon scattering amplitudes, have obtained a somewhat smaller Σ_{KN} . This can be understood in the chiral perturbation calculation of C.-H. Lee [146] where the only significant effect of higher chiral order terms can be summarized in the “range term”³⁷; namely Σ_{KN} is to be replaced by an effective Σ ,

$$(\Sigma_{KN})_{eff} = (1 - 0.37 \omega_K^{*2} / m_K^2) \Sigma_{KN}. \quad (10.22)$$

It should be pointed out that although the Σ_{KN} is important at low densities, ω_K decreases with m_K^* , this “range-term” correction becomes less important at higher densities. This effect – which is easy to implement – is included in the realistic calculations.

10.5 Partial Decoupling of the Vector Interaction

10.5.1 Theoretical and experimental evidences

There are both theoretical and empirical reasons why we believe that the vector interaction should decouple at high density.

³⁶The correction to this approximation which may become important as the nucleon mass drops comes as a “1/m” correction in the heavy-fermion chiral perturbation theory (as for the “range term” mentioned below) and can be taken into account systematically. It can even be treated fully relativistically using a special regularization scheme being developed in the field. Our approximation does not warrant the full account of such terms, so we will not include this correction here.

³⁷As mentioned, in the language of heavy-baryon chiral perturbation theory, this corresponds to a “1/m” correction term.

1. We first give the theoretical arguments. We know of three theoretical reasons why the vector coupling g_ω^* should drop with density.

- The first is the observation by Song et al [147] that describing nuclear matter in terms of chiral Lagrangian in the mean field requires the ratio g_ω^*/m_ω^* to at least be roughly constant or even decreasing as a function of density. In fact to quantitatively account for non-linear terms in a mean-field effective Lagrangian, a dropping ratio is definitely favored ³⁸. For instance, as discussed in [147], the in-medium behavior of the ω -meson field is encoded in the “FTS1” version of the non-linear theories of ref.[148]. In fact, because of the attractive quartic ω term in the FTS1 theory, the authors of [148] have (for the parameter $\eta = -1/2$ favored by experiments) $g_\omega^{*2}/m_\omega^{*2} \simeq 0.8g_\omega^2/m_\omega^2$ as modification of the quadratic term when rewritten in our notation . In other words, their vector mean field contains a partial decoupling already at $\rho \approx \rho_0$ although they do not explicitly scale g_ω as we do.

Historically, Walecka-type mean field theories with only quadratic interactions (i.e., linear Walecka model) gave compression modulus $K \sim 500$ MeV, about double the empirical value. This is cured in nonlinear effective field theories like FTS1 by higher-dimension non-renormalizable terms which effectively decrease the growth in repulsion in density. As suggested in [147], an effective chiral Lagrangian with BR scaling can do the same (by the increase in magnitude of the effective scalar field with density) but more economically and efficiently.

This decrease of g_ω^*/m_ω^* as density increases toward nuclear matter density contrasts with the increase of $g_{\rho NN}^*/m_\rho^*$ within the same density range discussed in Section 6.1. This can be explained as follows. In free space $g_\omega \equiv g_{\omega NN} = 3g_{\rho NN}$ whereas near chiral restoration, we expect (as in the case of the quark number susceptibility mentioned below) that $g_{\omega NN}^* \simeq g_{\rho NN}^*$. This implies that at low density, the ω coupling must fall faster than the ρ coupling by “shedding off” the factor of 3.

- The second reason is perhaps more theoretical. We mentioned in Section 4 that in an effective QCD Lagrangian theory with baryons, pions and vector mesons put together in hidden-gauge symmetric way, both g_V^* and m_V^* (where V stands for hidden gauge bosons) are predicted to fall very rapidly with baryon chemical potential [150] ³⁹ The main agent for this behavior is found in [150] to be the pionic one-loop contribution linked to chiral symmetry which is lacking in the mean-field treatment for BR scaling [2]. The Kim-Lee arguments were made for the ρ which has a simple interpretation in terms of hidden gauge symmetry but it will apply to the ω if the nonet symmetry is assumed to hold in nuclear

³⁸Since the non-linear terms – though treated in the mean field – are fluctuation effects in the effective field theory approach, this represents a quantum correction to the BR scaling.

³⁹Kim and Lee found that even the ratio g_V^*/m_V^* fell rapidly. This is at variance with what one would expect if the vector manifestation à la Harada-Yamawaki were realized. As noted, this may be due to the incompleteness of the renormalization group analysis of [150].

medium. It is difficult to be quantitative as to how fast the mass and coupling constant will fall but it is clear that the drop is substantial already near normal nuclear matter density.

On a more profound ground, the vector decoupling in approaching the chiral phase transition could be interpreted as a flow to a fixed point as argued by Harada and Yamawaki [12]. This point will be reinforced in the next section.

- Finally, close to chiral restoration in temperature, there is clear evidence from QCD for an equally rapid drop, specifically, from the quark number susceptibility that can be measured on the lattice [13]. The lattice calculation of the quark number susceptibility dealt with quarks and the large drop in the (isoscalar) vector mean field was found to be due chiefly to the change-over from hadrons to quarks as the chiral restoration temperature is approached from below. The factor of 9 in the ratio $g_{\omega NN}^2/g_{\omega QQ}^2$ (where Q is the constituent quark) should disappear in the change-over. Now since the electroweak properties of a constituent quark (quasiquark) are expected to be the same as those of a bare Dirac particle with $g_A = 1$ and no anomalous magnetic moment (i.e., the QCD quark) [149] with possible corrections that are suppressed as $1/N_c$ [151], there will be continuity between before and after the chiral transition. This is very much in accordance with the “Cheshire-Cat picture” developed elsewhere [11]. In fact, it is possible to give a dynamical (hadronic) interpretation of the above scenario. For instance in the picture of [124] sketched in Section 9, this may be understood as the “elementary” ω strength moving downwards into the “nuclear” ω , the $[N^*(1520)N^{-1}]^{J=1,I=0}$ isobar-hole state involving a single-quark spin flip [125]. The mechanism being intrinsic in the change-over of the degrees of freedom, we expect the same phenomenon to hold in density as well as in temperature. The upshot of this line of argument is that the suppression of the vector coupling is inevitable as density approaches the critical density for chiral transition. In Section 11.2, we will have an additional support for this from color-isospin locking in QCD both in low density and in high density.

We believe that the different behavior of vector and scalar mean fields, the latter to be discussed below, follows from their different roles in QCD. With the vector this is made clearer in the lattice calculations of the quark number susceptibility which involves the vector interactions. In Brown and Rho [13], it is shown that as the description changes from hadronic to quark/gluonic at $T \sim T_c$, the critical temperature for chiral restoration, the vector interaction drops by an order of magnitude, much faster than the logarithmic decrease due to asymptotic freedom. We expect a similar feature in density, somewhat like in the renormalization-group analysis for the isovector vector meson ρ of Kim and Lee [150]. The scalar interaction, on the other hand, brings about chiral restoration and must become more and more important with increasing density as the phase transition point is approached.

2. From the empirical side, the most direct indication of the decoupling of the vector

interaction is from the baryon flow [152] which is particularly sensitive to the vector interaction. The authors of [152] find a form factor of the form

$$f_V(\mathbf{p}) = \frac{\Lambda_V^2 - \frac{1}{6}\mathbf{p}^2}{\Lambda_V^2 + \mathbf{p}^2} \quad (10.23)$$

with $\Lambda_V = 0.9$ GeV is required to understand the baryon flow. Connecting momenta with distances, one finds that this represents a cutoff at

$$R_{cutoff} \sim \frac{\sqrt{6}}{\Lambda_V} \sim 0.5 \text{ fm.} \quad (10.24)$$

Furthermore it is well known that the vector mean field of the Walecka model must be modified, its increase as E/m_N removed, at a scale of ~ 1 GeV. The reason for this is presumably that inside of $R \sim 0.5$ fm, the finite size of the solitonic nucleon must be taken into account. A repulsion still results, but it is scalar in nature as found in [153] and for which there are direct physical indications [154].

10.5.2 Kaons at GSI

The K^+ and K^- energies in the top-down scenario are given by

$$\omega_{\pm} = \pm \frac{\omega_{\pm}}{m_K} V_K + \sqrt{k^2 + m_K^{*2}} \quad (10.25)$$

with V_K given in (10.27) below. Although at high densities it will decouple, the term linear in V_K that figures in the range correction in $(\Sigma_{KN})_{eff}$ will give a slightly different effective mass for K^+ and K^- before decoupling. Although the large distance vector mean field must arise from vector meson exchange, this must be cut off at a reasonably large distance, say, ~ 0.5 fm as indicated by the baryon-flow mentioned above.

For the GSI experiments with temperature ~ 70 MeV, the nucleon and kaon momenta are $|\mathbf{p}_N| \sim 444$ MeV and $|\mathbf{p}_K| \sim 322$ MeV, respectively, and

$$f_V(p) \sim 0.82. \quad (10.26)$$

We therefore propose to use

$$\frac{V_K}{m_K} \approx \frac{1}{3} f_V^2 V_N(p=0)/m_K \sim 0.15 \quad (10.27)$$

This is small. Furthermore we assume it to be constant above ρ_0 . This assumption amounts to taking the vector coupling to drop as $\sim 1/\rho$.

The above arguments could be quantified by a specific model. For example, as alluded to above, the low-lying ρ - and ω -excitations in the bottom-up model can be built up as N^* -hole excitations [124]. At higher densities, these provide the low-mass strength. One might attempt to calculate the coupling constants to these excitations in the constituent-quark (or quasi-quark) model, which as we have suggested would be expected to be more applicable at densities near chiral restoration. Riska and Brown [125] find the quark model couplings to be a factor ~ 2 lower than the hadronic ones [155].

10.6 Schematic Model

10.6.1 First try with the simplest form

On the basis of our above considerations, a first try in transport calculation might use the vector potential with the Song scaling [147] as $g_\omega^*/m_\omega^* = \text{constant}$ and the effective mass

$$m_K^{*2} \approx m_K^2 \left(1 - \frac{\rho(\Sigma_{KN})_{\text{eff}}}{f^2 m_K^2} \right) \quad (10.28)$$

with $\Sigma_{KN} = 400$ MeV and $(\Sigma_{KN})_{\text{eff}}$ given by eq. (10.22). While as argued above the vector coupling will decouple at very high densities, as ω_K drops, the vector potential will become less important even at moderate densities since the factor ω_K/m_K comes into the coupling of the vector potential to the kaon.

Our schematic model (10.28) gives roughly the same mass as used by Li and Brown [138] to predict kaon and antikaon subthreshold production at GSI. For $\rho \sim 3\rho_0$ it gives $m_{K^-}^* \sim 230$ MeV, less than half the bare mass. We predict somewhat fewer K^- -mesons because the (attractive) vector interaction is largely reduced if not decoupled. Cassing et al [142] have employed an $m_{K^-}^*$ somewhat lower than that given by eq.(10.28) to describe a lot of data.

The experimental data verify that our description is quite good up to the densities probed, i.e., $\sim 3\rho_0$. In order to go higher in density, we switch to our top-down description which through eq.(10.14) involves g_σ^2/m_σ^{*2} . Although the scalar interaction could have roughly the same form factor as the vector, cutting it off at ~ 0.5 fm as mentioned above, we believe that this will be countered by the dropping scalar mass m_σ^* which must go to zero at chiral restoration (viewed as an order parameter). Treating the scalar interaction linearly as a fluctuation (as in (10.14)) cannot be expected to be valid all the way to chiral restoration but approaching the latter the σ -particle becomes the “dilaton” in the sense of Weinberg’s “mended symmetry” [59, 60] with mass going to zero (in the chiral limit) together with the pion .

At high densities at which the vector interaction decouples, the K^+ and K^- will experience nearly the same very strong attractive interactions. This can be minimally expressed through the effective mass m_K^* . At low densities where the vector potential not only comes into play but slightly predominates over the scalar potential, the K^+ will have a small repulsive interaction with nucleons. It is this interaction, extrapolated without medium effects by Bratkovskaya et al [134] which gives the long equilibration time of 40 fm/c. However, clearly the medium effects will change this by an order of magnitude.

10.6.2 Implications on kaon condensation and maximum neutron-star mass

While in heavy-ion processes, we expect that taking m_σ^* to zero (or nearly zero in the real world) is a relevant limiting process, we do not have to take m_σ^* to zero for kaon condensation in neutron stars, since the K^- -mass m_K^* must be brought down only to the electron chemical potential $\mu_e \simeq E_F(e)$, the approximate equality holding because

the electrons are highly degenerate. We should mention that it has been suggested that the electron chemical potential μ_e could be kept low by replacing electrons plus neutrons by Σ^- hyperons (or more generally by exploiting Pauli exclusion principle with hyperon introduction) in neutron stars [156]. In this case, the μ_e might never meet m_K^* .

Hyperon introduction may or may not take place, but even if it does, the scenario will be more subtle than considered presently. To see what can happen, let us consider what one could expect from a naive extrapolation to the relevant density, i.e., $\rho \sim 3\rho_0$, based on the *best* available nuclear physics. The replacement of neutron plus electron will take place if the vector mean field felt by the neutron is still high at that density. The threshold for that would be

$$E_F^n + V_N + \mu_e \simeq M_{\Sigma^-} + \frac{2}{3}V_N + S_{\Sigma^-} \quad (10.29)$$

where E_F^n is the Fermi energy of the neutron, M_{Σ^-} the bare mass of the Σ^- and the S_{Σ^-} the scalar potential energy felt by the Σ^- . Here we are simply assuming that the two non-strange quarks of the Σ^- experience 2/3 of the vector mean field felt by the neutron. Extrapolating the FTS1 theory [148]⁴⁰ and taking into account in V_N the effect of the ρ -meson using vector dominance, we find $E_F^n + V_N \sim 1064$ MeV at $\rho \approx 3\rho_0$. From the extended BPAL 32 equation of state with compression modulus 240 MeV [157], the electron chemical potential comes out to be $\mu_e \simeq 214$ MeV. So the left-hand side of (10.29) is $E_F^n + V_N + \mu_e \sim 1278$ MeV. For the right-hand side, we use the scalar potential energy for the Σ^- at $\rho \approx 3\rho_0$ estimated by Brown, Lee and Rapp [158] to find that $M_{\Sigma^-} + \frac{2}{3}V_N + S_{\Sigma^-} \sim 1240$ MeV. The replacement of neutron plus electron by Σ^- looks favored but only slightly.

What is the possible scenario on the maximum neutron star mass if we continue assuming that the calculation we made here can be trusted? A plausible scenario would be as follows. K^- -condensation supposedly occurs at about the same density and both the hyperonic excitation (in the form of ΣN^{-1} – where N^{-1} stands for the nucleon hole – component of the “kaesobar” [158]) and K^- -condensation would occur at $T \sim 50$ MeV relevant to the neutron-star matter. Now if as is likely the temperature is greater than the difference in energies between the two possible phases, although the hyperons will be more important initially than the kaons, all of the phases will enter more or less equally in constructing the free energy of the system. In going to higher density the distribution between the different phases will change in order to minimize the free energy. Then it is clear that dropping from one minimum to another, the derivative of the free energy with density – which is just the pressure – will decrease as compared with the pressure from any single phase. This would imply that the maximum neutron star mass calculated with either hyperonic excitation or kaon condensation alone must be greater than the neutron star mass calculated with inclusion of both.

The story will be quite different if the vector field decouples. We showed in Section

⁴⁰There is nothing that would suggest that the effective Lagrangian valid up to $\rho \sim \rho_0$ will continue to be valid at $\rho \sim 3\rho_0$ without addition of higher mass-dimension operators, particularly if the chiral critical point is nearby. So this exercise can be taken only as indicative.

10.5.1 that the isoscalar vector mean field must drop by a factor $\gtrsim 9$ in the change-over from nucleons to quasiquarks as variables as one approaches the chiral restoration density. Hyperons will disappear during this drop. It is then highly likely that the kaon will condense *before* chiral restoration and that the kaon condensed phase will persist through the relevant range of densities which determine the maximum neutron star mass.

10.7 Discussions

In this section, we have given arguments to support that not only the kaon mass but also its coupling to vector mesons should drop in matter with density. In particular, with the introduction of medium effects the apparent equilibration found in strangeness production at GSI can be increased from the baryon number density of $\sim \frac{1}{4}\rho_0$ up to the much more reasonable $\sim 2\rho_0$. These properties do not appear at first sight to be connected to BR scaling *per se*. But they must be connected in an albeit indirect way.

From the baryon flow analysis we have direct indications that the vector interaction decouples from the nucleon at a three-momentum of $|\mathbf{p}| \sim 0.9$ GeV/c or at roughly 0.5 m_{NC} . In colliding heavy ions this is reached at a kinetic energy per nucleon of $\sim \frac{1}{8}m_{NC}c^2$ which means a temperature of 78 MeV when equated to $\frac{3}{2}T$. This is just the temperature for chemical freeze-out at GSI energies. We have given several theoretical arguments why the vector coupling should drop rapidly with density.

Once the vector mean field, which acts with opposite signs on the K^+ and K^- mesons is decoupled, these mesons will feel the same highly attractive scalar meson field. Their masses will fall down sharply; e.g., from eq.(10.28) with proposed parameters,

$$\frac{m_K^*}{m_K} \sim 0.5 \quad (10.30)$$

at $\rho \approx 3\rho_0$ and possibly further because of the dropping m_σ^* . The differing slopes of K^+ and K^- with kinetic energy will then develop after chemical freeze-out, as suggested by Li and Brown [138].

In this section we have focused on the phenomenon at GSI energies. Here the chief role that the dropping K^- -mass played was to keep the combination $\mu_B + \omega_{K^-}^*$ nearly constant so that low freeze-out density in the thermal equilibration scenario became irrelevant for the K^+/K^- -ratio. We suggest that the same scenario applies to AGS physics, where the freeze-out density in the thermal equilibration picture comes out to be $\sim 0.35\rho_0$ [159]. In fact, there is no discernible dependence on centrality in the K^-/K^+ -ratios measured at 4A GeV, 6A GeV, 8A GeV and 10.8A GeV [160]. From this it follows either that the ratio of produced K^- -to hyperons is nearly independent of density or that the negative strangeness equilibrates down to a lower freeze-out density and then disperses. Given the relative weakness of the strange interactions, we believe the former to be the case. In fact, we suggest that near constancy with multiplicity of the K^-/K^+ -ratio found experimentally be used to determine temperature dependence of $\omega_{K^-}^*$ in the region of temperatures reached in AGS physics. As was done for GSI energies, the temperature can be obtained from the inverse slopes of the kaon and antikaon distributions of p_\perp and

then the temperature dependence of $\omega_{K^-}^*$ can be added to the density dependence as in [139], in such a way that $\mu_B + \omega_{K^-}^*$ stays roughly constant as function of density. At least this can be done in the low-density regime considered in [159] when the approximation of a Boltzmann gas is accurate enough to calculate μ_B . Our “broad-band equilibration”; i.e., the production of the same, apparently equilibrated ratio of K^- -mesons to hyperons over a broad band of densities, avoids complications in the way in which the K^- degree of freedom is mixed into other degrees of freedom at low density [161]. Most of the K^- -production will take place at the higher densities, as shown in Fig. 12, where the degrees of freedom other than K^- have been sent up to higher energies by the Pauli principle.

Unless the electron chemical potential in dense neutron star matter is prevented from increasing with density (as might happen if the repulsive Σ -nuclear interaction turns to attraction at $\rho > \rho_0$), kaon condensation will take place *before* chiral restoration. This has several implications at and beyond chiral restoration. For instance, its presence would have influence on the conjectured color superconductivity at high density, in particular regarding its possible coexistence with Overhauser effects, skyrmion crystal and other phases with interesting effects on neutron star cooling.

The phenomenon of vector decoupling, if confirmed to be correct, will have several important spin-off consequences. The first is that it will provide a refutation of the recent claim [162] that in the mean-field theory with a kaon-nuclear potential given by the vector-exchange (Weinberg-Tomozawa) term – both argued to be valid at high density – kaon condensation would be pushed up to a much higher density than that relevant in neutron-star matter. Our chief point against that argument is that the vector decoupling and the different role of scalar fields in QCD (e.g., BR scaling) described in this article cannot be accessed by the mean field reasoning used in [162] or by any other standard nuclear physics potential models. The second consequence that could be of a potential importance to the interpretation of heavy-ion experiments is that if the vector coupling rapidly diminishes with density, the strong-coupling perturbation calculation of the vector response functions used in terms of “melting” vector mesons to explain [121], e.g., the CERES dilepton data must break down rapidly as density increases. This could provide a specific mechanism for the quasiparticle description of BR scaling found to be successful in nuclear matter [73]). It is of course difficult to be quantitative as to precisely where this can happen.

Finally we should stress that the scenario presented in this section – which is anchored on Brown-Rho scaling – should not be considered as an *alternative* to a possible quark-gluon scenario currently favored by the heavy-ion community. It is once again more likely a sort of complementarity of the same physics along the line that the Cheshire-Cat Principle [11] embodies that would continue to apply at higher energies.

11 EFFECTIVE FIELD THEORIES FOR DENSE QCD

Thus far we have been climbing up in density in what may be aptly called “bottom-up” approach. In this section, we will start at some asymptotic density and come down to the density regime relevant to dense compact stars and possibly in certain regimes of heavy-ion collisions. This will be a “top-down” approach exploiting once more how chiral symmetry in nature manifests itself through (Nambu-)Goldstone mode. There is an intense activity on this matter, comprehensively reviewed in the recent literature [163], so we will not go into most of the topics. Here we will focus on the most intriguing aspect of dense QCD that reflects an intriguing repeat of the Cheshire-Cat phenomenon. We wish to highlight the seemingly continuous role of chiral symmetry from low-density strong-coupling regime to high density weak-coupling regime in the form of a skyrmion replica that maps high-density excitations to low-density excitations. In view of the rapid development on this matter, our discussion will necessarily be incomplete and primitive but the general feature of the Cheshire Cat phenomenon is likely to survive the test of the time.

11.1 Color-Flavor Locking for $N_F = 3$

11.1.1 *Instability at high density*

Asymptotic freedom of QCD suggests that at very high density with $\mu \rightarrow \infty$, the QCD gauge coupling becomes very weak and so interactions disappear. However if there is an attraction in a certain channel, now matter how weak, the same renormalization group consideration discussed above in connection with Landau Fermi liquid state [72] tells us that the system will be unstable against a phase change. Indeed in the weak coupling limit, one gluon exchange that survives asymptotic freedom has an attraction in the channel that involves diquarks sitting on the opposite side of the Fermi sphere, namely, the BCS channel and this inevitably leads to the Cooper pair condensation as in superconductivity. That this must occur at asymptotic density is without doubt as dictated by the renormalization group argument. Whether or not – and in what manner – this will occur in a physically relevant regime of density cannot be addressed by the asymptotic QCD and it appears most plausible that the scenario is much richer in various different ways than just the Cooper pairing type as one approaches top-down to the density regime of relevance. This matter is amply discussed in the literature [163] but the situation is totally unclear. It is not our aim to dwell on the multitude of possibilities. We will focus on one particular aspect of this phenomenon, that is, the situation where color and flavor of QCD get locked, i.e., the color-flavor-locked (CFL) phase which renders the discussion simple and transparent.

11.1.2 Symmetry breaking and excitations

We shall discuss first the case of $N_c = N_F = 3$ which is relevant at asymptotic density, returning to the case of $N_c = 3$, $N_F = 2$ in the next subsection.

Gluon exchange between two quarks is attractive in the color $\bar{\mathbf{3}}$ channel and repulsive in the $\mathbf{6}$ channel. So one expects diquarks would condense in the $\bar{\mathbf{3}}$ channel. We shall ignore a small mixing to the $\mathbf{6}$ channel which is allowed by symmetry. The diquark condensate would be in the form

$$\langle q_{L\alpha}^{ia} q_{L\beta}^{jb} \rangle = -\langle q_{R\alpha}^{ia} q_{R\beta}^{jb} \rangle = \kappa \epsilon^{ij} \epsilon^{abI} \epsilon_{\alpha\beta I} \quad (11.1)$$

where κ is a constant, i, j are $SL(2, C)$ indices, a, b are color indices and α, β are flavor indices. This condensation breaks the symmetry

$$G \rightarrow H \quad (11.2)$$

with

$$G = SU(3)_c \times SU(3)_L \times SU(3)_R \times U(1)_B, \quad (11.3)$$

$$H = SU(3)_{c+L+R} \times Z_2. \quad (11.4)$$

At superdensity, instantons are suppressed, but the anomaly never disappears, so the $U(1)_A$ symmetry is never truly restored. We shall not be concerned with it here. The color is completely broken and since the vectorial color is locked to both L and R , chiral symmetry is also broken so the resulting invariance group is $SU(3)_{c+L+R}$. Since $\langle q_{L\alpha}^a q_{L\beta}^b \bar{q}_{R\alpha}^{\gamma} \bar{q}_{R\beta}^{\delta} \rangle \sim \kappa^2 \epsilon_{\alpha\beta\gamma\delta} \epsilon^{\gamma\delta\Gamma}$ is gauge invariant, it can be used as an order parameter but while it breaks chiral symmetry, it leaves Z_2 invariant, thus its appearance in H .

The spontaneous symmetry breaking induces Goldstone bosons: eight from the breaking of the color $SU(3)_C$, eight from chiral symmetry breaking and one from $U(1)_B \rightarrow Z_2$. We shall forget the last one since it does not concern us here. The striking feature we would like to focus on here is the uncanny resemblance of the spectrum in the CFL phase to the that of low density in terms of a hidden local symmetry [63]. The scalar Goldstones are eaten up by the gluons thereby the vector bosons becoming massive. The octet of the massive gluons in the CFL are the analogs to the (octet) massive light-quark vector mesons in the low-density vacuum. The octet pseudoscalar Goldstones in the CFL are the analog to the octet pions in the low density vacuum, the dynamics of which can be described by an analogous chiral Lagrangian. The quarks in the system are gapped – and hence massive – and bear the quantum numbers of the octet baryon of the zero-density vacuum. We shall show below that this can be understood by looking at the solitons in the chiral Lagrangian [164]. Since the soliton corresponds to a gapped colored quark, we call it “qualiton” in analogy to the qualiton considered by Kaplan for the constituent quark [165]. (The breaking of $U(1)_B$ leads to superfluidity which resembles the same in nuclear matter, another uncanny correspondence.) The one-to-one matching between the low density spectrum in terms of hadronic variables and the high density spectrum in terms of quark-gluon variable is referred to as “quark-hadron continuity.” [166]. We will identify this as belonging to the class of the Cheshire Cat phenomenon in the strong interaction physics [11].

11.1.3 Chiral Lagrangians and qualitons

As suggested in [164, 167], the dynamics of the surviving Goldstone modes can be described by an effective chiral field theory as in the zero-density situation. We introduce the chiral effective field ⁴¹

$$\xi_{La\alpha}(x) \sim \epsilon^{ij} \epsilon_{abc} \epsilon_{\alpha\beta\gamma} q_{Li}^{b\beta}(-\mathbf{v}_F, x) q_{Lj}^{c\gamma}(\mathbf{v}_F, x) \quad (11.5)$$

corresponding to the map $SU(3)_c \times SU(3)_L / SU(3)_{c+L}$ and similarly for R ,

$$\xi_{Ra\alpha}(x) \sim \epsilon^{ij} \epsilon_{abc} \epsilon_{\alpha\beta\gamma} q_{Ri}^{b\beta}(-\mathbf{v}_F, x) q_{Rj}^{c\gamma}(\mathbf{v}_F, x) \quad (11.6)$$

corresponding to the map $SU(3)_c \times SU(3)_R / SU(3)_{c+R}$.

Under an $SU(3)_c \times SU(3)_L \times SU(3)_R$ transformation by unitary matrices (g_c, g_L, g_R) , ξ_L transforms as $\xi_L \mapsto g_c^* \xi_L g_L^\dagger$ and ξ_R transforms as $\xi_R \mapsto g_c^* \xi_R g_R^\dagger$. In the ground state of the CFL superconductor, ξ_L and ξ_R take the same constant value. QCD symmetries with (11.1) imply

$$\langle \xi_{La\alpha} \rangle = -\langle \xi_{Ra\alpha} \rangle = \kappa \delta_{a\alpha}. \quad (11.7)$$

The Goldstone bosons are the low-lying excitations of the condensate, given as unitary matrices $\xi_L(x) = g_c^T(x) g_L(x)$ and $\xi_R(x) = g_c^T(x) g_R(x)$. For the present decomposition, we note the extra invariance under the (hidden) local transformation $g_{c+L+R}(x)$ – which is an analog to the hidden gauge transform $h(x)$ of [63] – within the diagonal $SU(3)_{c+L+R}$ through

$$g_c^T(x) \rightarrow g_c^T(x) g_{c+L+R}^\dagger(x) \quad g_{L,R}(x) \rightarrow g_{c+L+R}(x) g_{L,R}(x) \quad (11.8)$$

Hence, the spontaneous breaking of $SU(3)_c \times (SU(3)_L \times SU(3)_R) \rightarrow SU(3)_{c+L+R}$ can be realized non-linearly through the use of $\xi_{L,R}(x)$ or linearly through the use of $g_{c,L,R}(x)$ with the addition of an octet vector gauge field transforming inhomogeneously under local $g_{c+L+R}(x)$. This can be identified with the hidden local symmetry [63] ⁴². Clearly the

⁴¹One has to be careful with a singularity in the product of two fermion fields at one point. See [164] for a more proper definition.

⁴²We comment as a side remark on a technical detail which is somewhat outside of the scope of this review but may be helpful to those interested in subtlties involved in hidden-gauge-symmetry aspects of the problem.

As mentioned, when the color is completely broken, the octet gluons become massive by Higgs mechanism with the mass proportional to the chemical potential μ . These were found to have the same quantum numbers as those of the light-quark vector mesons present at zero density. The hidden gauge bosons excited at high density discussed here belong to the unbroken diagonal subgroup $SU(3)_{c+L+R}$. How are these vectors related to the massive gluons?

In [168], the hidden gauge bosons $\in SU(3)_{c+L+R}$ were identified with the spin-1 two-quark bound states with the properties that match with the Georgi vector limit at some non-asymptotic density. At the leading order in $1/\mu$, these states seem to have nothing to do with the Higgsed gluons: The overlap is zero. But this cannot be correct. In nature, the low-lying vector excitations at large density must be a coherent mixture of the two but at the leading order, they must be equivalent. This is analogous to the complementary description of the pion as a Goldstone mode and as a zero-mass bound state of a quark and

composites carry color-flavor in the unbroken subgroup, with a mass of the order of the superconducting gap.

The current associated with $\det \xi_L$ ($\det \xi_R$) is the left (right)-handed $U(1)_L$ ($U(1)_R$) baryon number current. Because of the $U(1)$ axial anomaly, the field $\det \xi_L / \det \xi_R$ is massive due to instantons. We decouple the massive field from the low energy effective action by imposing $\det \xi_L / \det \xi_R = 1$. The Goldstone boson associated with spontaneously broken $U(1)_B$ symmetry is described by $\det \xi_L \cdot \det \xi_R$ and responsible for baryon superfluidity. But since it is not directly relevant for our problem, we further choose $\det \xi_L \cdot \det \xi_R = 1$ to isolate the Goldstone bosons resulting from the spontaneous breaking of chiral symmetry, from the massive ones eaten up by the gluons. We now parameterize the unitary matrices $\xi_{L,R}$ as

$$\xi_L(x) = \exp(i\pi_L^A T^A/f), \quad \xi_R(x) = \exp(i\pi_R^A T^A/f), \quad (11.9)$$

where T^A are $SU(3)$ generators, normalized as $\text{Tr}(T^A T^B) = \delta^{AB}/2$. The Goldstone bosons π^A transform nonlinearly under $SU(3)_c \times SU(3)_L \times SU(3)_R$ but linearly under the unbroken symmetry group $SU(3)_{c+L+R}$.

The effective Lagrangian for the CFL phase at asymptotic densities follows by integrating out the ‘hard’ quark modes at the edge of the Fermi surface [171]. The effective Lagrangian for $U_{L,R}$ is a standard non-linear sigma model in D=4 dimensions including the interaction of Goldstone bosons with colored but “screened” gluons G . Expanding in

antiquark. Indeed this complementarity has also been verified in the pion channel in dense QCD in terms of bound diquarks [169, 168]. To see this aspect in the vector channel, we follow the CCWZ (Callan-Coleman-Wess-Zumino) formalism [170]. Consider the symmetry group $G = SU(3)_L \times SU(3)_R \times SU(3)_c$ broken down to $H = SU(3)_{L+R+c}$. Using a notation slightly different from what is used in this subsection, let the G transformation be represented in the block diagonal form $g = \text{diag}(L, R, C)$ corresponding to the left, right and color transformations. Let the generator of the diagonal subgroup be given by $h = \text{diag}(U, U, U)$. Now we would like to write $\Xi(x) \in G$, the *rotation matrix that transforms the standard vacuum configuration to the local field configuration*. One choice consistent with the CCWZ prescription is

$$\Xi(x) = \text{diag}(\xi_L(x), \xi_R(x), 1)$$

which transforms as

$$g\Xi h^{-1} = \text{diag}(L\xi_L U^{-1}, R\xi_R U^{-1}, CU^{-1}).$$

It is clear that we are required to take

$$CU^{-1} = 1$$

which means that $U = C$ and that $\xi_{L,R}$ transform as

$$\begin{aligned} \xi_L &\rightarrow L\xi_L C^{-1}, \\ \xi_R &\rightarrow R\xi_R C^{-1}. \end{aligned}$$

Now U is a non-linear function of L , R , ξ_L and ξ_R , and so must be C . In HGS, this is the group that is gauged. Therefore the “hidden gauge symmetry” can be equated to the color symmetry of QCD as was done by Casalbuoni and Gatto [167]. This can be seen also in Eq.(11.10) given below.

powers of derivative, the effective Lagrangian for the Goldstone bosons is then

$$\mathcal{L} = + \frac{f_T^2}{4} \text{Tr}(\partial_0 \xi_L \partial_0 \xi_L^\dagger) - \frac{f_S^2}{4} \text{Tr}(\partial_i \xi_L \partial_i \xi_L^\dagger) + g_s G \cdot J_L + (L \rightarrow R) + \dots \quad (11.10)$$

Here the ellipsis stands for higher derivative terms including the Wess-Zumino-Witten term [19] that is needed to account for anomalies. The vectorial coupling to the gluon field G_μ via the color current J_μ indicates that the left-right chiral symmetry is also locked to each other. In the presence of a chemical potential, the $SL(2, C)$ breaks down to $O(3)$, so the ‘decay constant’ f has two different values for the time and space components. The temporal and spatial decay constants $f_{T,S}$ are fixed by the ‘hard’ modes at the Fermi surface. Their exact values are determined by the dynamics at the Fermi surface. They go like $f_S \sim f_T \sim \mu$.

The effective Lagrangian (11.10) in the CFL phase bears much in common with Skyrme-type Lagrangians [11], with the screened color mediated interaction analogous to the exchange of massive vector mesons. Indeed in the CFL phase the ‘screened’ gluons and the ‘Higgsed’ gauge composites are the analog of the massive vector mesons in the low density phase. In the CFL phase the WZW term is needed to enforce the correct flavor anomaly structure.

The ‘Higgsed’ gluons are very massive in the large μ limit, so can be integrated out from the Lagrangian (11.10). This is very much like the hidden gauge symmetry theory wherein the vector mesons can be integrated out to give rise to a nonlinear sigma model. The theory then can have a soliton as suggested by Hong, Rho and Zahed [164] if there are higher derivative terms that stabilize it. The qualiton will be colored. However the pair-condensed ground state is colored also, so combined with the background, the excitation will be effectively color-singlet. In other words, the chiral field from which the soliton arises can be considered as color-singlet fluctuation. This means that one can rewrite the effective field theory in terms of the *color-singlet field*

$$U_i^j \equiv \xi_{Lai} \xi_R^{*aj} \quad (11.11)$$

which transforms $U \rightarrow g_L U g_R^\dagger$. The Lagrangian (11.10) can then be rewritten in the form familiar from low density

$$\mathcal{L} = \frac{f_T^2}{4} \text{Tr}(\partial_0 U \partial_0 U^\dagger) - \frac{f_S^2}{4} \text{Tr}(\partial_i U \partial_i U^\dagger) + \mathcal{O}(\partial^4) + \mathcal{O}(\mathcal{M}^2) + \dots \quad (11.12)$$

The resulting theory is essentially identical to the familiar nonlinear sigma model giving rise to the Skyrme soliton [11], except that the mass terms which we did not specify here should be quadratic in the quark mass matrix \mathcal{M} because of the Z_2 invariance. The qualiton can be collective-quantized in a way paralleling the low-density skyrmions. This was worked out recently in [172] in which the authors argue that since a qualiton is a quark on top of the condensed state, it would correspond to the quasiparticle of the particle-hole complex and the qualiton mass that is obtained as a soliton solution must therefore correspond to 2Δ where Δ is the gap.

11.2 Complementarity of Hidden Gauge Symmetry and Color Gauge Symmetry and BR Scaling

The $N_c = 3$, $N_F = 2$ case is a bit more intricate and involved than the $N_c = N_F = 3$ CFL discussed above. It turns out, however, that color-flavor locking in this case [174] is more relevant in the density regime closer to nature, both in high density and in low density. It can also be mapped as we shall argue to hidden local symmetry discussed in the previous sections.

11.2.1 Quark number susceptibility

It was observed in [13, 176] that the quark number susceptibility $\chi_{\pm} = (\partial/\partial\mu_u \pm \partial/\partial\mu_d)(\rho_u \pm \rho_d)$ where $\rho_{u,d}$ and $\mu_{u,d}$ are respectively u, d -quark number density and chemical potential measured on lattice as a function of temperature [175] exhibited a smooth change-over from a flavor-gauge symmetry or hidden gauge symmetry to QCD color-gauge symmetry at the chiral phase transition critical temperature T_c . It was suggested [13] that at the phase transition, the flavor gauge symmetry – which is induced and hence not fundamental – gets *converted directly* to the color gauge symmetry – which is fundamental, implying that they could be related in an intricate way. In this subsection, following [177], we suggest how this can be realized in terms of color-flavor-locked (CFL) quark-antiquark and diquark condensates and “vector manifestation” (VM) of chiral symmetry explained in Section 4. It will be seen how BR scaling can be fit into the general scheme that results from these developments: Its proof will be the most convincing case for the validity of BR scaling.

Our argument relies on two recent remarkable developments that come from seemingly unrelated sectors. One is the suggestion by Harada and Yamawaki [12] that the phase transition from the Nambu-Goldstone phase to the Wigner-Weyl phase involves “vector manifestation” of chiral symmetry, that is, at the phase transition, the longitudinal components of the light-quark vector mesons (i.e., the triplet ρ in the 2-flavor case) and the triplet pions (π^a) come together becoming massless in the chiral limit, the vectors decoupling à la Georgi’s vector limit [62] but with the pion decay constant f_π vanishing at that point. The other important development is the proposal by Berges and Wetterich [173, 174] that color and flavor get completely locked in the Nambu-Goldstone phase (a) for three flavors ($N_f = 3$) [173] by the quark-antiquark condensate in the color-octet **(8)** channel

$$\chi = \langle \bar{q}_\alpha^a \sum_{i=1}^3 (\tau_i)_{\alpha\beta} (\lambda_i)^{ab} q_\beta^b \rangle \quad (11.13)$$

and (2) for two flavors ($N_F = 2$) [174] by (11.13) together with the diquark condensate in the color-antitriplet **(\bar{3})** channel

$$\Delta = \langle q_\alpha^a (\tau_2)_{\alpha\beta} (\lambda_2)^{ab} q_\beta^b \rangle. \quad (11.14)$$

In (11.13) and (11.14), the indices α, β denote the flavors and a, b the colors. In the Berges-Wetterich scenario, the chiral phase transition and deconfinement occur through the melting of the condensates χ and Δ .

11.2.2 Color-isospin locking

The scenario for color-flavor-locking (CFL) is a bit different depending on the number of flavors N_F . For our purpose, the case of two flavors is more relevant, so we shall focus on this case. In [174], Berges and Wetterich argue that both the χ and Δ condensates can be nonzero in the vacuum, thereby completely breaking the color. Should one of the condensates turn out to be zero, then color would be only partially broken (see [163] for a simple explanation for this and references). This pattern of color breaking and color-flavor locking renders the octet gluons and six quarks massive by the Higgs mechanism and generates three Goldstone pions due to the broken chiral symmetry. All of the excitations are integer-charged. Among the eight massive gluons, three of them are identified with the isos triplet ρ 's with the mass

$$m_\rho = \kappa g_c \chi \quad (11.15)$$

where κ is an unknown constant and g_c the color gauge coupling. The fourth vector meson is identified with the isosinglet ω with the mass

$$m_\omega = \kappa' g_c \Delta \quad (11.16)$$

where κ' is another constant. The remaining four vector mesons turn out to have exotic quantum numbers and are presumably heavy. We assume that they decouple from the low-energy regime. As for the fermions, there are two baryons with the quantum numbers of the proton and neutron with their masses proportional to the scalar condensate ϕ ,

$$\phi = \langle \bar{q}_\alpha^a q_\alpha^a \rangle. \quad (11.17)$$

The four remaining fermions are also of exotic quantum numbers with zero baryon number and heavier, so we assume that they also decouple from the low-energy sector. What concerns us in this Letter is therefore the three pions, the proton and neutron, the ρ -mesons and the ω -meson.

11.2.3 Implications of the lattice measurements of quark number susceptibility

It was argued in [78] that the “measured” singlet and non-singlet QNS's [175] indicate that both the ρ and ω couplings vanish at the transition temperature T_c . This meant that the ωNN coupling which is ~ 3 times the ρNN coupling at zero temperature became equal to the latter at near the critical temperature. This also meant that the both vector mesons became massless and decoupled. Viewed from the CFL point of view, it follows from (11.15) and (11.16) that the condensates χ and Δ “melt” at that point. This is consistent with the observation by Wetterich [173] that for three-flavor QCD, the

phase transition – which is both chiral and deconfining – occurs at T_c with the melting of the color-octet condensate χ . The transition is first-order for $N_F = 3$ in agreement with lattice calculations, so the vector meson mass does not go to zero smoothly but makes a jump from a finite value to zero. We expect however that in the case of $N_F = 2$ the transition will be second-order with the vector mass dropping to zero continuously.

Noting that both the CFL formulas (11.15)-(11.16) and the vector manifestation result (4.6) are of the Higgsed type, we invoke the lattice results to arrive at

$$a g_V f_\pi \approx \kappa g_c \chi \approx \kappa' g_c \Delta. \quad (11.18)$$

We admit that this relation follows neither from the group-theoretical considerations of Berges and Wetterich [174, 173] nor from the vector manifestation of HLS [12]. We are proposing that this is indicated by the lattice data, at least near the phase transition point. It holds empirically at zero temperature and zero density, so we are led to assume that it holds at least approximately from $T = 0$ up to $T = T_c$ ⁴³. It should be noted that the vanishing of the hidden gauge coupling g_V corresponds to the vanishing of the condensates χ and Δ with the color gauge coupling remaining non-vanishing, $g_c \neq 0$.

Next, we have shown in [78] that above the chiral transition temperature $T \gtrsim T_c$, the QNS's can be well described by perturbative gluon exchange with a gluon coupling constant $\frac{g_c^2}{4\pi} \approx 0.19$ and argued that the flavor gauge symmetry *cedes* to the fundamental QCD gauge symmetry. Now the HLS theory is moot on what it could be beyond the chiral restoration point since the theory essentially terminates at T_c . We propose that this is where the color-flavor locking of [173, 174] phrased in the QCD variables takes over by supplying a logical language for crossing-over from below T_c to above T_c . Indeed (11.18) describes the *relay* that must take place in terms of the hidden flavor gauge coupling g_V on one side and the color gauge coupling g_c on the other side. Now above T_c , the color and flavor must unlock, with the gluons becoming massless and releasing the scalar Goldstones. The dynamics of quarks and gluons in this regime will then be given by hot QCD in the proper sense. The way the two condensates melt as temperature is increased is a dynamical issue which seems to be difficult to address unambiguously within the present scheme. It will have to be up to lattice measurements to settle this issue. Our chief point here is that their melting is intricately connected.

⁴³This would imply that the nonet symmetry for $N_F = 3$ or the quartet symmetry $N_F = 2$ is a good symmetry not only at $T = 0$ but also for $T \neq 0$. Why this symmetry should hold at any non-zero temperature or density is not obvious either in CFL QCD or in HLS effective theory. In discussing color-flavor locking in two-flavor QCD, Berges and Wetterich [174] entertain among others the possibility that the two condensates χ and Δ could be different at the critical point. As for the HLS theory, at one-loop order, the RG flows are expected to be different for the ρ and ω properties, so it is not obvious that the ρ and ω mesons would reach the chiral restoration with the Georgi vector limit at the same temperature. Nonetheless if our interpretation of QNS is correct, it seems most plausible and appealing that the nonet or quartet symmetry does hold at the phase transition. Proving this conjecture remains as a theoretical challenge.

11.2.4 Link to BR scaling and Landau parameter F_1

The situation appears to be quite different in dense medium. Since there is no guidance from lattice as it is impossible at present to put density on lattice except for unphysical cases of two colors or adjoint quarks, we shall simply assume that the above scenario holds in density up to $n = n_c$ ⁴⁴. Certain models indicate that the phase structure near chiral restoration could be quite involved and complex. As suggested by Schäfer and Wilczek [166], an intriguing possibility is that the three-flavor color-flavor locking operative at asymptotic density continues all the way down to the “chiral transition density” (n_c) in which case there will be no real phase change since there will then be a one-to-one mapping between hadrons and quark/gluons, e.g., in the sense of “hadron-quark continuity.” However the non-negligible strange-quark mass is likely to spoil the ideal three-flavor consideration. One possible alternative scenario is that viewed from “bottom-up,” one gets into the phase where $\chi = \sigma = 0$ and $\Delta \neq 0$ corresponding to the two-flavor color superconducting (2csc) phase [163]. Unless Δ goes to zero at ρ_c , this would mean that the ρ mesons become massless but the ω meson remains massive. One cannot say that this is inconsistent with the vector manifestation since the HLS does not require that $U(2)$ symmetry hold at the chiral restoration point or in medium in general. But this seems unlikely. On the other hand, it is highly plausible that both χ and Δ approach zero (or near zero if it is first-order) from below n_c and then Δ picks up a non-zero value at or above n_c in which case we will preserve the mass formula (4.6) as one approaches n_c . This is the scenario that we favor.

Among the scaling relations implied by BR scaling [2, 78], the one most often discussed in the literature is the dropping of the ρ -meson mass in medium. This relation has been extensively discussed recently in connection with the CERN-CERES data on dilepton production in heavy-ion collisions. The simplest explanation for the observed dilepton enhancement at an invariant mass ~ 400 MeV is to invoke BR scaling for the excitations relevant in the process [179]. It turns out however that this explanation is not unique. One could explain it equally well if the ρ meson “melted” in dense medium with a broadened width [121]. Since the process is essentially governed by a Boltzmann factor, all that is needed is the shift downward of the ρ strength function: the expanding width simply does the job as needed for the dilepton yield. If one calculates the current-current correlation function in low-order perturbation theory with a phenomenological Lagrangian, it is clear, because of the strong coupling of the ρ meson with the medium, that the meson will develop a large width in medium and “melt” at higher density. The upshot of the dilepton experiments then is that they cannot distinguish the variety of scenarios that probe average properties of hadrons in the baryon density regime – which is rather dilute – encountered in the experiments.

In the vector manifestation scenario, the width should become narrower, decreasing like $\sim g_V^2$. Then the vector mesons become more a quasiparticle at high density than at lower density. *This is the underlying picture of BR scaling.* Now what about the matter that is not so dense, say, near nuclear matter density? By far the most clear-cut indication

⁴⁴In this subsection, we again denote density by n reserving ρ for the vector meson.

for BR scaling comes from observations in nuclei, that is, up to nuclear matter density. In nuclei, the evidence is mostly indirect but the data are more precise and hence more quantitative. Several cases evidencing BR scaling are discussed in a recent review [177]. Some are somewhat model-dependent and hence subject to objections. The most direct case is the $(e, e'p)$ response functions in nuclei [1, 177] where the effect of BR scaling is more convincingly exposed.

Thus far, we have made a link between the color-flavor-locked condensates and hidden gauge symmetry. We can go even one step further and via BR scaling, make an intriguing connection between QCD “vacuum” properties and many-body nuclear interactions. This connection was discussed in Section 5. Simply put, it comes about because nuclear matter owes its stability to a Fermi-liquid fixed point [72]. Certain interesting nuclear properties were found to be calculable in terms of the Fermi-liquid fixed point parameters [74]. Among others, it was shown that the Landau parameter F_1 – which is a component of quasiparticle interactions – can be expressed in terms of the BR scaling factor $\Phi(n) \equiv m_\rho^*(n)/m_\rho(0)$

$$\tilde{F}_1 = 3(1 - \Phi^{-1}) + \tilde{F}_1(\pi) \quad (11.19)$$

where $\tilde{F}_1(\pi)$ is the contribution from the pion which is completely fixed by chiral dynamics. One of the most remarkable prediction was Eq.(6.4) for the anomalous gyromagnetic ratio δg_l in nuclei

$$\delta g_l = \frac{4}{9} \left[\Phi^{-1} - 1 - \frac{1}{2} \tilde{F}_1(\pi) \right] \tau_3. \quad (11.20)$$

At nuclear matter density $n = n_0$, we have $\tilde{F}_1(\pi)|_{n=n_0} = -0.153$. Note that (11.20) depends on only one parameter, Φ . This parameter can be extracted from various sources and all give about the same value, $\Phi(n_0) \approx 0.78$. Given that this is not very accurately determined, it is probably a better strategy to determine Φ from the data on δg_l . In any event, given Φ at nuclear matter density, Eq.(11.20) makes a simple prediction,

$$\delta g_l = 0.23\tau_3 \quad (11.21)$$

which should be compared with the measurement in the Pb region [84],

$$\delta g_l^p = 0.23 \pm 0.03. \quad (11.22)$$

We believe this to be a good agreement within the theoretical uncertainty involved. It is intriguing that what is an intrinsic QCD quantity can be related to what appears to be a standard many-body nuclear interaction summarized in the Landau quasiparticle parameter F_1 .

11.3 Kaon Condensation: *Encore Cheshire Cat*

In addition to the “continuity” in excitations and chiral phase transitions between the hadronic phase and the quark phase, meson condensations can occur in high density

matter with $n > n_c$ and in hadronic matter with $n < n_c$ where n_c is the presumed critical density for the so-called “chiral restoration” – whatever that may be. Pion condensation is unlikely in the density regime that is relevant for laboratory or astrophysical observations, but the negatively charged kaon K^- can condense at a relatively low density as well as at an asymptotically high density providing yet another support for “continuity” or Cheshire Cat. For completeness we briefly describe this phenomenon although the story is by no means final.

• K^- Condensation in the Hadronic Sector

Since this matter was discussed already in Section 10, we shall simply summarize the pertinent feature in a slightly different language. As originally pointed out by Kaplan and Nelson [180] and reinterpreted by Brown et al [144], the S-wave condensation of K^- ’s is driven by “rotating away” of the kaon mass associated with both the explicitly broken chiral symmetry and spontaneously broken chiral symmetry. As is widely discussed, hyperons can also participate through P-wave coupling with the kaons but near the condensation transition, the P-wave coupling would be “irrelevant”⁴⁵ in contrast to the S-wave that has to do with “relevant” terms [181] and hence may be ignored in this qualitative discussion. The condensation therefore occurs when the kaon mass is eaten up by attractive interactions. Negative kaons have attractive interactions with nucleons by exchanging the vector mesons ρ and ω as well as scalar mesons, e.g., the σ meson. The vector exchange is dictated by the vector current conservation and is given by the Weinberg-Tomozawa term and the σ exchange by the Σ_{KN} – the KN sigma term. When many-body interactions through many-Fermi contact terms in the Lagrangian are implemented through BR scaling, one then has a Lagrangian of the form (10.12). One can generate this effective Lagrangian in chiral perturbation theory as reviewed e.g. by Lee [146]. The condensation occurs when these relevant terms drive the system to instability [181]. In neutron star matter, the kaon energy ω_K need not go all the way to zero. It suffices to drop to the electron chemical potential μ_e . Since the μ_e increases as a function of density in nonrelativistic nuclear systems and the ω_K must fall, the crossing is bound to occur at some density. However exactly at what density it will occur will depend upon details of the dynamics and this is still a controversial issue [162]. In Section 10, we have proposed that the critical density is rather low, $\rho_c^K \sim 3\rho_0$.

• K^- Condensation in the CFL Phase

The effective chiral Lagrangian discussed above, (11.12), implemented with mass terms predicts [182, 169, 183, 184, 185] at high density where the color-flavor locking sets in that the kaon mass is of the form

$$m_{K^\pm} = cm_d(m_u + m_s) \quad (11.23)$$

where c is a constant that can be evaluated in the weak-coupling QCD, $c = \frac{3\Delta^2}{\pi^2 f_\pi^2}$ where Δ is the pairing gap and the subscripts u, d and s stand for up, down and strange quarks

⁴⁵This presumably is related to Migdal theorem. See Polchinski in Ref.[72] for a related discussion in condensed matter physics.

respectively. Because the Goldstone bosons in this phase are of $q^2\bar{q}^2$ configuration, the kaon is less massive than the pion which has the mass

$$m_{\pi^\pm} = cm_s(m_u + m_d). \quad (11.24)$$

It is found numerically that for $\mu \sim 500 - 1000$ MeV, the kaon mass ranges from ~ 5 MeV to ~ 1 MeV. The reason for this small mass is easy to understand. First of all, because of the Z_2 symmetry, the Goldstone mass is quadratic in the quark mass and secondly, the mass is proportional to $(\Delta/\mu)^2$ that goes to zero as $\mu \rightarrow \infty$.

For large density, one can ignore the attractive kaon-quark interaction analogous to the kaon-nuclear since the interaction is suppressed by $(1/\mu)^2$. Considering the Fermi sea filled with non-interacting massless up, down and strange quarks, the electron chemical potential μ_e is found in this case to drop as $\sim m_s/k_F$. This contrasts with the increasing μ_e found in the nonrelativistic hadronic system. Schäfer found that for a reasonable range of parameters involved for the CFL phase, the kaon mass is *always* less than the electron chemical potential [186]. This means that the electron will undergo the transformation $e^- \rightarrow K^- + \nu_e$ with the kaons condensing. Here the mechanism for the condensation is again the mass effect in the presence of dense electrons as in the hadronic sector. It would be exciting if the condensation were continuous from that in the hadronic sector to that in the CFL sector. If so, this would be yet another case of Cheshire Cat.

Acknowledgments

We are grateful for discussions with and comments from Bengt Friman, Masayasu Harada, Youngman Kim, Kuniharu Kubodera, Shoji Nagamiya and Koichi Yamawaki. This work was initiated while both of us were visiting Korea Institute for Advanced Study in June 2000 and completed when one of us (MR) was spending the Spring 2001 at Seoul National University and Yonsei University. We acknowledge the generous hospitality of the host institutes. The work of GEB was supported by the US Department of Energy under Grant No. DE-FG02-88 ER40388.

References

- [1] J. Moregenstern and Z.-E. Meziani, “Is the Coulomb sum rule violated in nuclei?” to appear; private communication.
- [2] G.E. Brown and M. Rho, Phys. Rev. Lett. **66** (1991) 2720.
- [3] M. Rho and G.E. Brown, Comments Part. Nucl. Phys. **10** (1981) 201; M. Rho, Ann. Rev. Nucl. Part. Science **34** (1984) 531.
- [4] M. Chemtob and M. Rho, Nucl. Phys. **A163** (1971) 1.
- [5] D.O. Riska and G.E. Brown, Phys. Lett. **38B** (1972) 193.
- [6] B. Frois and J.-F. Mathiot, Comments Part. Nucl. Phys. **18** (1989) 291.
- [7] G.E. Brown and M. Rho, Phys. Lett. **B82** (1979) 177; G.E. Brown, M. Rho and V. Vento, Phys. Lett. **B84** (1979) 383.
- [8] S. Théberge, A.W. Thomas and G.A. Miller, Phys. Rev. **D22** (1980) 2838.
- [9] T.H.R. Skyrme, Nucl. Phys. **31** (1962) 556.
- [10] E. Witten, Nucl. Phys. **B223** (1983) 422, 433
- [11] M.A. Nowak, M. Rho and I. Zahed, *Chiral Nuclear Dynamics* (World Scientific, Singapore, 1996).
- [12] M. Harada and K. Yamawaki, Phys. Rev. Lett. **86** (2001) 757, hep-ph/0010207.
- [13] G.E. Brown and M. Rho, Phys. Rep. **269** (1996) 333.
- [14] A. Chodos, R.L. Jaffe, K. Johnson and C.B. Thorn, Phys. Rev. **10** (1974) 10; T. DeGrand, R.L. Jaffe, K. Johnson and J. Kiskis, Phys. Rev. **12** (1975) 2060.
- [15] A. Chodos and C.B. Thorn, Phys. Rev. **D12** (1975) 2733.
- [16] S. Nadkarni, H.B. Nielsen and I. Zahed, Nucl. Phys. **B253** (1984) 308; ref.[11].
- [17] G.E. Brown, A.D. Jackson, M. Rho and V. Vento, Phys. Lett. **B140** (1984) 285.
- [18] A.W. Thomas, Adv. Nucl. Phys. **13** (1984) 1.
- [19] J. Wess and B. Zumino, Phys. Lett. **B37** (1971) 95; E. Witten, Nucl. Phys. **B223** (1983) 422.
- [20] N. Dorey, J. Hughes and M.P. Mattis, Phys. Rev. Lett. **73** (1994) 1211.
- [21] P.H. Damgaard, H.B. Nielsen and R. Sollacher, Nucl. Phys. **B414** (1994) 227.

- [22] G.E. Brown and M. Rho, *Comments on Nucl. Part. Phys.* **18** (1988) 1; M. Rho, *Phys. Rep.* **240** (1994) 1.
- [23] A. Hosaka and H. Toki, *Phys. Rep.* **277** (1996) 65.
- [24] H.B. Nielsen, M. Rho, A. Wirzba and I. Zahed, *Phys. Lett.* **B269** (1991) 389; *Phys. Lett.* **B281** (1992) 345.
- [25] S. Ansoldi, C. Castro and E. Spallacci, “Chern-Simons hadronic bag from quenched large-N QCD,” [hep-th/0011013](#).
- [26] A.V. Manohar, *Phys. Lett.* **B336** (1994) 502.
- [27] D.I. Diakonov and V.Yu. Petrov, “Nucleons as chiral solitons,” [hep-ph/0009006](#).
- [28] V. Vento, J.H. Jun, E.M. Nyman, M. Rho and G.E. Brown, *Nucl. Phys.* **A345** (1980) 413.
- [29] R. Jackiw and C. Rebbi, *Phys. Rev. Lett.* **36** (1976) 1116.
- [30] M. Rho, A.S. Goldhaber and G.E. Brown, *Phys. Rev. Lett.* **51** (1983) 747.
- [31] J. Goldstone and R.J. Jaffe, *Phys. Rev. Lett.* **51** (1983) 1518.
- [32] B.-Y. Park and M. Rho, *Zeit. für Physik* **A331** (1988) 151; B.-Y. Park, D.-P. Min and M. Rho, *Nucl. Phys.* **A551** (1993) 657.
- [33] H.-J. Lee, D.-P. Min, M. Rho and V. Vento, *Nucl. Phys.* **A657** (1999) 75.
- [34] See for a recent review, K. Saito, [nucl-th/0010035](#)
- [35] S. Weinberg, *Physica* **96A** (1979) 327; [hep-ph/9702027](#); *Quantum field theory II* (Cambridge University Press, Cambridge, 1998). .
- [36] For a recent review, see U.-G. Meissner, “Chiral QCD: Baryon dynamics,” [hep-ph/0007092](#).
- [37] M. Rho, *Prog. Part. Nucl. Phys.* **8** (1982) 103.
- [38] S. Weinberg, *Phys. Lett.* **B251** (1990) 288; *Nucl. Phys.* **B363** (1991) 3.
- [39] T.-S. Park, D.-P. Min and M. Rho, *Phys. Rev. Lett.* **74** (1995) 4153; *Nucl. Phys.* **A596** (1996) 515; T.-S. Park, K. Kubodera, D.-P. Min and M. Rho, *Phys. Lett.* **B472** (2000) 232.
- [40] J.-W. Chen and M.J. Savage, *Phys. Rev.* **C60** (1999) 065205.
- [41] T.-S. Park, K. Kubodera, D.-P. Min and M. Rho, [nucl-th/0005069](#).

- [42] T.-S. Park, K. Kubodera, D.-P. Min and M. Rho, “An effective field theory prediction for the solar HEP process,” to appear.
- [43] L.E. Marcucci, R. Schiavilla, M. Viviani, A. Kievsky and S. Rosati, Phys. Rev. Lett. **84** (2000) 5959; L.E. Marcucci, R. Schiavilla, M. Viviani, A. Kievsky, S. Rosati and J. F. Beacom, Phys. Rev. **C63** (2000) 015801.
- [44] S.R. Beane, P.F. Bedaque, W.C. Haxton, D.R. Phillips and M.J. Savage, “From hadrons to nuclei: Crossing the border,” nucl-th/0008064.
- [45] D.B. Kaplan, M.J. Savage and M.B. Wise, Nucl. Phys. **534** (1998) 329; Phys. Lett. **B424** (1998) 390.
- [46] C. Ordonez, L. Ray and U. van Kolck, Phys. Rev. Lett. **72** (1994) 1982; Phys. Rev. **C53** (1996) 2086; U. van Kolck, Prog. Part. Nucl. Phys. **43** (1999) 409.
- [47] M. Rho, Phys. Rev. Lett. **66** (1991) 1275.
- [48] T.-S. Park, D.-P. Min and M. Rho, Phys. Rep. **233** (1993) 341; Phys. Rev. Lett. **74** (1995) 4153; T.-S. Park, K. Kubodera, D.-P. Min and M. Rho, Phys. Rev. **C58** (1998) 637; Phys. Lett. **B472** (2000) 232; nucl-th/0005069.
- [49] J. Carlson and R. Schiavilla, Rev. Mod. Phys. **70** (1998) 743; V.R. Pandharipande, Nucl. Phys. **A654** (1999) 157c.
- [50] R.B. Wiringa, V.G.J. Stoks and R. Schiavilla, Phys. Rev. **C51** (1995) 38.
- [51] K. Kubodera, J. Delorme and M. Rho, Phys. Rev. Lett. **40** (1978) 755.
- [52] T. Mehen, I.W. Stewart and M.B. Wise, Phys. Rev. Lett. **83** (1999) 931; Phys. Lett. **B474** (2000) 145.
- [53] D.R. Phillips and T.D. Cohen, Nucl. Phys. **A668** (2000) 45.
- [54] C.H. Hyun, T.-S. Park and D.-P. Min, Phys. Lett. **473** (2000) 6.
- [55] S.R. Beane and M.J. Savage, “Rearranging pionless effective theory,” nucl-th/0011067.
- [56] J.-W. Chen and M.J. Savage, Phys. Rev. **C60** (1999) 065205; G. Rupak, nucl-th/9911018.
- [57] T.-S. Park, K. Kubodera, D.-P. Min and M. Rho, Astrophys. J. **507** (1998) 443.
- [58] M. Butler and J.-W. Chen, “Proton-proton fusion in effective field theory to fifth order,” nucle-th/0101017.

[59] S. Weinberg, in *Salamfestschrift: A Collection of Talks*, World Scientific Series in 20th Century Physics, eds. A. Ali, J. Ellis and S. Randjabar-Daemi (World Scientific, 1993)

[60] S. Beane and U. van Kolck, Phys. Lett. **B328** (1994) 137.

[61] R. Pisarski and F. Wilczek, Phys. Rev. **D52** (1984).

[62] H. Georgi, Phys. Rev. Lett. **63** (1989) 1917; Nucl. Phys. **B331** (1990) 217.

[63] M. Bando, T. Kugo and K. Yamawaki, Phys. Rep. **164** (1988) 217.

[64] M. Harada and K. Yamawaki, Phys. Rev. Lett. **83** (1999) 3374.

[65] M. Harada and K. Yamawaki, hep-ph/0009163.

[66] M. Harada, T. Kugo and K. Yamawaki, Phys. Rev. Lett. **71** (1993) 1299.

[67] R.D. Pisarski, Phys. Rev. **D52** (1995) 3773.

[68] T. Appelquist, J. Terning and L.C.R. Wijewardhara, Phys. Rev. Lett. **77** (1996) 1214; T. Appelquist, A. Ratnaveera, J. Terning and L.C.R. Wijewardhara, Phys. Rev. **D56** (1998) 105017.

[69] See, e.g., R.A. Batty and P.M. Sutcliffe, Phys. Rev. Lett. **79** (1997) 363; C.J. Houghton, N.S. Manton and P.M. Sutcliffe, Nucl. Phys. **B510** (1998) 507

[70] B.W. Lynn, Nucl. Phys. **B402** (1993) 281.

[71] M. Lutz, B. Friman and Ch. Appel, Phys. Lett. **B474** (2000) 7.

[72] R. Shankar, Rev. Mod. Phys. **66** (1994) 129; J. Polchinski, *Recent Directions in Particle Theory: From Superstrings and Black Holes to the Standard Model*, edited by J. Harvey and J. Polchinski (World Scientific, Singapore, 1994) p235-274; T. Chen, J. Fröhlich, and M. Seifert, “Renormalization group methods: Landau Fermi liquid and BCS superconductors,” lectures at Les Houches summer school, August 1994, cond-mat/9508063; G. Benfatto and G. Gallavotti, “Perturbation theory of the Fermi surface in a quantum liquid. A general quasiparticle formalism and one-dimensional systems,” J. Stat. Phys. **59**, 541 (1990); “Renormalization-group approach to the theory of the Fermi surface,” Phys. Rev. B **42** (1990) 9967.

[73] A.B. Migdal, *Theory of Finite Fermi Systems and Applications to Finite Nuclei* (Interscience, London, 1967).

[74] B. Friman and M. Rho, Nucl. Phys. **A606**, 303 (1996); C. Song, G. E. Brown, D.-P. Min, and M. Rho, Phys. Rev. C **56**, 2244 (1997); C. Song, D.-P. Min, and M. Rho, Phys. Lett. **B424**, 226 (1998); B. Friman, M. Rho, and C. Song, Phys. Rev. **C59**, 3357 (1999).

- [75] C. Song, Phys. Rep., to appear; nucl-th/0006030.
- [76] M. Rho, “Effective field theories, Landau-Migdal Fermi-liquid theory and effective chiral Lagrangians for nuclear matter,” nucl-th/0007060.
- [77] G. Gelmini and B. Ritzi, Phys. Lett. B **357**, 431 (1995); T.-S. Park, D.-P. Min and M. Rho, Nucl. Phys. **A596**, 515 (1996).
- [78] G.E. Brown and M. Rho, Nucl. Phys. **A506** (1996) 503.
- [79] B.D. Serot and J.D. Walecka, Adv. Nucl. Phys. **16**, 1 (1986).
- [80] T. Matsui, Nucl. Phys. **A370** (1981) 365 .
- [81] T. Hatsuda and S.H. Lee, Phys. Rev. **C46** (1992) R34; X. Jin and D.B. Leinweber, Phys. Rev. **C52** (1995) 3344.
- [82] G.E. Brown and M. Rho, Phys. Lett. **B222** (1989) 324.
- [83] G.E. Brown and M. Rho, Phys. Lett. **B237** (1990) 3.
- [84] R. Nolte, A. Baumann, K.W. Rose and M. Schumacher, Phys. Lett. **B173** (1986) 388.
- [85] E.K. Warburton, Phys. Rev. Lett. **66** (1991) 1823; Phys. Rev. C **44** (1991) 233; E.K. Warburton and I.S. Towner, Phys. Lett. B **294** (1992) 1.
- [86] T. Minamisono *et al.*, Phys. Rev. Lett. **82** (1999) 1644.
- [87] P. Baumann *et al.*, Phys. Rev. C **58** (1998) 1970.
- [88] A. Van Geert et al, “Meson-exchange enhancement in the first-forbidden beta transition of ^{205}Hg ,” to appear
- [89] K. Kubodera and M. Rho, Phys. Rev. Lett. **67** (1991) 3479.
- [90] M. Rho, Nucl. Phys. **A 231** (1974) 493; K. Ohta and M. Wakamatsu, Nucl. Phys. **A234**, 445 (1974); E. Oset and M. Rho, Phys. Rev. Lett. **42** (1979) 47.
- [91] A. Arima, T. Cheon, K. Shimizu, H. Hyuga and T. Suzuki, Phys. Lett. **B122** (1983) 126.
- [92] A. Arima, T. W. Bentz, T. Suzuki and T. Suzuki, “Delta-Hole Interaction in Nuclei and the Gamow-Teller Strength in ^{90}Nb ,” nucl-th/0008029.
- [93] M. Rho, Phys. Rev. Lett. **66** (1991) 1275.
- [94] A. Heger, K. Langanke, G. Matrtinez-Pinedo and S.E. Woosley, Phys. Rev. Lett. **86** (2001) 1678.

- [95] Y. Kim, G.E. Brown and M. Rho, to appear.
- [96] P.B. Ratha, D.J. Dean, S.E. Koonin, K. Langanke and P. Vogel, Phys. Rev. **C56** (1997) 3079.
- [97] E. Caurier, K. Langanka, G. Martinez-Pinedo and F. Nowacki, Nucl. Phys. **A653** (1999); K. Langanka and G. Martinez-Pinedo, Nucl. Phys. **A673** (2000) 481.
- [98] G. Martinez-Pinedo, , A. Poves, E. Caurier and A.P. Zuker, Phys. Rev. **C53** (1996) R2602; G. Martinez-Pinedo, A.P. Zuker, A. Poves, and E. Caurier, Phys. Rev. **C55** (1997) 187.
- [99] F. Klingl, T. Waas and W. Weise, Nucl. Phys. **A650** (1999) 299.
- [100] E. Marco and W. Weise, “Photoproduction of quasibound omega mesons in nuclei,” nucl-th/0012052.
- [101] G.J. Lolos et al, Phys. Rev. Lett. **80** (1998) 241.
- [102] K. Ozawa et al, “Observation of ρ/ω meson modification in nuclear matter,” nucl-exp/0011013.
- [103] K. Ozawa, private communication.
- [104] M. Soyeur, G.E. Brown and M. Rho, Nucl. Phys. **A556** (1993) 355.
- [105] G.E. Brown, M. Rho and M. Soyeur, Acta Physica Polonica **B24** (1993) 491.
- [106] J. Jourdan, Phys. Lett. **B312** (1993) 189; Nucl. Phys. **A603** (1996) 117.
- [107] D. Onley, Y. Jin and E. Wright, Phys. Rev. **C45** (1992); **C55** (1999) 168.
- [108] D.R. Yennie, F.L. Boos and D.G. Ravenhall, Phys. Rev. **137** (1965) B882.
- [109] P. Guèye et al, Phys. Rev. **C60** (1999) 044308-1.
- [110] K.S. Kim, L.E. Wright, Y. Jin and D.W. Kosik, Phys. Rev. **C54** (1996) 2575
- [111] K. Saito, K. Tsushima and A.W. Thomas, Phys. Lett. **B405** (1999) 27.
- [112] G.E. Brown, M. Buballa and M. Rho, Nucl. Phys. **A609** (1996) 579.
- [113] D.E. Miller, hep-ph/0008031.
- [114] T. Schäfer and E.V. Shuryak, Phys. Rev. **D53** (1996) 6522.
- [115] V. Koch and G.E. Brown, Nucl. Phys. **A560** (1993) 345.
- [116] J.B. Kogut, D.K. Sinclair and K.C. Wang, Phys. Lett. **B263** (1991) 101.

- [117] G.E. Brown, A.D. Jackson, H.A. Bethe and M. Pizzochero, Nucl. Phys. **A560** (1993) 1035.
- [118] M. Gilg et al, KEK Preprint 99-54; K. Itakashi et al, KEK Preprint 99-55.
- [119] T.-S. Park, H. Jung and D.-P. Min, “In-medium effective pion mass from heavy-baryon chiral perturbation theory,” nucle-th/0101064.
- [120] N. Kaiser and W. Weise, “Systematic calculation of s-wave pion and kaon self-energies in asymmetric nuclear matter,” nucl-th/0102062.
- [121] See for review R. Rapp and J. Wambach, hep-ph/9909229.
- [122] G.E. Brown, C.Q. Li, R. Rapp, M. Rho and J. Wambach, Acta Physica Polonica **B29** (1998) 2309.
- [123] G.E. Brown, Y. Kim, R. Rapp and M. Rho, AIP Proceedings, nucl-th/9902009.
- [124] Y. Kim, R. Rapp, G.E. Brown and M. Rho, Phys. Rev. **C62** (2000) 015202
- [125] D.O. Riska and G.E. Brown, Nucl. Phys. **A**, in press, hep-ph/0005049.
- [126] J. Alam, S. Sarkar, T. Hatsuda, T.K. Nayak and B. Sinha, “Photons from Pb-Pb collisions at CERN SPS,” hep-ph/0008074.
- [127] S. Sarkar, J. Alam and T. Hatsuda, “Low-mass dileptons from Pb+Au collisions at CERN-PS,” nucl-th/0011032.
- [128] M.A.B. Bég and S.-S. Shei, Phys. Rev. **D12** (1975) 3092.
- [129] J. Alam, S. Sarkar, P. Roy, T. Hatsuda and B. Sinha, hep-ph/9909267, Ann. Phys., in press.
- [130] G.E. Brown, M. Rho and C. Song, “Strangeness Equilibration at GSI energy,” nucl-th/0010008
- [131] R. Hagedorn, CERN Yellow Report 71-12 (1971).
- [132] J. Cleymans, D. Elliot, A. Keränen and E. Suhonen, Phys. Rev. **C57** (1998) 3319.
- [133] J. Cleymans, H. Oeschler and K. Redlich, Phys. Rev. **C59** (1999) 1663; Phys. Lett. **485** (2000) 27.
- [134] E.L. Bratkovskaya, W. Cassing, C. Greiner, M. Effenberger, U. Mosel and A. Sibirtsev, nucl-th/0001008, Nucl. Phys. **A675** (2000) 661.
- [135] P. Koch, B. Müller and J. Rafelski, Phys. Rep. **142** (1986) 167.
- [136] P. Braun-Munzinger, J. Stachel, J.P. Wessels, and N. Xu, Phys. Lett. **B365** (1996) 1.

[137] M. Menzel et al., nucl-ex/0010013, to be published in Phys. Lett.; M. Menzel, University of Marburg PhD thesis, 2000; D. Best et al, Nucl. Phys. **A625** (1997) 307.

[138] G.Q. Li and G.E. Brown, Phys. Rev. **C58** (1998) 1698.

[139] G.E. Brown, C.M. Ko, Z.G. Wu and L.H. Xia, Phys. Rev. **C43** (1991) 1881.

[140] W.S. Chung, G.Q. Li and C.M. Ko, Nucl. Phys. **A625** (1997) 347.

[141] X.S. Fang, C.M. Ko, G.Q. Li and Y.M. Zheng, Nucl. Phys. **A575** (1994) 766.

[142] W. Cassing, E.L. Bratkovskaya, U. Mosel, S. Teis and A. Sibertsev, Nucl. Phys. **A614** (1997) 415.

[143] E. Friedman, A. Gal and J. Mares, Nucl. Phys. **A625** (1997) 272.

[144] G.E. Brown, K. Kubodera and M. Rho, Phys. Lett. **B192** (1987) 273.

[145] K. F. Liu, S. J. Dong, T. Draper, D. Leinweber, J. Sloan, W. Wilcox and R. M. Woloshyn, Phys. Rev. **D59** (1999) 112001.

[146] C.-H. Lee, Phys. Rep. **275** (1996) 256.

[147] C. Song, Phys. Rep., to appear; nucl-th/0006030; C. Song, G. E. Brown, D.-P. Min, and M. Rho, Phys. Rev. C **56** (1997) 2244.

[148] R.J. Furnsthal, H.-B. Tang and S.D. Serot, Phys. Rev. **C52** (1995) 1368.

[149] S. Weinberg, Phys. Rev. Lett. **65** (1990) 1181.

[150] Y. Kim and H. K. Lee, Phys. Rev. C **62**, 037901 (2000).

[151] S. Peris, Phys. Lett. **B268** (1991) 415.

[152] P.K. Sahu, A. Hombach and W. Cassing, Nucl. Phys. **A640** (1998) 493; P.K. Sahu, W. Cassing, U. Mosel and A. Ohnishi, Nucl. Phys. **A672** (2000) 376.

[153] V. Vento, M. Rho and G.E. Brown, Phys. Lett. **B103** (1981) 285.

[154] K. Holinde, AIP Conference, Particles and Fields Series 43, Proc. LAMPF Workshop on (π, K) Physics, eds. B.F. Gibson, W.R. Gibbs and M.B. Johnson, Los Alamos, 1990.

[155] B. Friman, M. Lutz and G. Wolf, nucl-th/0003012.

[156] N.K. Glendenning, Ap. J. **293** (1985) 470; *Compact stars* (Springer, New York, 1996); nucl-th/0009082.

- [157] M. Prakash, I. Bambaci, M. Prakash, P.J. Ellis, J.M. Lattimer and R. Knorren, Phys. Rep. **280** (1997) 1.
- [158] G.E. Brown, C.-H. Lee and R. Rapp, Nucl. Phys. **A639** (1998) 455c.
- [159] P. Braun-Munzinger, J. Stachel, J.P. Wessels and N. Xu, Phys. Lett. **B344** (1995) 43.
- [160] J. Dunlop, MIT PhD thesis, 1999; L. Ahle et al., Phys. Lett. **B490** (2000) 53.
- [161] A. Ramos and E. Oset, Nucl. Phys. **A671** (2000) 481.
- [162] J. Carlson, H. Heiselberg and V. Pandharipande, nucl-th/9912043.
- [163] For a comprehensive review and updated references, K. Rajagopal and F. Wilczek, “The condensed matter physics of QCD,” hep-ph/0011333 and references given therein.
- [164] D.K. Hong, M. Rho and I. Zahed, hep-ph/9906551, Phys. Lett. **B468** (1999) 261.
- [165] D.B. Kaplan, Phys. Lett. **B235** (1990) 163.
- [166] T. Schäfer and F. Wilczek, Phys. Rev. Lett. **82** (1999) 3956.
- [167] R. Casalbuoni and R. Gatto, hep-ph/9908227, Phys. Lett. **B464** (1999) 111.
- [168] M. Rho, E. Shuryak, A. Wirzba and I. Zahed, Nucl. Phys. **A676** (2000) 273.
- [169] M. Rho, A. Wirzba and I. Zahed, Phys. Lett. **B473** (2000) 126.
- [170] C.G. Callan, S. Coleman, J. Wess and B. Zumino, Phys. Rev. **177** (1969) 2247.
- [171] D.K. Hong, hep-ph/9812510, Phys. Lett. **B473** (2000) 118; hep-ph/9905523, Nucl. Phys. **B582** (2000) 451.
- [172] D.K. Hong, S.-T. Hong and Y.-J. Park, “Bosonization of QCD at high density,” hep-ph/0011027.
- [173] C. Wetterich, Phys. Lett. **B462**, 64 (1999); hep-th/0012023, hep-ph/0008150, hep-ph/0102248.
- [174] J. Berges and C. Wetterich, “Higgs description of two-flavor QCD vacuum,” hep-ph/0012311; J. Berges, “Quark description of nuclear matter,” hep-ph/0012013.
- [175] S. Gottlieb, W. Liu, D. Toussaint, R.C. Renken and R.L. Sugar, Phys. Rev. Lett. **59** (1987) 2247.
- [176] T. Hatsuda and T. Kunihiro, Phys. Rep. **247** (1992) 221.

- [177] G.E. Brown and M. Rho, “Color-flavor locking, hidden local symmetry and BR scaling,” nucl-th/0101015
- [178] M. Harada and K. Yamawaki, Phys. Lett. B **297** (1992) 151.
- [179] C.Q. Li, C.M. Ko and G.E. Brown, Phys. Rev. Lett. **75** (1995) 4007.
- [180] D.B. Kaplan and A.E. Nelson, Phys. Lett. **B175** (1986) 57.
- [181] H.K. Lee, M. Rho and S.J. Sin, Phys. Lett. **B348** (1995) 290.
- [182] D.T. Son and M. Stephanov, Phys. Lett. **B464** (1999) 111. 126.
- [183] D.K. Hong, T. Lee and D.-P. Min, Phys. Lett. **B477** (2000) 137.
- [184] C. Manuel and M.H. Tytgat, Phys. Lett. **B479** (2000) 190.
- [185] S.R. Beane, P.F. Bedaque and M.J. Savage, Phys. Lett. **483** (2000) 131.
- [186] T. Schäfer, Phys. Rev. Lett. **85** (2000) 5531.

